(NASA-CR-150811) MODEL VERIFICATION OF LARGE STRUCTURAL SYSTEMS Final Report, 13 Apr. 1976 - 15 Jul. 1978 (Wiggins (J. H.) Co., Redondo Beach, Calif.) 241 p HC A11/MF A01 CSCL 20K G3/39

N78-31464

Unclas 30295

MODEL VERIFICATION OF LARGE STRUCTURAL SYSTEMS

TECHNICAL REPORT 78-1300 • PREPARED FOR GEORGE C. MARSHALL SPACE FLIGHT CENTER, NATIONAL AERONAUTICS AND SPACE ADMIN.

j.h.wiggins company

FOREWORD

The material documented in this report describes the work accomplished under NASA Contract No. NAS8-31950, during the period 13 April 1976 through 15 July 1978. During this period, a methodology has been formulated and a general computer code implemented and checked out, for processing sinusoidal vibration test data to simultaneously make adjustments to a prior mathematical model of a large structural system, and resolve measured response data to obtain a set of orthogonal modes representative of the test article.

The general procedure is referred to as "model verification". The term "model verification" is used herein to denote a procedure with two distinct and equally important objectives: (1) to establish a proper model configuration by examining different variations of configuration with respect to their ability to match available test data, and (2) to estimate specific parameter values for a selected model configuration. The first objective is met by providing a general modeling capability within the logical structure of the computer code. The practical utility provided by this modeling capability is intended to facilitate a "man-in-the-loop" type of function, where the user may apply his judgement and modeling skill to achieve a proper model configuration. The second objective is met by providing fully automated parameter estimation programs to optimize the fit of any selected model configuration to the given test data.

The basic methodology for the three step procedure described herein has been described in detail in the interim report [2]

and will not be repeated here. The procedure involves three operations:

1) A linear perturbation of the prior modal model which directly incorporates experimental mode-shape and frequency data when available;

2) Bayesian estimation of the modal mass, stiffness and damping parameters, using the modulus of (measured) complex sine response for selected locations on the structure, at selected frequencies; and

3) Bayesian estimation of component scaling parameters associated with component submatrices of the original mass and stiffness matrices of the given dynamic model using the revised modal model from step 2 as input to the estimation.

The method has been applied to two problems associated with the Space Shuttle project: the Quarter-Scale SRB and the Quarter-Scale Orbiter. Much has been learned about the procedures, although changes to the dynamic models of these two structures cannot at this time be recommended.

ACKNOWLEDGEMENTS

This project was fortunate in having two co-technical monitors, Larry Kiefling of the Marshall Space Flight Center and George Zupp of the Johnson Space Center, who were both interested in and supportive of the effort. Their assistance is very much appreciated.

The work could not have been completed without the willing cooperation and assistance of the Vehicle and Systems Dynamics Group (Mr. L.S. Nogawski, Supervisor) at Rockwell International - Space Division. All members of the Group were particularly helpful during the four-month period in which the Quarter-Scale Orbiter was studied at Rockwell Plant in Downey using the Rockwell Cyber-174 computer. Information on Rockwell procedures and their computer system was always available when needed. Any time a problem was encountered, someone would drop what he was doing to lend a hand. Particular thanks is made to those individuals who provided the Quarter-Scale SRB and Orbiter data, under the direction of Bohdan Bejmuk, and facilitated our use of that data: J.A. Barrett, M.Y. Hion, J.S. Kanno, and B.H. Ujihara.

Many other individuals contributed to the performance of this work. Particular note is made of the contribution made by Jon D. Chrostowski in the development of the computer codes and Jerrold Isenberg in the development of the Bayesian estimator. Other company personnel who contributed to the development of the methodology and furthered our understanding of the processes involved are Jon D. Collins and David A. Evensen.

TABLE OF CONTENTS

TABLE OF CONTENTS (CONTINUED)

LIST OF FIGURES

LIST OF TABLES

LIST OF TABLES (CONTINUED)

NOTATION

C	dynamic model damping matrix
F	object function
I	identity matrix
I_{xx}, I_{yy}, I_{zz}	mass moments of inertia
K	dynamic model stiffness matrix
k	analytic model stiffness matrix
M	dynamic model mass matrix
m	analytic model mass matrix
P	applied forces
r, r_e	estimated parameter (new, old respectively)
r_o	prior estimate of parameters
S_{rr}	covariance matrix of prior parameters (always diagonal)
$S_{\varepsilon\varepsilon}$	covariance matrix of observed responses (may be diagonal)
u	calculated responses
u_o	observed (i.e., test) responses or dynamic model coordinates
w	observation weight matrix
$\hat{w}$	parameter (i.e., prior model) weight matrix
x	analytic model coordinates
α	dynamic model scaling parameters

η, δ	intermediate FOC calculations
λ	eigenvalue
σ	standard deviation
T	sensitivity matrix
ψ, ϕ	mode shapes
Ω	excitation frequency

1. INTRODUCTION

1.1 Background

This project was begun in April of 1976 with its objective to develop a computer program for the application of parameter identification on the structural dynamic models of the Space Shuttle. This effort was a natural continuation of research that the Marshall Space Flight Center has been involved in since 1969 to improve the techniques by which analytic models can be verified and upgraded.

The dynamic response of the structure is a critical consideration in the operation and performance of all aerospace vehicles. Many of these vehicles are never subjected to their design environment until some time during their operational life. And many are so expensive that pre-operational testing is very limited in scope. Tests to destruction are often impractical because the test hardware must be preserved for more testing. Consequently, the success of the project often hinges on the adequacy and sophistication of the analytic models used to predict both the loads and their effect on the structure.

Because of their recognized importance, these analytic models have for many years been verified by test. This is usually accomplished with a modal test in which the normal modes and natural frequencies are measured. If the test data fail to verify the mathematical model, the model is modified until a satisfactory correlation is obtained. This is very often a tedious trial-and-error procedure which may depend for its success on the engineering intuition of the practitioner.

There have been many attempts in recent years to put the modification of the analytic model on a more rigorous footing. The resulting field of investigation, often called parameter identification, uses the dynamic-test results to modify (i.e., identify) the parameters (i.e., mass, stiffness, and damping) in the equations of motion. To date, however, no method has really been proven or generally accepted as a reliable technique to derive a useful analytic model from test data. Most are successful under certain situations, but none appears to work for the most general case. Many are successful on small models involving only a few degrees-of-freedom, but become intractable when applied to models with hundreds of degrees-of-freedom.

The J. H. Wiggins Company has been involved in this field of investigation since 1970. A computer program called MOUSE (Modal Optimization Using Statistical Estimation) was developed for NASA/MSFC and delivered in 1973 [1]. Some of the more important features of this program are:

- A prior estimate of the model parameters and their uncertainties are used.
- The test data consist of mode shape and natural frequency information.
- Incomplete information can be used.
- Specific finite element parameters, such as the bending or shear stiffness, are estimated.

The program is not, however, directly applicable to large models with hundreds of degrees-of-freedom, such as those

developed for the Space Shuttle. This project was, therefore, initiated (1) to extend that methodology to large models and (2) to demonstrate its application to real problems using Space Shuttle mathematical models and test data.

1.2 Objectives

A number of specific objectives were established as a first step in achieving the major goals of the project. These objectives are separated into two groups, the first supporting the development of the general methodology and computer program, the second supporting the demonstration of the methodology and computer program for practical applications.

Specific objectives which have shaped the present methodology are as follows:

1) To provide a general capability which is fully compatible with currently used methods of analysis and testing, so that it may be used in support of the Space Shuttle Program, as well as other present and future NASA programs. In particular, the interface with math models should be such that the output from any structural analysis program such as applied to any structural configuration, NASTRAN, SPAR, etc., may be used directly. And, the processed data from either show sine-sweep tests or resonant dwell tests should be directly usable.

2) To provide a capability which places no demands or limitations on the amount of data required.

3) To be able to estimate the modal damping characteristics of a structure as well as its mass and stiffness parameters.

4) To be applicable to structures with high modal density, i.e., closely spaced modes with respect to frequency.

5) To provide a capability which, in addition to serving as an instrument for refining a math model, may serve as an instrument for filtering, interpolating, and extrapolating test results, and if possible, help to resolve modal information from tests which were unable to isolate some of the modes experimentally.

6) To estimate mass and stiffness parameters which are physically meaningful from the standpoint of their association with localized areas, components, or elements of the physical structure itself.

7) To provide a quantitative measure of the significance of estimated parameter values, based on the quantity and quality of data used in the Bayesian Estimator.

8) To provide for a computerized data interface among the separately executable computer codes comprising the computer program, and between the program and the analysis and test data files pertaining to Space Shuttle applications.

9) To provide user instructions for operating the computer program, and guidelines for formulating and interpreting the results of specific applications.

The objectives guiding the selection, formulation, execution, and interpretation of demonstration problems were defined as follows:

1) To demonstrate, first and foremost, that the methodology and computer program work on real problems.

2) To demonstrate that an "outsider" (i.e., a person who has not previously been involved in either the analysis or the testing of a structure) may access the two corresponding sets of data and use this computer program to perform meaningful analysis-test correlation.

3) To identify some of the pitfalls which may be encountered in the unconventional use of conventional data, thereby developing a better awareness for planning future activities.

4) To gain general experience with the behavior of the computer program, so that practical guidelines may be offered for the benefit of new users.

5) To provide insight for any further development which might enhance the utility of the present computer program.

It is believed that all of the above objectives have been substantially achieved. The original methodology consisting of

a two-phase Bayesian Estimator driven by frequency response data, has been extended to incorporate an initial first order correction (linear perturbation) of the prior model based on experimental mode shapes and frequencies when available. This initial step has been found to improve the convergence of the Bayesian Estimator in a number of cases. However, its use is optional.

To augment the basic methodology and facilitate practical use of the computer program, an expedient alternative to generating component submatrices from the detailed finite element model has been developed and demonstrated. The technique requires only that the reduced mass and stiffness matrices corresponding to the dynamic model be available, and that these matrices correspond to physical displacement coordinates distributed over the structure. Component submatrices are generated from orthogonal (or nearly orthogonal) displacement shapes induced by selecting appropriate equilibrium load distribution.

It is perhaps worth emphasizing here that a fundamental assumption, underlying the development of this methodology, is that the resulting computer program will be used as a tool for computation and analysis, and not as a "black box" for blindly correlating analysis and test. The concept of "man-in-the-loop" is essential to the proper understanding and utilization of this tool. In short, the computer program automates Part (2) of the "model verification" process described in the Foreword. The analyst must use his experience and insight to accomplish Part (1).

2. METHODS OF ANALYSIS

2.1 Analytical Approach

The analytical approach was previously presented in the Interim Report [2] issued during June of 1977. No substantial changes have been made since that time except to upgrade the estimator algorithm to a more truly Bayesian formulation. All of the steps incorporated or proposed in 1977 have been made part of the estimation procedures and incorporated into the computer program triad: FOCOR, ESTIMA, ESTIMB. The three phases of the procedure are:

1) Make direct use of measured modal data to condition the prior analytic model so as to improve the frequency match between "model" and test.

2) Use the Bayesian estimator to generate an improved analytical model. Use a linear estimator in an iterative fashion on highly non-linear equations.

3) Use the Bayesian estimator to generate mass and stiffness scaling parameters for an improved finite element model. Since these equations are linear, the optimum set of parameters is obtained in one step.

The revised estimator is described in detail in Reference [3]. Brief summaries of it and each phase of the procedures are provided in the following sections.

Before proceeding we should define the hierarchy of mathematical models used to represent the structural system. Four models are germane to the present discussion:

- Finite Element Model - This model represents the most detailed model of the system.

- Dynamic Model - This model is obtained by taking the finite element model, or the components of that model, through several stages of coordinate reduction. At least some of these degrees-of-freedom must relate directly to physical structural displacements so that a comparison to measured test data can be made. In the development this model is referred to as the "u" system.

- Analytic Model - This model is obtained by selecting a limited number of modes of the dynamic model and using them as the basis for an additional coordinate reduction. The size (i.e., number of degrees-of-freedom) of the analytical model is the number of modes being used. These are the modes which should and can be verified with vibration test data. In the development, this model is referred to as the "x" system.

- Modal Model - Prior to the estimation, the modal model does not exist because the coordinate reduction described above diagonalizes the dynamic model mass and stiffness matrices. There is then no need for another transformation. However, once an estimation has been performed, the analytic model mass and stiffness matrices are no longer diagonal. Now a second coordinate transformation can be defined using the modes of the perturbed analytic model. The resulting coordinates are referred to as the modal model or the "q" system.

2.2 The Bayesian Estimator

In Bayesian estimation [3] we are given a prior estimate of the parameters, r_o, along with the associated covariance matrix S_{rr}. We then seek to minimize the object function

$$F = \sum_{i=1}^{n} \sum_{j=1}^{n} w_{ij}\left(u_{o_i} - u_i\right)\left(u_{o_j} - u_j\right)$$

$$+ \sum_{i=1}^{p} \sum_{j=1}^{p} \hat{w}_{ij}\left(r_{o_i} - r_i\right)\left(r_{o_j} - r_j\right) \qquad (1)$$

where $w = S_{\varepsilon\varepsilon}^{-1}$ (2)

and $\hat{w} = S_{rr}^{-1}$ (3)

and S_{rr} is a symmetric matrix as is $S_{\varepsilon\varepsilon}$.

w and $\hat{w}$ are weight matrices for the observation data and the prior model respectively. The second summation accounts for our knowledge of the Bayesian prior. The new parameter estimate obtained via this equation will be a compromise between our knowledge concerning the experimental data (the first double series term) and the Bayesian prior. If the weighting matrix for the prior model, $\hat{w}$, is set to zero this formulation reduces to a minimum variance estimator.

Minimizing this equation with respect to each parameter gives

$$\frac{\partial F}{\partial r_k} = -\sum_i \sum_j w_{ij} \left[\left(u_{o_i} - u_i \right) \frac{\partial u_j}{\partial r_k} + \left(u_{o_j} - u_j \right) \frac{\partial u_i}{\partial r_k} \right]$$

$$+ \sum_j \hat{w}_{kj} \left(r_{o_j} - r_j \right) \frac{\partial \left(r_{o_k} - r_k \right)}{\partial r_k}$$

$$+ \sum_i \hat{w}_{ik} \left(r_{o_i} - r_i \right) \frac{\partial \left(r_{o_k} - r_k \right)}{\partial r_k} = 0 \qquad (4)$$

Since the function u is nonlinear, expand it into a truncated Taylor series evaluated at an estimated value, r_e:

$$u_\ell \approx u_{e_\ell} + R_1 T_{\ell 1} + R_2 T_{\ell 2} + \ldots + R_P T_{\ell P} \qquad (5)$$

and note that

$$\frac{\partial u_\ell}{\partial r_k} = T_{\ell k} = \text{element of sensitivity matrix} \qquad (6)$$

and

$$\frac{\partial \left(r_{o_k} - r_k \right)}{\partial r_k} = -1. \qquad (7)$$

Substituting Equations 5, 6, and 7 into Equation 4 gives

$$\sum_{1}\sum_{j} w_{1j}\left(u_{o_j} - u_{e_j} - R_1T_{j1} - R_2T_{j2} - \ldots - R_pT_{jp}\right)T_{ik}$$

$$+ \sum_{1}\sum_{j} w_{ij}\left(u_{o_i} - u_{e_i} - R_1T_{i1} - R_2T_{12} - \ldots - R_pT_{1p}\right)T_{jk}$$

$$+ \sum_{j} \hat{w}_{kj}\left(r_{o_j} - r_j\right) + \sum_{i} \hat{w}_{ik}\left(r_{o_1} - r_i\right) = 0 \qquad (8)$$

Since $S_{\varepsilon\varepsilon}$ and S_{rr} are symmetric, w and $\hat{w}$ are also symmetric. Therefore the two double series terms of Equation 8 are identical as are the two single series terms. Equation 8 then simplifies to

$$\sum_{1}\sum_{j} \overline{w_{ij}\left(u_{o_j} - u_{e_j} - R_1T_{j1} - R_2T_{j2} - \ldots - R_pT_{jp}\right)}T_{1k}$$

$$+ \sum_{j} \hat{w}_{kj}\left(r_{o_j} - r_j\right) = 0 \qquad (9)$$

We then note that

$$r_{o_j} - r_j = r_{o_j} - r_{e_j} - R_j \qquad (10)$$

which upon insertion into Equation 9 and some manipulation gives a set of linear equations of the form

$$CR = V \tag{11}$$

where the elements of C and V are defined by

$$C_{k\ell} = \hat{w}_{k\ell} + \sum_{i=1}^{n} \sum_{j=1}^{n} w_{ij} T_{ik} T_{j\ell} \tag{12}$$

$$V_k = \sum_{j=1}^{p} \hat{w}_{kj} \left(r_{o_j} - r_{e_j} \right) + \sum_{j=1}^{n} \left(u_{o_j} - u_{e_j} \right) \sum_{i=1}^{n} w_{ij} T_{ik} \tag{13}$$

As seen from Equation 12, the C matrix is symmetric which eases much of the computation.

In matrix form the parameter estimate is obtained by iteratively solving the relation

$$r = r_e + \left(\hat{w} + T^t w T \right)^{-1} \left[\hat{w} \left(r_o - r_e \right) + T^t w \left(u_o - u_e \right) \right] \tag{14}$$

The iteration starts with r replacing r_e, calculating T as a function of the independent variables, and then generating r by Equation 14. When r converges to r_e the iterations are terminated.

2.3 The First Order Correction

The First Order Correction was developed to utilize certain test information, namely mode shape and frequency data, not explicitly used elsewhere in the parameter identification. This information is used in a linear perturbation technique to adjust the analytic model so as to provide a better frequency match between the new analytic model and the test modes. Five steps are involved:

1) Compute the frequency difference (rad^2/sec^2)

$$\Delta\lambda_j = \hat{\lambda}_j - {}^{\circ}\lambda_j \tag{15}$$

where the ^ refers to the test data and the ° to the prior model.

2) Compute the cross-orthogonality between the analytic modes and the test modes. Only modes which can be matched test to analysis can be used.

$$[\hat{\psi}] = [{}^{\circ}\phi]^t [{}^{\circ}M] [\hat{\phi}] \tag{16}$$

3) Compute $\Delta\eta_{ij}$.

$$\Delta\eta_{ij} = \hat{\psi}_{ij} - \delta_{ij} \tag{17}$$

where $\delta_{ij} = 1$ when $i = j$

$= 0$ when $i \neq j$

4) Compute the perturbations to the analytic mass and stiffness matrices.

$$\Delta m_{jj} = -2\Delta\eta_{jj} \tag{18a}$$

$$\Delta m_{ij} = -(\Delta\eta_{ij} + \Delta\eta_{ji}) \tag{18b}$$

$$\Delta k_{jj} = \Delta\lambda_j + {}^{o}\lambda_j \Delta m_{jj} \tag{18c}$$

$$\Delta k_{ij} = ({}^{o}\lambda_j - {}^{o}\lambda_i)\Delta\eta_{ij} + {}^{o}\lambda_j \Delta m_{ij} \tag{18d}$$

2.4 The Analytic-Model Estimator

The Analytic-Model Estimator is also called the Phase I Estimator. It refines the parameters of the analytic and modal models using measured response data. The objective is to develop revised generalized mass and stiffness matrices for the analytic model and a revised generalized damping matrix for the modal model which will provide a better match between the calculated and the measured frequency response. The approach used to develop the new analytic model mass matrix, [m]; new analytic model stiffness matrix, [k]; and new generalized damping matrix, [ξ]; is as follows:

1) Calculate the response of the system at the measurement locations. [φ], [λ], and [ξ] are taken from the unperturbed dynamic model.

$$[M]\{\ddot{u}\} + [C]\{\dot{u}\} + [K]\{u\} = \{f(t)\} \tag{19a}$$

$$\{u\} = [\phi]\{x\} = [H(\Omega)]\{P\}g(t) \tag{19b}$$

$$[H(\Omega)] = [\phi][\tilde{H}(\Omega)][\phi]^t \tag{20}$$

$$[\tilde{H}(\Omega)] = \left[-[I]\Omega^2 + [c]\Omega\hat{i} + [\lambda]\right]^{-1} \tag{21}$$

2) Calculate the sensitivity matrix [T] and the "observation" vector. The effective "observation" vector is the difference between the measured responses and the calculated responses.

3) Use the Bayesian estimator to provide new mass and stiffness matrices for the analytic system. Input to the estimator consists of the "observation" vector, the sensitivity matrix, and the previous estimate of the mass and stiffness matrices. The new equations of motion for the "x" system are

$$[m]\{\ddot{x}\} + [c]\{\dot{x}\} + [k]\{x\} = \{\tilde{P}\}g(t). \tag{22}$$

4) Solve for the eigenvalues [λ] and eigenvectors [ψ] of the modified "x" system. Normalize these modes such that they have the characteristics:

$$[\psi]^t[m][\psi] = [I] \quad \text{diagonal}$$

$$[\psi]^t[k][\psi] = [\lambda] \quad \text{diagonal} \tag{23}$$

5) The revised eigenvectors for the dynamic model, the u-coordinate system, are given by

$$[\phi] = [^{\circ}\phi][\psi]. \tag{24}$$

6) Revise the damping matrix [ξ] to reflect the new eigenvalues while retaining the same damping ratios as were assumed for the initial dynamic model. The damping parameters are estimated by a separate operation.

7) Calculate the response using the new eigenvalues [λ] and new dynamic-model modes [ϕ].

8) Repeat the above steps until convergence is obtained.

9) Lastly, perform a similar iterative scheme to estimate elements of the damping matrix, [ξ].

2.5 The Dynamic-Model Estimator

The goal of the Phase II estimator is to develop a set of scaling parameters, α_1, which will improve the mass and stiffness matrices of the dynamic model. It still remains the responsibility of the analyst to select a set of submatrices which when multiplied by scaling factors will improve the model. The analyst must select submatrices which he thinks might be successful or enlightening based on his experience and knowledge of the structure being investigated. In general, a number of trial configurations may be run before a useful and realistic modified model is obtained.

The basic approach used to estimate the new dynamic model mass and stiffness matrices is as follows:

1) Complete Phase I to provide "observation data" in the form of generalized mass [m] and stiffness [k]

3. DEMONSTRATION PROBLEM: QUARTER-SCALE SRB

3.1 Background and Conclusions

At the start of this investigation, the Quarter-Scale Solid Rocket Booster at end-of-action (SRB - Figure 3-1) was selected as a demonstration problem to provide an example of relatively modest proportions. It was believed at that time that this relatively simple structure could be adequately characterized with six beam bending modes, one torsion mode, and one axial mode.

The first problem that came to light centered on the aft skirt (Figure 3-1). First, the analytic model, based on flight hardware, differs from the test item in the launch pad stiffness. Second, the analytic model has 8 "launch pad" modes between 30 and 130 Hz, some of which are highly coupled with the "second" body bending modes. This, as will be shown later, means that a unique set of body bending modes (first, second, third bending modes) cannot be extracted from the analytic set of modes. Since only the "primary body bending" modes were recorded during the test, this leads to an incompatibility between test and analysis.

The second difficulty with this particular vehicle is its near axi-symmetry. This results in non-unique bending modes with repeated frequencies. Those analytic modes that could be uniquely identified as primary body bending (first and third bending in the Y and Z planes) lie in mutually orthogonal planes. The corresponding test modes, plus the two second body bending modes, do not lie in such mutually orthogonal planes (Figure 3-15 on page 3-37 and Figures 3-17 and 3-18 on page 3-41). Since the test article is so nearly axi-symmetric, it is not clear if the test modes are unique or

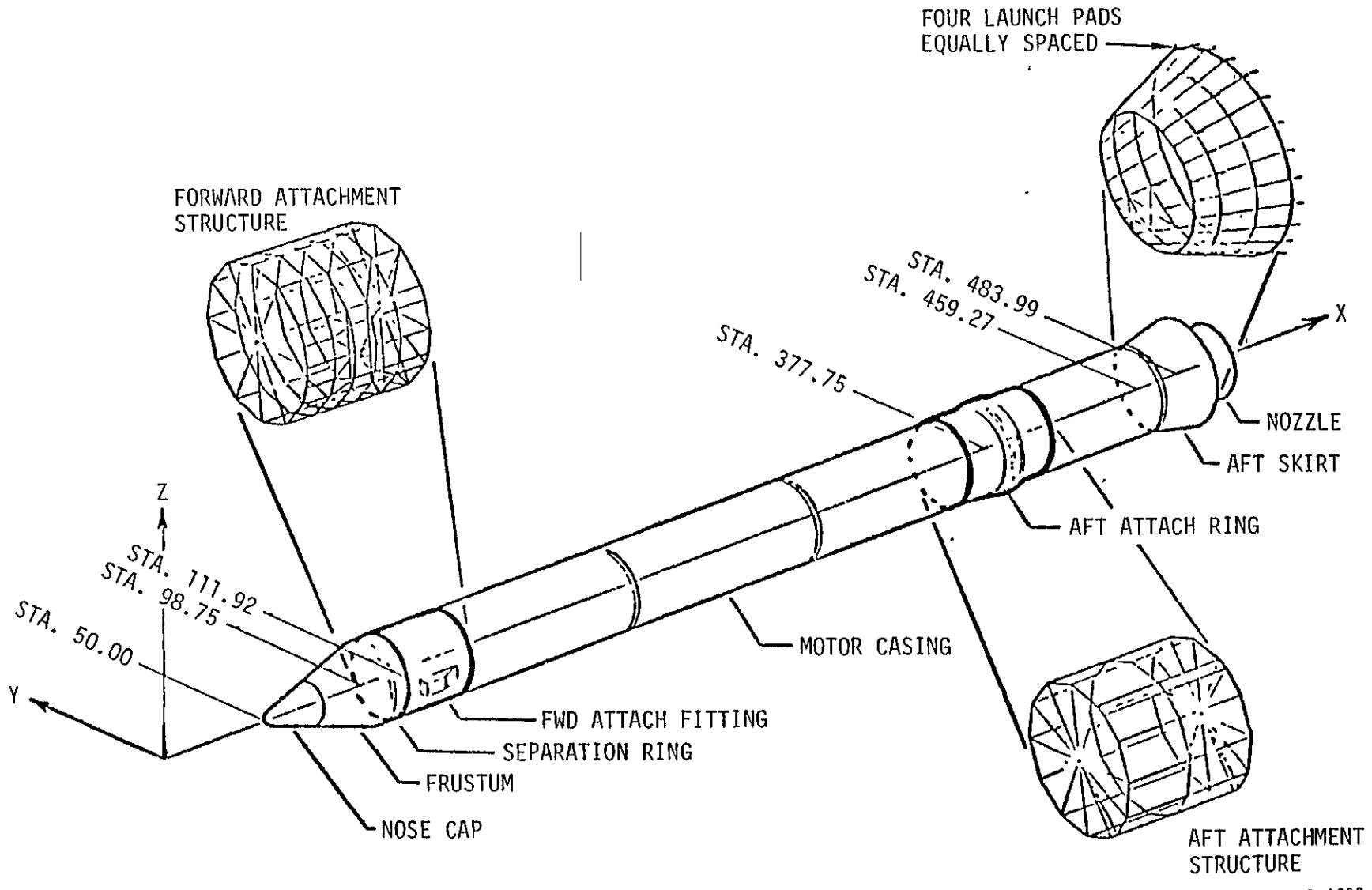

Figure 3-1. Quarter-Scale SRB

if the spacial non-orthogonality means that the best orthogonal modes were missed. Even if the modes are unique, their orientation with respect to the Y and Z axis is probably very sensitive to small stiffness changes. The non-uniqueness quality of the bending modes of a slender axi-symmetric body clouds the problem, making it difficult to interpret the estimator's behavior. The study of this example has led us to the following conclusions regarding closely spaced modes of similar shape, except for global orientation.

- Although closely spaced modes may be distinct in a mathematical sense, they appear to be much less distinct in a physical sense. That is, (1) they are difficult to isolate experimentally, (2) their orientation (experimental) may be ambiguous and somewhat arbitrary, and (3) because of (1) and (2) they are difficult to correlate with analytical modes.

- Particularly in the case of closely spaced modes, it may be more meaningful to correlate the modulus of complex response (analysis and test) than to attempt to correlate modes. This should be done at resonant frequencies, however.

- Since closely spaced modes tend to be non-distinct (in a practical sense), one should probably not try to read in too much physical significance to individual mode shapes, either analytical modes or experimental modes.

Another difficulty encountered with the Quarter-Scale SRB was that the stiffness matrix corresponding to the modes provided by Rockwell (end-of-action time configuration) was not available. This meant that Step 2 of the estimation procedure, modifying the [M] and [K] matrices of the dynamic model, could not be performed in its totality. We, therefore, concentrated our investigation on evaluating the ability of the First Order Correction(FOC) and the Phase I Estimator to produce an improved set of "analytic" modes. We then used the results of one of the examples and generated four scaling parameters for the mass matrix. Although the usefulness of these parameters in the absence of concurrent adjustments to the stiffness matrix can not be ascertained, the adjusted masses provide a somewhat improved fit of the data.

The following conclusions have been drawn with respect to the First Order Correction, and the Phase I and Phase II Estimators:

First Order Correction

- The FOC improves the frequency match.
- The FOC appears to worsen the mode shapes by changing the generalized mass (i.e., a scaling problem).
- When used with the Phase I parameter estimation, the FOC improves the final results significantly as measured by the reduction of the object function.

Phase I Estimator

- The basis of comparison between analysis and test should be total resonant response, rather than

quadrature response or individual mode shapes. Kinetic energy at resonant response would appear to be a good basis of comparison (single number).

- Successful reduction of the object function (particularly with FOC) indicates significant improvement of analytic mode shapes. The object function is reduced by more than a factor of 2. The remaining residual "error" (final value of object function) may be due (at least in part) to the fact that test modes do not satisfy conservation of momentum. The reason for this apparent discrepancy in test modes has not been resolved. It is evidently not caused by external forces applied by suspension system because these forces are too small (soft mount). Neither does it seem to be caused by external forces applied by the shakers, because these are supposedly out of phase by 90°, i.e., the test modes are determined from the quadrature response.

- Parameter estimation using this program has been successfully applied in the case where data are available only at selected resonant frequencies. It thus appears to retain the successful features of MOUSE while adding several new capabilities: (1) damping, (2) closely spaced modes, (3) drift limiter (stability), (4) much more general modeling capability.

- All of the modes must be retained in the analytic model up to the maximum frequency being considered. (See Section 3.5, Example One.)

Dropping analytic modes not found in the test, constrains the Estimator in what it can accomplish. (See Section 3.6, Example Two.)

Phase II Estimator

- The Phase B Estimator can successfully produce mass scaling parameters to improve the model/"test" correlation ("test" means output from Phase I).

3.2 Analytic Model

A detailed mathematical model of the quarter-scale model was prepared by NASA [4]. This model has 54 nodes, 240 static degrees of freedom (DOF) and 121 dynamic degrees of freedom. The dynamic model (i.e. the matrices used for the eigensolution) is derived from the top level model using a static reduction technique to remove the 119 DOF with zero mass. The algorithm used by Rockwell for this reduction is capable of restoring the reduced coordinates.

A brief description of the model is shown in Tables 3-1 and 3-2. The overall mass properties are:

weight	2707.82	lb
I_{xx}	179.02	slug-ft^2
I_{yy}	10323.04	slug-ft^2
I_{zz}	10323.04	slug-ft^2

The first 24 analytical modes (excluding shell modes) are described in Table 3-3. Included within these 24 modes are:

6 rigid body modes
6 bending modes

Table 3-1. Quarter-Scale SRB: Degree-of-Freedom Schedule

NODE	STATION	DESCRIPTION	DEGREE-OF-FREEDOM SCHEDULE					
			X	Y	Z	θ_x	θ_y	θ_2
400	52 3	NOSE CAP	1	2	3	4	-	-
401	68.8	NOSE CAP - FRUS INT.	5	6	7	8	-	-
402	82 5	FRUSTUM	9	10	11	12	13	14
403	98 8	FRUSTUM - SEP. RING INT.	15	16	17	18	19	20
404	100 2	SEP. RING - FWD SKIRT INT	21	22	23	24	-	25
411	131.0	FWD SKIRT - SRB MOTOR INT	26	27	28	29	-	-
412	166 2	SRB MOTOR CASE	30	31	32	33	34	35
417	201.5	SRB MOTOR CASE	36	37	38	39	40	41
418	235 8	SRB MOTOR CASE	42	43	44	45	46	47
423	270 0	SRB MOTOR CASE	48	49	50	51	52	53
424	304 2	SEB MOTOR CASE	54	55	56	57	58	59
429	338.5	SRB MOTOR CASE	60	61	62	63	64	65
430	361 1	SRB MOTOR CASE	66	67	68	69	70	71
436	394 4	SRB MOTOR CASE	72	73	74	75	76	77
441	420 5	SRB MOTOR CASE	78	79	80	81	82	83
442	459.3	SRB MOTOR CASE	84	85	86	87	88	89
446	484 0	SRB LAUNCH PAD NODE,	90	91	92	93	-	94
447	484 0	SRB LAUNCH PAD NODE	95	96	97	98	-	99
448	484 0	SRB LAUNCH PAD NODE	100	101	102	103	-	104
449	484 0	SRB LAUNCH PAD NODE	105	106	107	108	-	109
450	468 8	NOZZLE C.G AT IGN.	110	111	112	113	114	115
452	468.7	NOZZLE ACT. MT.	116	117	118	119	120	121

Table 3-2. Quarter-Scale SRB: Analytical Mass and Inertia

NODE	MASS	I_x	I_y	I_z	REGION
400	.02343	.26662	0	0	NOSE AND FRUSTUM
401	.08552	3.75801	0	0	
402	.23037	24.67760	2.79774	7.51883	
403	.09533	19.03527	4.17703	7.50403	
404	.15084	41.48915	0	2.30727	
411	.49033	137.43280	0	0	MOTOR CASE - FORWARD
412	.47452	156.95210	38.13876	40.56774	
417	.45714	149.59420	307.25549	300.56289	
418	.45622	149.69290	441.67120	499.53799	
423	.46100	151.22910	457.20180	516.59059	
424	.47100	154.10350	473.49880	476.06839	
429	.37572	123.69130	386.32259	412.69939	MOTOR CASE - AFT
430	.42522	140.15090	370.74569	371.52579	
436	.47952	158.69010	390.78559	391.82970	
441	.48219	159.55970	347.54859	349.67450	
442	.55716	172.04230	104.78490	102.83480	
446	.050575	6.46250	0	.30090	SKIRT
447	.050575	6.46250	0	.30090	
448	.050575	6.46250	0	.30090	
449	.050575	6.46250	0	.30090	
450	.46038	148.67690	48.84528	60.01895	NOZZLE
452	.63616	84.99609	115.04300	115.14840	

Table 3-3. Quarter-Scale SRB: Analytic Pre-Test Modes Computed by NASA

MODE NO.	FREQUENCY (Hz)	MODE DESCRIPTION
1-6	0	RIGID BODY MODES (FREE-FREE)
7	30.064	NOZZLE MODE COUPLED WITH FIRST Z-BENDING
8	30.389	NOZZLE MODE COUPLED WITH FIRST Y-BENDING
9	38.136	FIRST Z-BENDING
10	38.321	FIRST Y-BENDING
11	81.218	LAUNCH PADS MODE
12	82.907	LAUNCH PADS MODE COUPLED WITH SECOND Y-BENDING
13	85.501	LAUNCH PADS MODE COUPLED WITH SECOND Z-BENDING
14	87.453	LAUNCH PADS MODE COUPLED WITH SECOND Y-BENDING
15	90.769	LAUNCH PADS MODE COUPLED WITH SECOND Z-BENDING
16	92.688	SECOND Z-BENDING COUPLED WITH LAUNCH PADS MODE
17	93.528	LAUNCH PADS MODE COUPLED WITH SECOND BENDING (Y & Z)
18	96.588	SECOND Y-BENDING COUPLED WITH LAUNCH PADS MODE
19	115.400	LAUNCH PADS MODE
20	121.020	FIRST TORSION
21	129.783	LAUNCH PADS MODE COUPLED WITH THIRD Z-BENDING
22	155.936	THIRD Y-BENDING
23	158.630	THIRD Z-BENDING
24	177.028	FIRST AXIAL

1 torsion mode
1 axial mode
2 nozzle modes
8 "launch pad" modes

These modes are shown graphically in Figures 3-2 to 3-14.* In the corresponding frequency band, the test developed 8 modes (excluding shell modes):

6 bending modes,
1 axial mode, and
1 torsion mode.

The two nozzle modes are obviously lacking in the test data because apparently the flexibility which generates these modes was not incorporated into the test hardware. Why the "launch pad" modes are missing from the test data is not known. It may have been that the known differences between the test hardware and the flight hardware, in the aft skirt area, moved these modes out of the frequency range of interest. Or, it may have been just that there was no attempt to measure these modes.

3.3 Test Data

The quarter-scale ground vibration tests of the SRB were conducted during November and December of 1976 and January of 1977 at the Downey facility of Rockwell Space Division. The

*In some of these figures, launch pad and nozzle deflections have not been plotted. The intent is to illustrate the degree to which launch pad and nozzle motion is coupled with body bending, since this is the information used in parameter estimation.

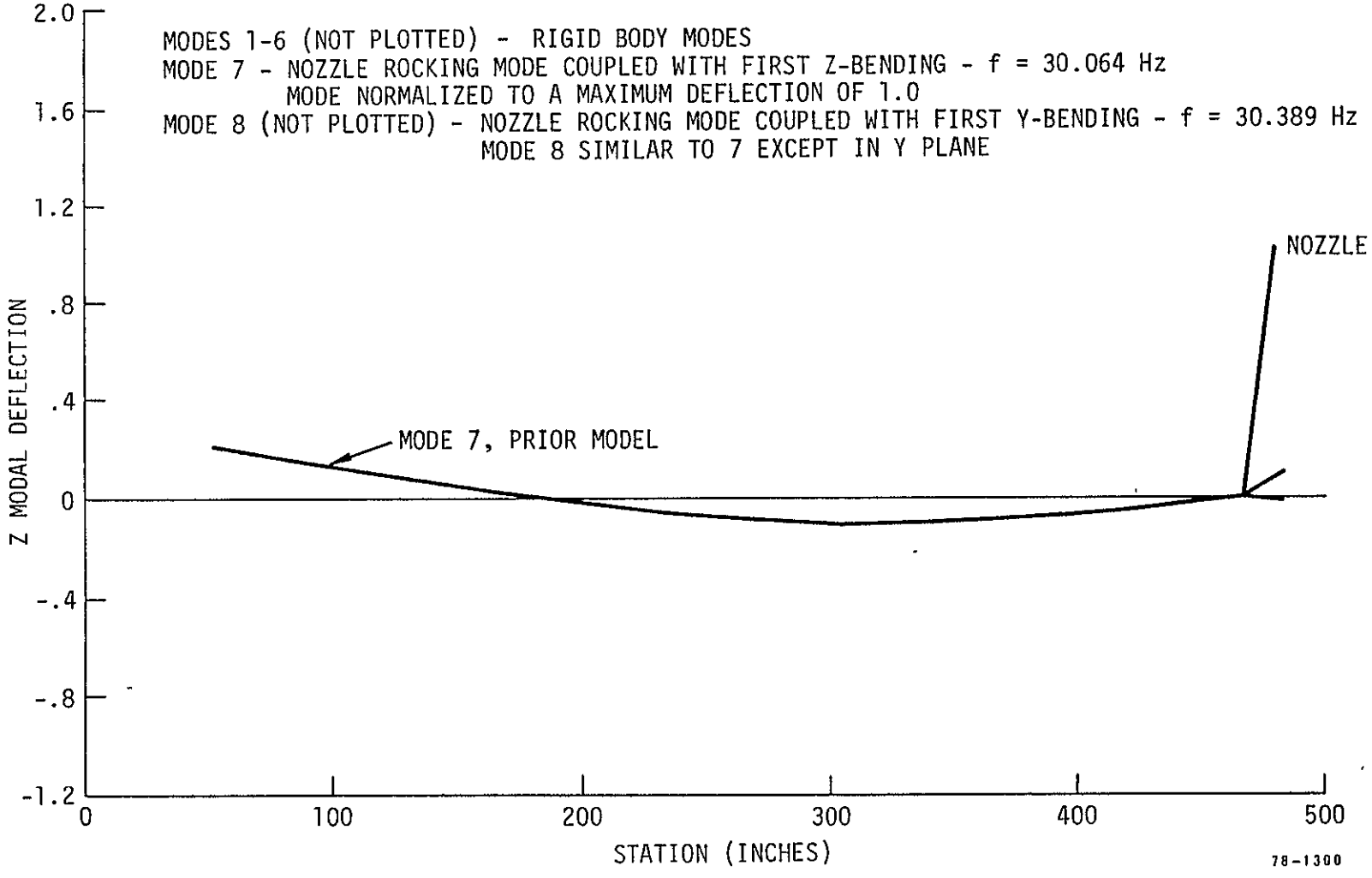

Figure 3-2. SRB Prior Model Mode - End-of-Action Time

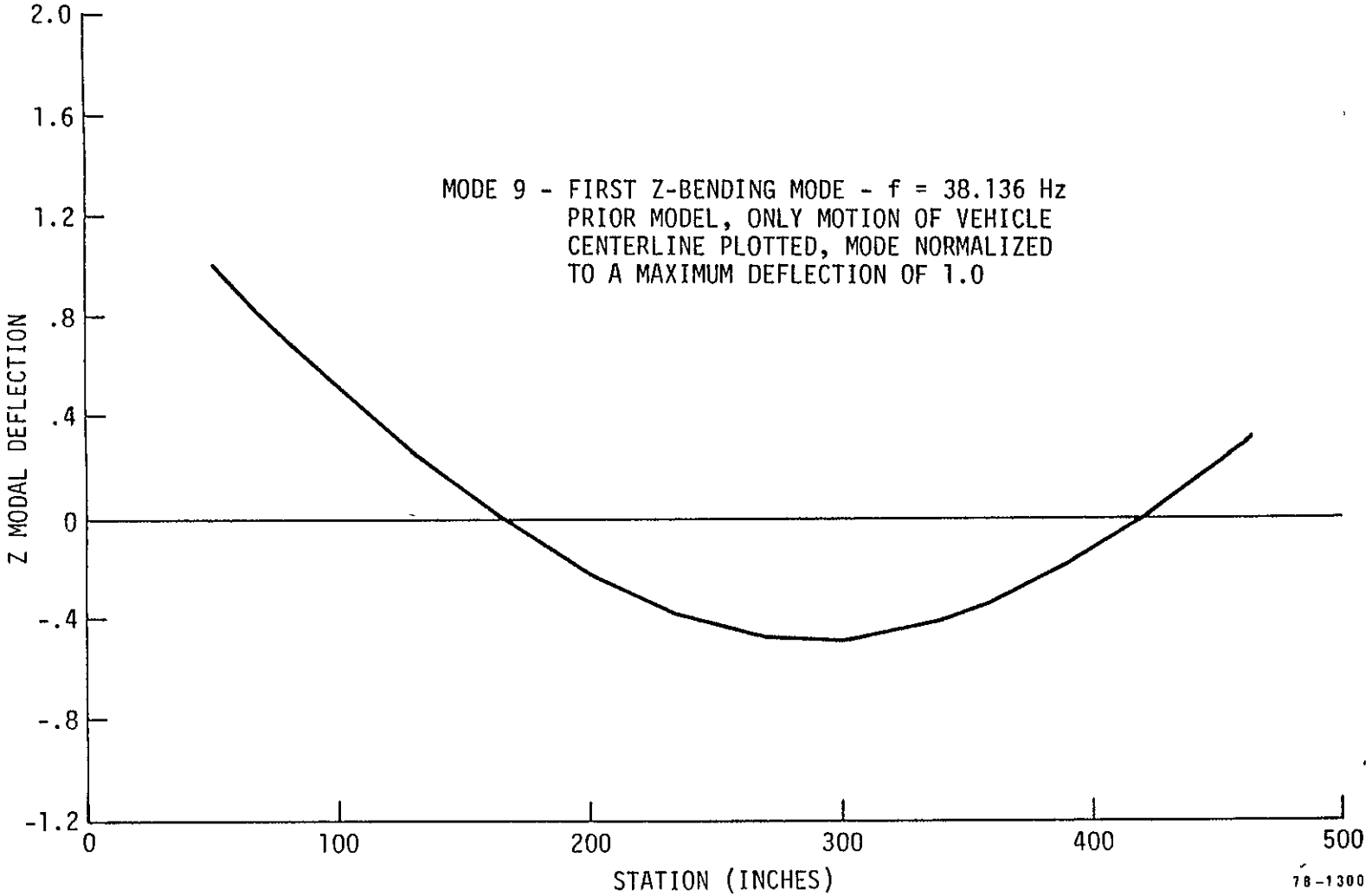

Figure 3-3. SRB Prior Model Mode - End-of-Action Time

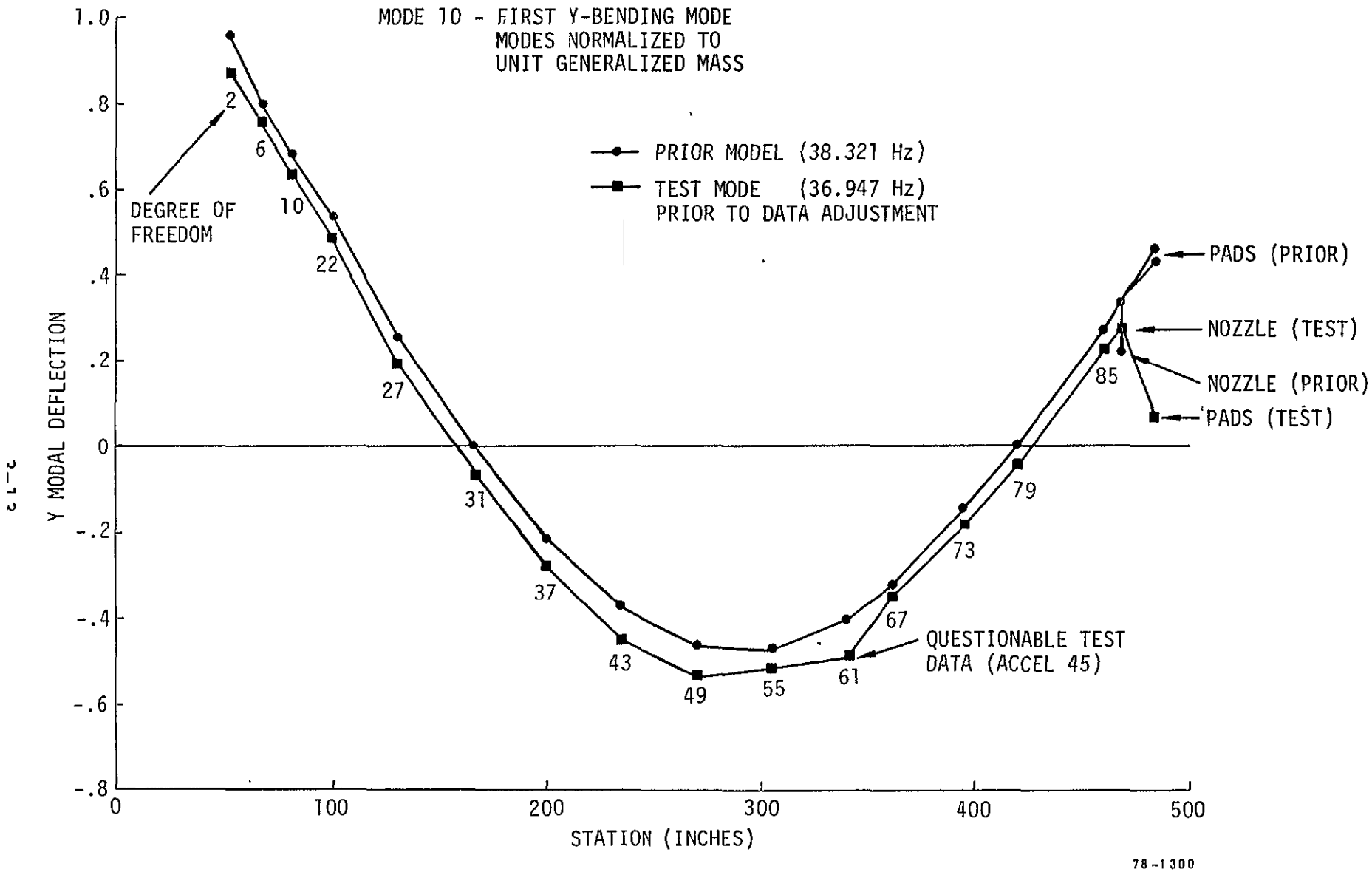

Figure 3-4. SRB Prior Model and Test Mode - End-of-Action Time

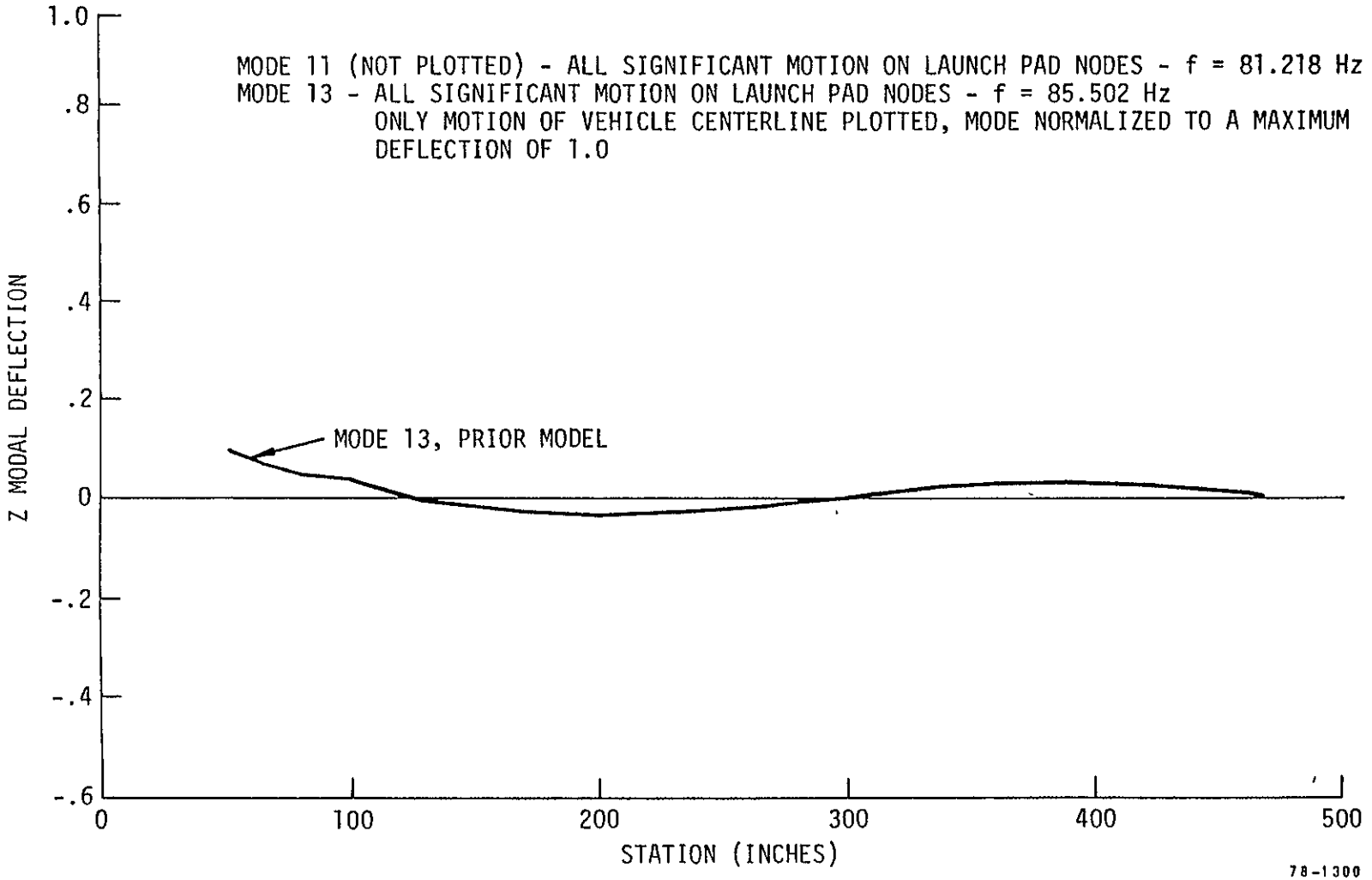

Figure 3-5. SRB Prior Model Mode - End-of-Action Time

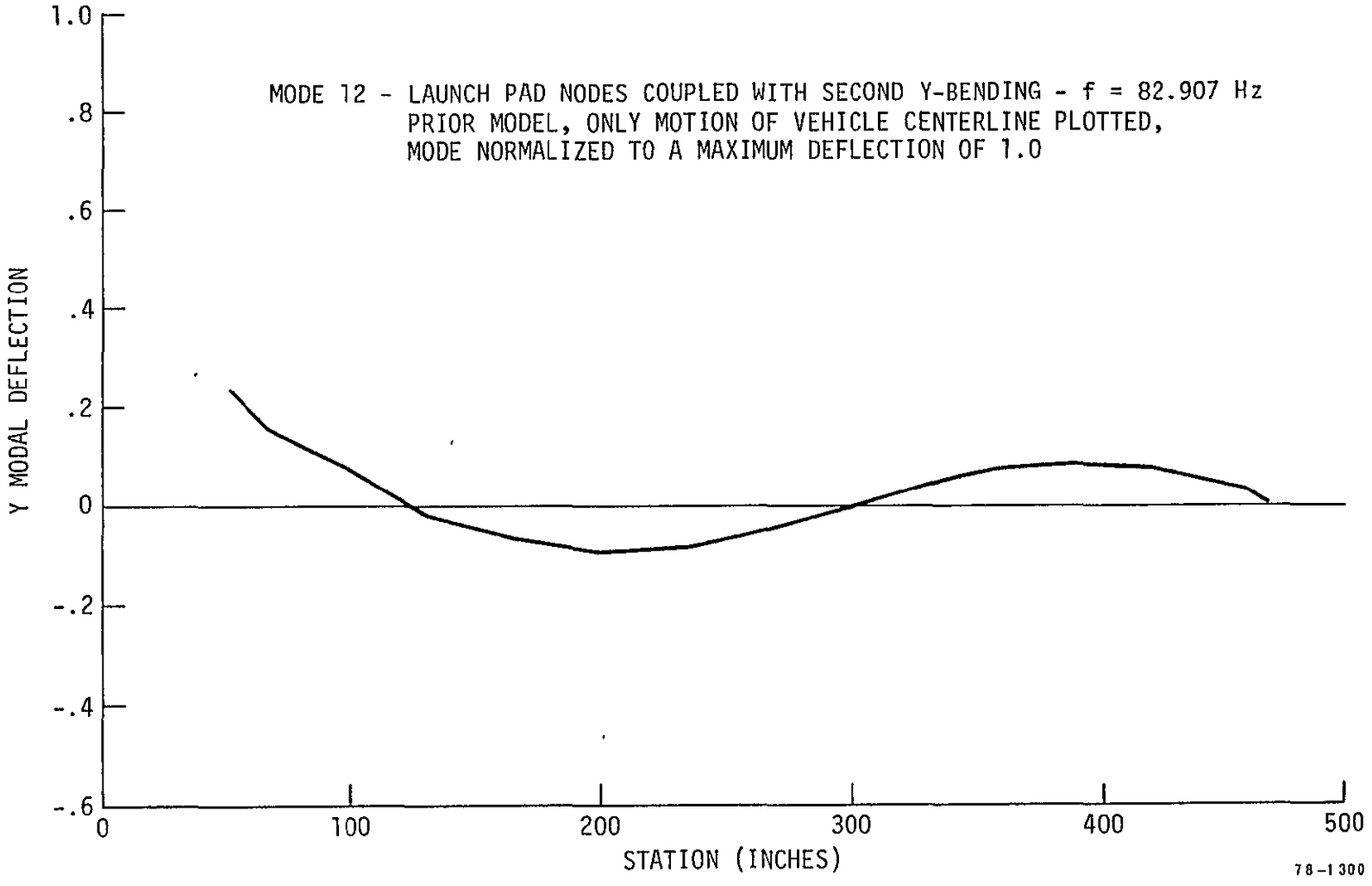

Figure 3-6. SRB Prior Model Mode - End-of-Action Time

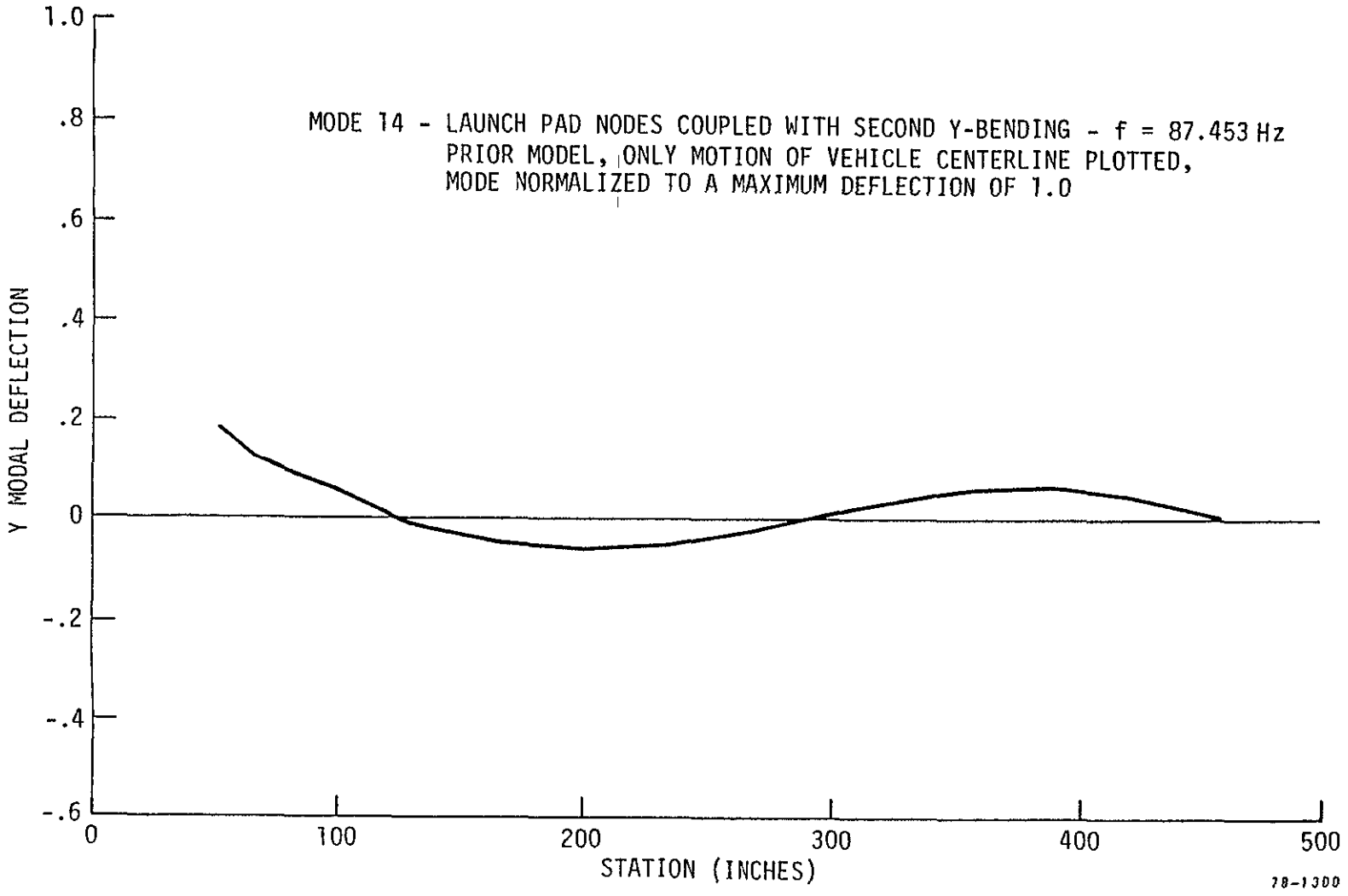

Figure 3-7. SRB Prior Model Mode - End-of-Action Time

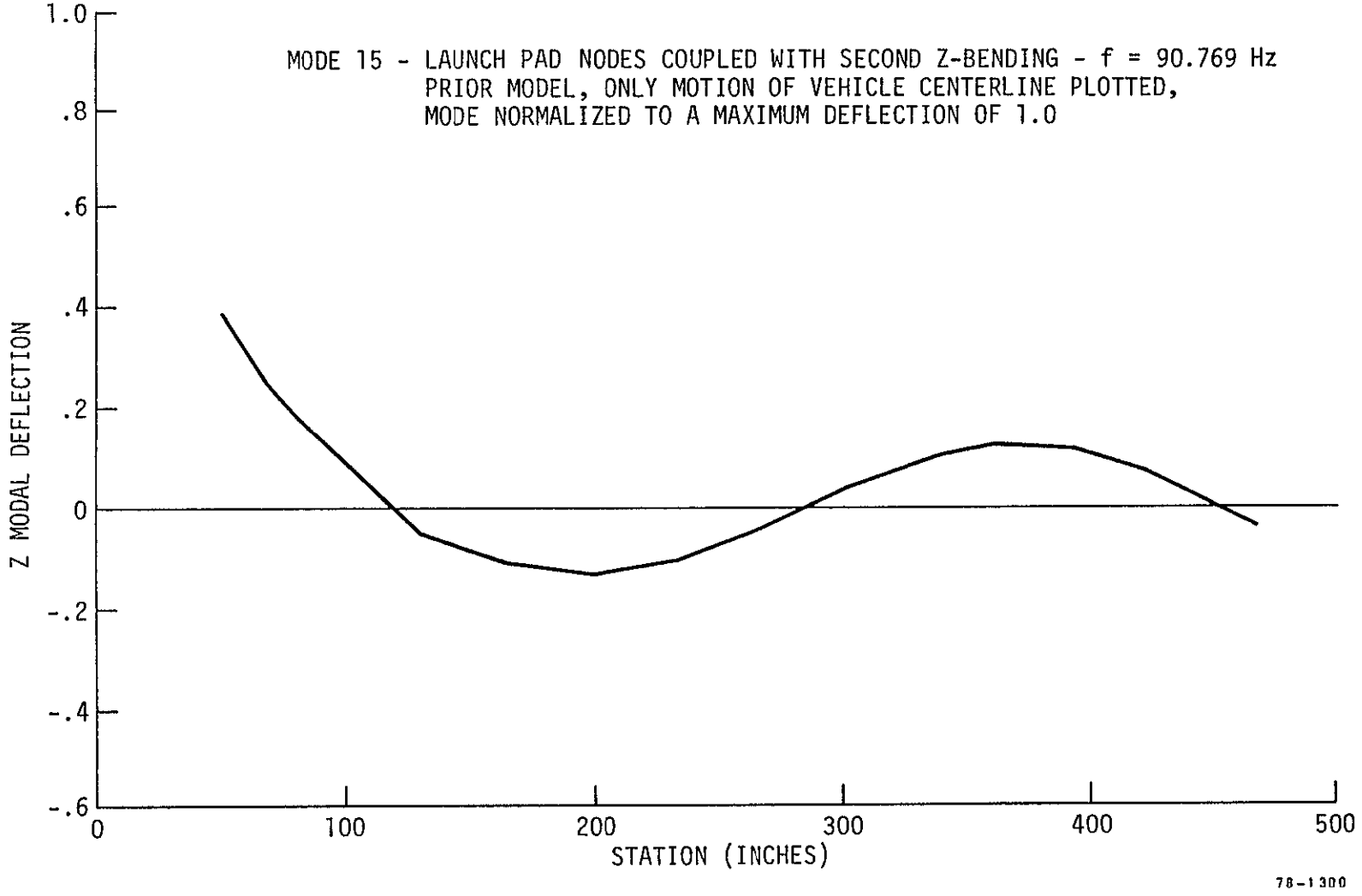

Figure 3-8. SRB Prior Model Mode - End-of-Action Time

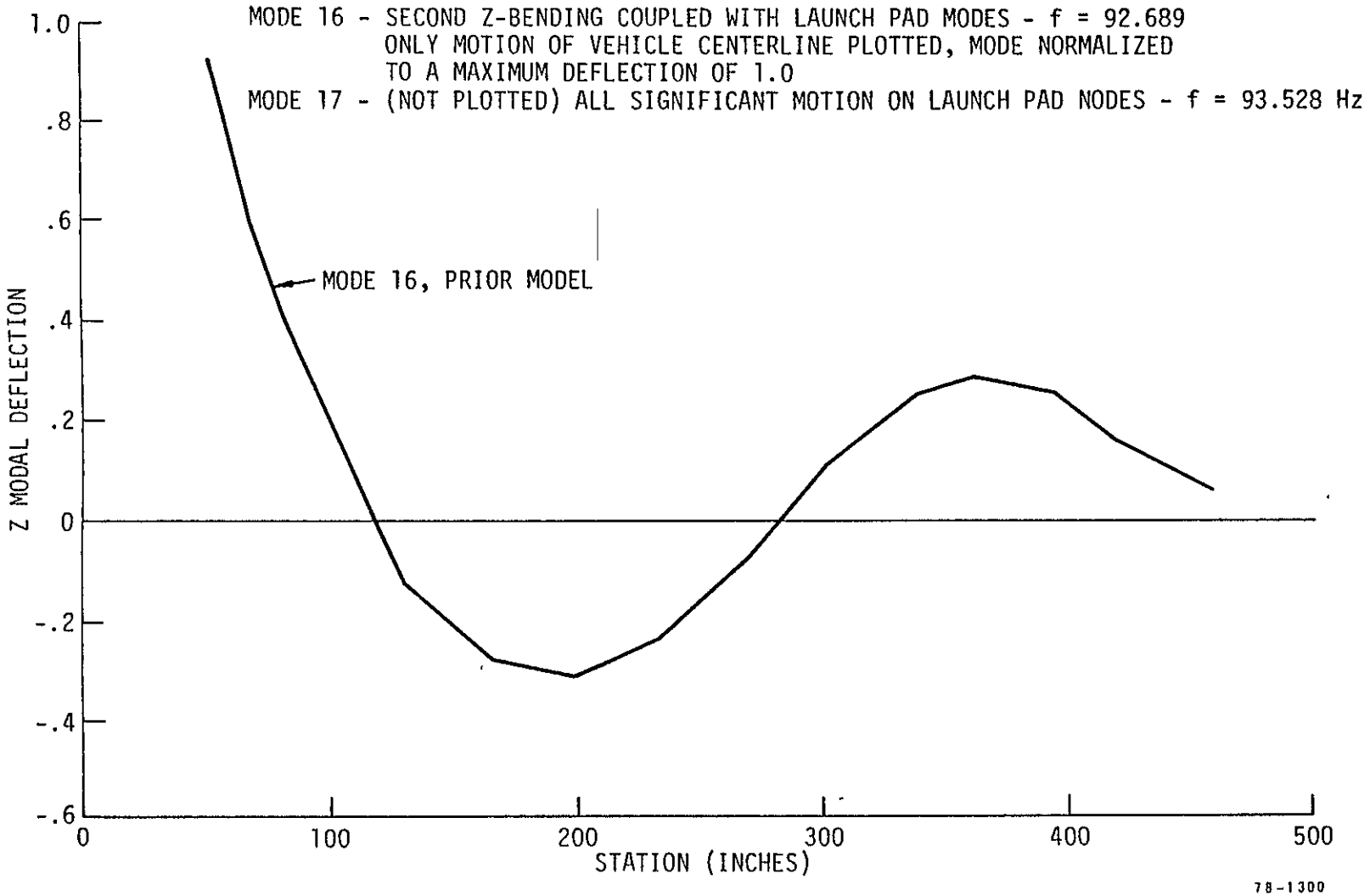

Figure 3-9. SRB Prior Model Mode - End-of-Action Time

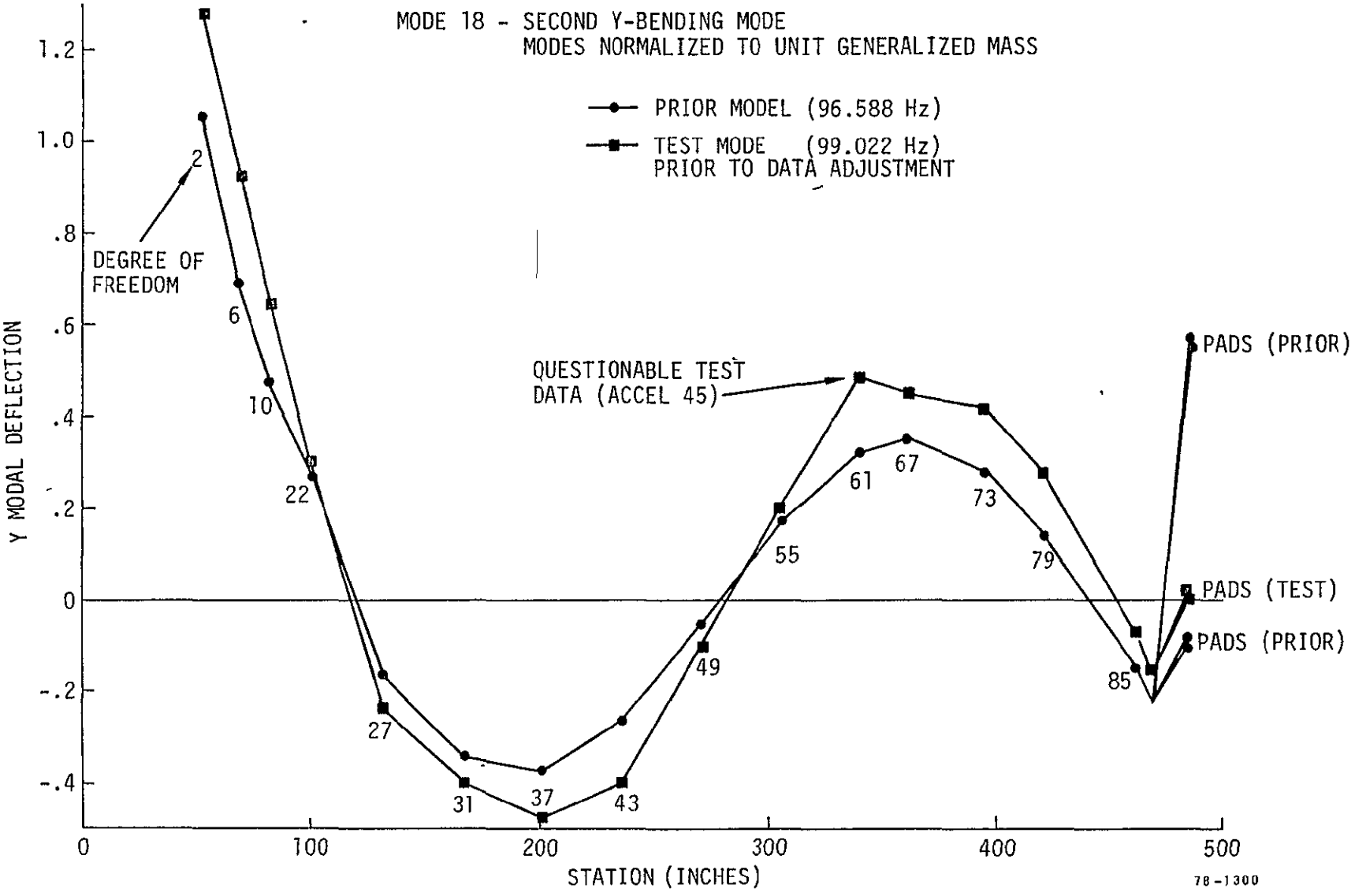

Figure 3-10. SRB Prior Model and Test Mode - End-of-Action Time

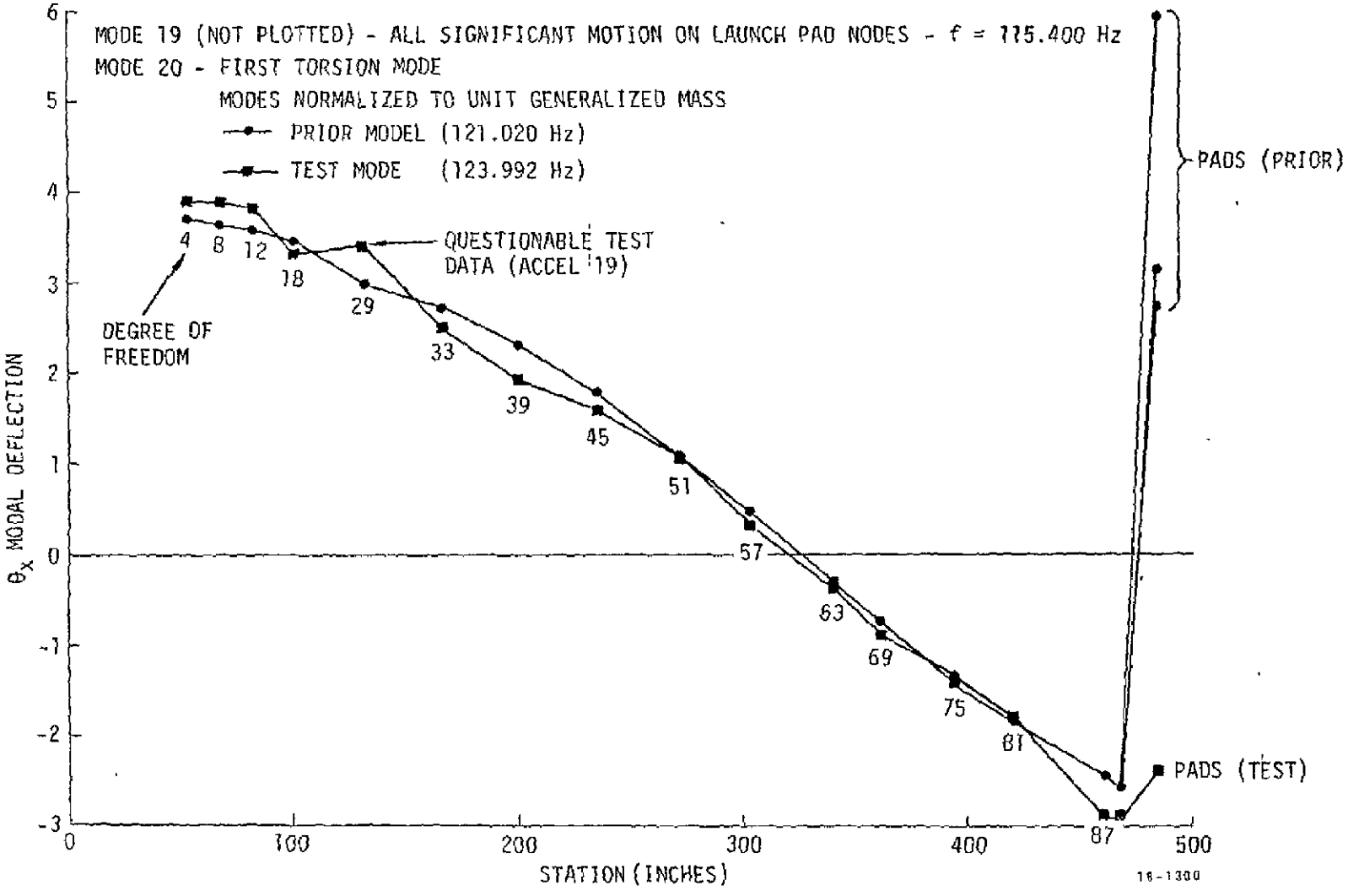

Figure 3-11. SRB Prior Model Mode and Test Mode - End-of-Action Time

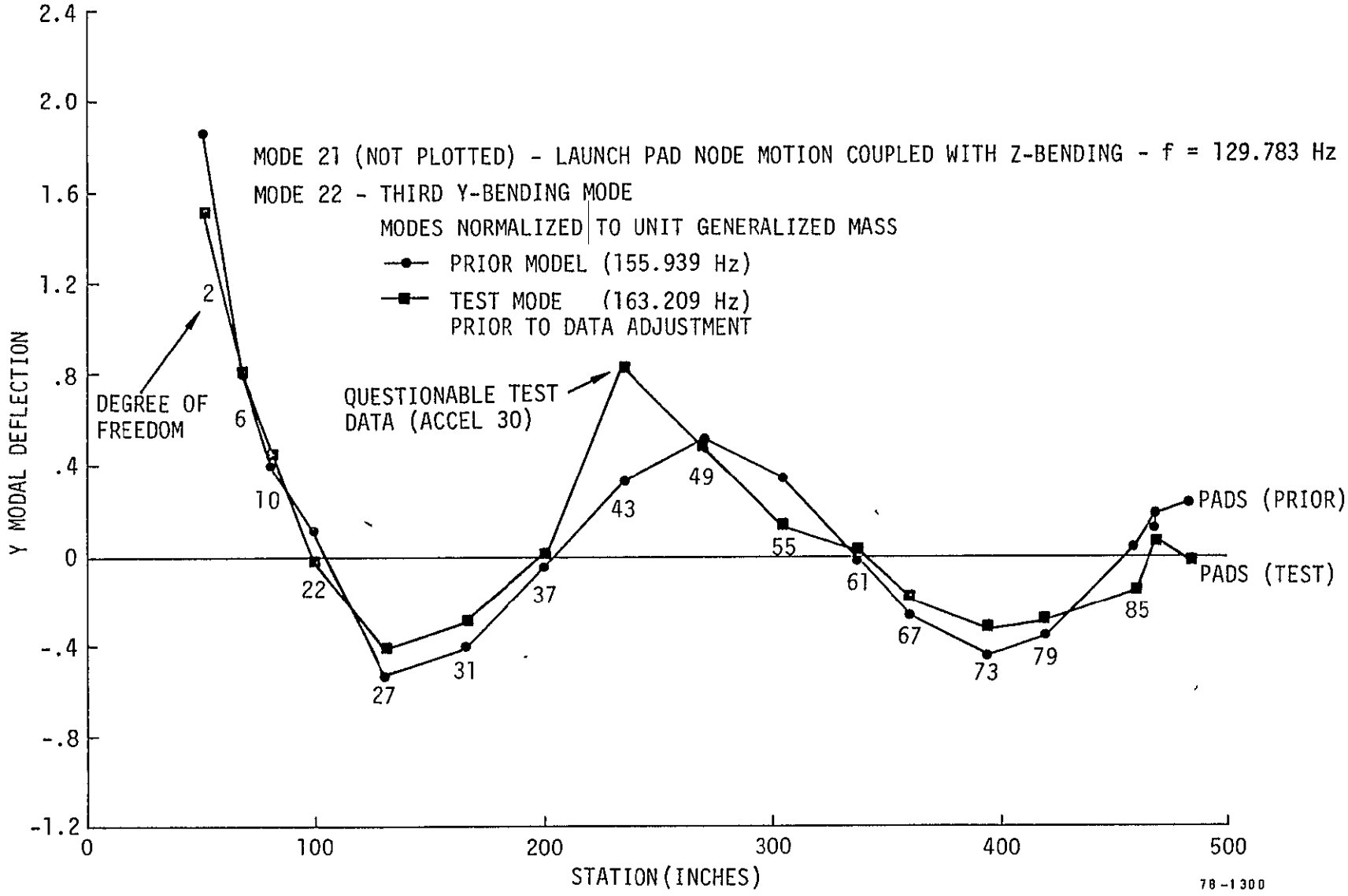

Figure 3-12. SRB Prior Model and Test Mode - End-of-Action Time

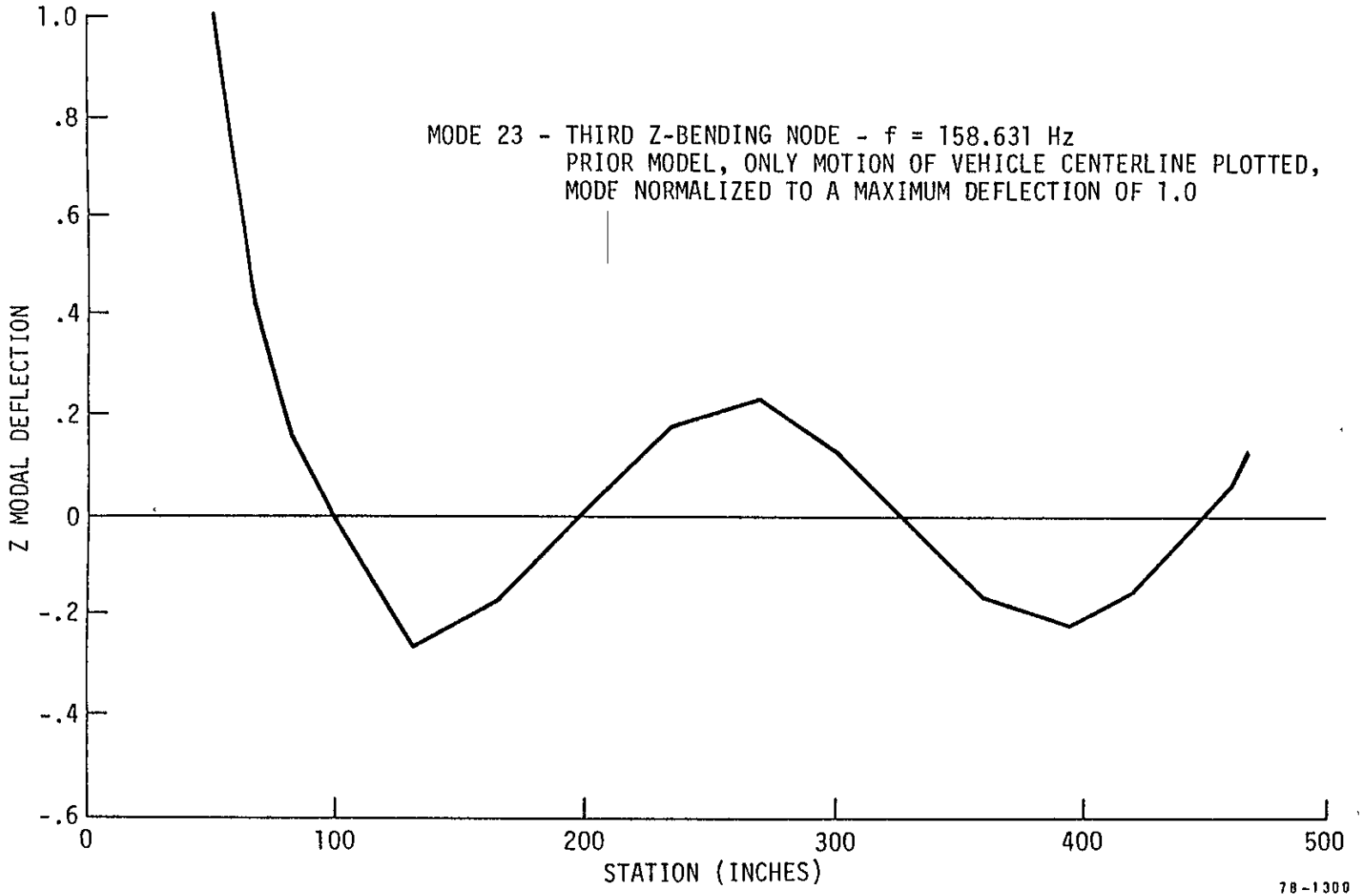

Figure 3-13. SRB Prior Model Mode - End-of-Action Time

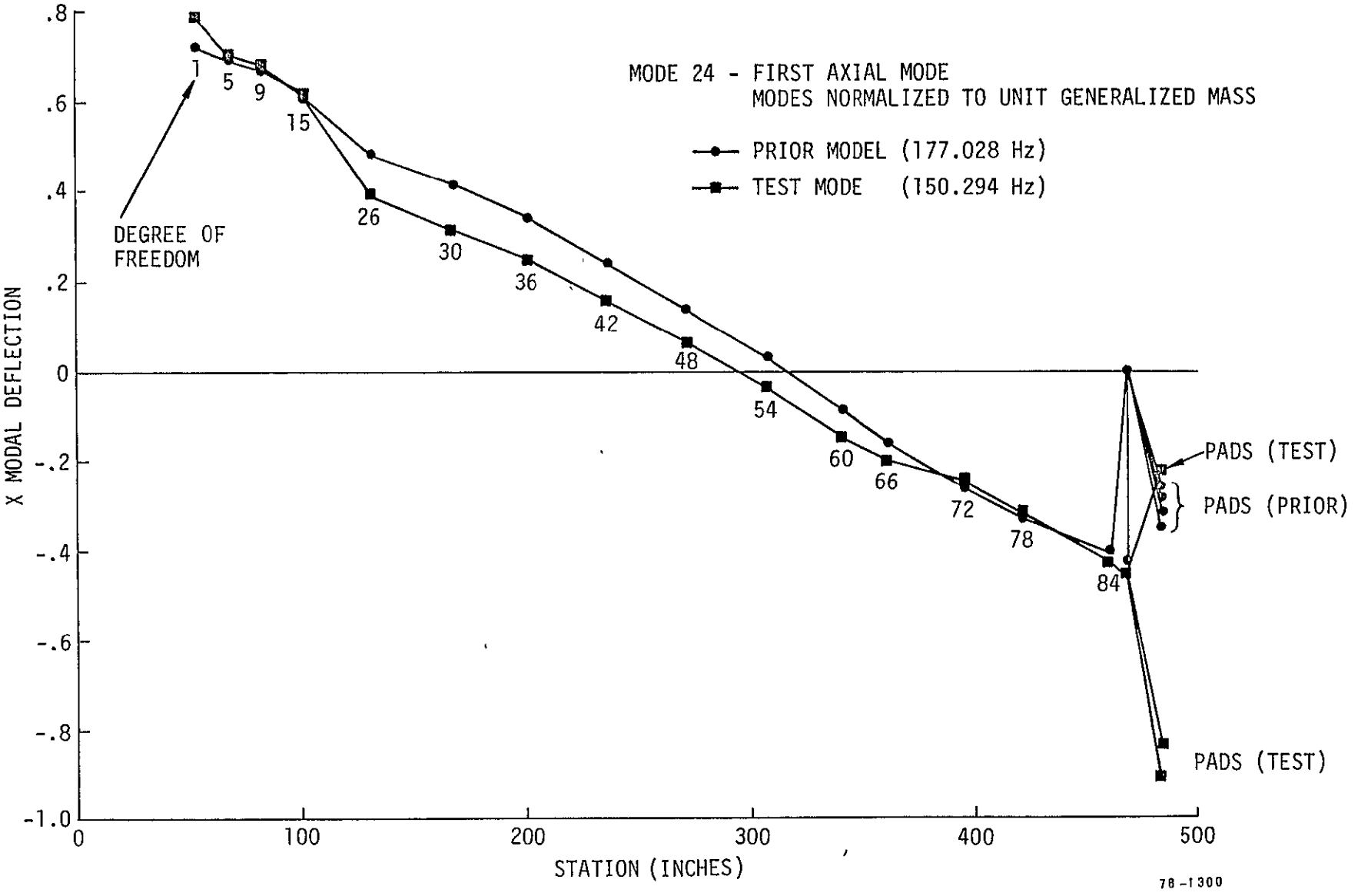

Figure 3-14. SRB Prior Model and Test Mode - End-of-Action Time

instrumentation list for these tests is presented in Reference [5]. The test data used for this exercise were taken from Reference [6]. Only resonant dwell data are available. Some of the test modes are shown in Figures 3-4, 3-10, 3-11, 3-12, and 3-14.

There were 111 accelerometers mounted on the test article, but only 85 of them are applicable to the beam modes being used for this parameter identification problem. At each resonant frequency, five pieces of information were recorded for each accelerometer:

Peak acceleration (G)
Coincident response (G/lb)
Quadrature response (G/lb)
Phase (degrees)
Reference shaker

The applicable accelerometers are numbered consecutively from 1 to 85. Twenty shakers were used to excite the vehicle.

The analytic model actually used by Rockwell for test correlation reflects a Guyan reduction to only 78 active DOF. Although the transformation from the accelerometer coordinates to the 78 DOF model was available, the mass and stiffness matrices for that model were not. Consequently, we developed our own transformation from the accelerometer coordinates to the 121 DOF model. The transformation is shown in Appendix 2.

A similar scheme was used to convert the shaker forces to generalized forces. The force transformation which we developed is shown in Appendix 2. The 20 shakers provide a maximum of

14 generalized forces. The shaker orientations given in Reference [6] were found to be inconsistent with the actual test configuration. This became apparent when the calculated test response was found to be grossly different from the measured response. The correct orientations were subsequently provided by Rockwell and are reflected in the transformation, as are other changes discussed below.

All of the test modes were at first assumed to be free-free modes directly comparable to the analytical model. However, a comparison of the analytical and test modes as is done in Figure 3-4 shows cause for concern. The first Y-bending mode is particularly graphic.

For free-free modes, linear momentum must be conserved. But for the first Y-bending mode (Figure 3-4) this can not be true for both the analytical and test modes since one is entirely shifted from the other. This anomaly was quantified by evaluating the linear momentum for all eight modes. The results are shown in Table 3-4. The significance of the value shown for the test modes is apparent when one recalls that the modes have been normalized to a generalized mass of one.

$$\sum M_i \phi_i^2 = 1.0$$

Possible reasons for this discrepancy were investigated; however, no explanation was found. The effect of the suspension system has been checked. But if the rigid body suspension modes as reported in Reference [7] are any indication, the stiffness of the suspension system is so low as to have virtually no influence on the vehicle modes.

Table 3-4. Quarter-Scale SRB: Modal Momentum Computed from Test Modes*

MODE DESCRIPTION	x-MOMENTUM		y-MOMENTUM		z-MOMENTUM	
	ORIGINAL	ADJUSTED†	ORIGINAL	ADJUSTED	ORIGINAL	ADJUSTED
FIRST Y-BENDING	- 009	- 009	-.391	-.375	031	.032
FIRST Z-BENDING	011	.011	.226	.132	.287	- 401
SECOND Z-BENDING	- 010	-.010	-.066	-.066	.160	.160
SECOND Y-BENDING	- 005	- 005	-.180	-.159	.095	096
FIRST TORSION	-.014	-.014	.167	.232	- 095	- 039
FIRST AXIAL	- 338	-.338	.133	133	- 106	-.106
THIRD Z-BENDING	-.026	-.026	.050	.050	-.090	-.090
THIRD Y-BENDING	-.045	-.051	-.197	-.024	- 042	- 048

*All analytic modes have "zero" momentum

†Accelerometer data such as those indicated for accelerometer numbers 45 and 30 in Figures 3-4, 3-10 and 3-12 were adjusted so as to be consistent with the rest of the mode shape. Momentum calculations which incorporate these adjustments are shown for comparison with those obtained from the original data provided.

The mode plots (Figures 3-4, 3-10, and 3-12) also reveal some questionable test points

- accelerometer 19 (first Z-bending and torsion modes)
- accelerometer 45 (first and second Y-bending modes)
- accelerometer 30 (third Y-bending mode).

For the third Y-bending mode, the erroneous data point has a large effect on the First Order Correction although it can be disregarded for the basic estimation procedure.

Several adjustments were made in the test data to remove some of the above anomalies. These included changing the "recorded" accelerations at the three locations described above to be consistent with the mode shape being measured. In these instances, the recorded values are totally out of line with both the adjacent accelerometer readings and the mode shape being measured. In addition, the phases of four shakers were reversed based on our inability to generate the measured responses using the reported shaker forces. The revised test modes now produce the measured responses when excited with the revised test forces, using the damping reported herein.

3.4 First Order Correction

The First Order Correction was applied to the SRB using FOCOR. The modified generalized mass and generalized stiffness matrices resulting from this procedure are shown in Tables 3-5 and 3-6. The original matrices were diagonal with unity for the mass and ω_o^2 for the stiffness. Of special interest is the cross-orthogonality matrix (Equation 16),

$$[\phi_{anal}]^t [M_{anal}] [\phi_{test}],$$

Table 3-5. Quarter-Scale SRB: FOC Generalized Stiffness Matrix
$[k] = [\omega_o^2] + [\Delta k]$

FIRST Y	65668							
FIRST Z	-6555	72296						
SECOND Z	-3434	4039	674548			SYMMETRIC		
SECOND Y	3796	17430	-113502	574188				
FIRST TORSION	1066	-9098	13080	-19760	813982.			
FIRST AXIAL	10779	5489	-13718.	-5419	-57691	1147156		
THIRD Z	-18217	-59438	-32881.	37333	14780.	14729	1528176	
THIRD Y	26178	04066	24651	-27083	27108	35800	78738	1308491

Table 3-6. Quarter-Scale SRB: FOC Generalized Mass Matrix
$[m] = [I] + [\Delta m]$

FIRST Y	1.2031							
FIRST Z	-0 1120	1 2965						
SECOND Z	-0 0055	0 0270	1 8833			SYMMETRIC		
SECOND Y	-0.0457	0 0167	-0.3282	1.5080				
FIRST TORSION	0.0320	0.0167	0 0216	-0 0534	1.3581			
FIRST AXIAL	0.0588	0 0420	-0 0304	-0 0313	-0 0843	1.2064		
THIRD Z	-0 0057	0 0624	-0 0421	0 0357	0 0022	0 0040	1 5582	
THIRD Y	0 1071	-0 0047	0 0311	-0 0373	0 0339	-0 0251	0 0802	1 2676

because it is a quantitative measure of how well the prior model describes the test configuration. This matrix is shown in Table 3-7. Except forthe second Z-bending modes, the test and analytic modes agree to about .70 - .90. The worst frequency match is on the axial mode where there is a 20 percent difference in frequency.

The "corrected" generalized mass and stiffness matrices were used to generate "corrected" modes and frequencies. The "corrected" frequencies are shown in Table 3-8.

In most cases the "corrected" mode is closer to the prior model mode than to the test mode. It must be recognized that all three versions are normalized with the prior-model mass matrix so any difference in total weight between test and analysis is not considered.

3.5 Phase I Model Estimation - Example One

This example uses the 12 analytic bending modes between 38 and 130 Hertz as the prior modes (Table 3-3) and the 4 test data-sets (excluding torsion) identified in the same frequency band. Three cases were investigated: the first used the prior model directly while the second and third applied the First Order Correction prior to executing the estimation program. These runs are summarized in Tables 3-9 and 3-10.

The same 32 test data points were used for all cases. These data consist of the measured total response (deflection) at seven stations along the length of the vehicle. Eight data points were used at each of the four frequencies: seven in the primary direction of motion and one in the perpendicular lateral direction. These data are given in Appendix 2. The

Table 3-7. Cross Orthogonality $[\phi_{anal}]^t[M_{anal}]\,[\phi_{test}]$

ANALYTICAL MODES ↓ / TEST MODES → FREQUENCY Hz	36.9472	37.4168	97.4560	99.0215	123.9922	150.2935	157.0450	163.2094
38.8214	0.8984	0.2264	-0.0056	0.0664	-0.0335	-0.0526	-0.0134	-0.0850
38.1362	-0.1144	0.8517	-0.0182	0.0362	-0.0361	-0.0394	-0.1297	0.0005
92.6887	0.0111	-0.0088	0.5583	0.2531	0.0024	0.0266	0.0137	-0.0083
96.5884	-0.0208	-0.0530	0.0751	0.7460	0.0530	0.0384	0.0029	0.0148
121.0205 FIRST TORSION	0.0015	0.0193	-0.0240	0.0004	0.8210	0.0708	0.0303	-0.0142
177.0280 FIRST AXIAL	-0.0062	-0.0026	0.0038	-0.0071	0.0136	0.8978	-0.0440	-0.2159
158.6306	0.0191	0.0673	0.0284	-0.0387	-0.0325	0.0399	0.7209	-0.0532
155.9386	-0.0221	0.0042	-0.0227	-0.0225	-0.0197	0.2410	-0.0269	0.8662

MODES NORMALIZED FOR UNIT GENERALIZED MASS:

$[\phi]^t\,[M_{anal}]\,[\phi] = [I]$

Table 3-8. Quarter-Scale SRB: Comparison of Modal Frequencies

MODE DESCRIPTION	PRIOR* MODEL	FIRST ORDER CORRECTION**	TEST
FIRST Y-BENDING	38.321	36.295	36.947
FIRST Z-BENDING	38.136	37.241	37.417
SECOND Z-BENDING	92.689	95.176	97.456
SECOND Y-BENDING	96.588	98.562	99.022
FIRST TORSION	121.020	123.280	123.992
FIRST AXIAL	177.028	153.459	150.294
THIRD Z-BENDING	158.631	158.405	157.045
THIRD Y-BENDING	155.939	164.179	163.209

* PRIOR MODEL WAS A MODEL OF FLIGHT HARDWARE, NOT A MODEL OF TEST CONFIGURATION. THE PRIOR MODEL FREQUENCIES LISTED ARE THOSE ESTIMATED TO BE MOST COMPARABLE TO THE TEST MODES. HOWEVER, THE PRIOR MODEL HAS 10 ADDITIONAL LOW FREQUENCY MODES WHICH EXTENSIVELY COUPLE WITH THE SECOND Y AND Z BENDING MODES. (SEE TEXT)

**FIRST ORDER CORRECTION IS BASED ON ADJUSTED DATA.

Table 3-9. Goodness of Fit for Quarter-Scale SRB Parameter Identification Using 4 Test Data-Sets

PARAMETER	PRIOR MODEL	WITH FIRST ORDER CORREC-TION	ITER ONE	ITER TWO	ITER THREE	ITER FOUR	ITER FIVE	ITER. SIX	
CASE A WITHOUT FIRST ORDER CORRECTION; ESTIMATE DIAGONAL PLUS FIRST OFF-DIAGONAL TERMS OF [m] & [k]									
OBJECT FUNCTION	3954	--	2802	2754	2640	2624			
RMS DIFFERENCE (ALL E-2)*	8445	--	8090	.6086	.6004	.5981			CONVERGED, STEP SIZE SMALLER THAN CUTOFF
MEAN DIFFERENCE (ALL E-2)	.5719	--	.5315	.4024	.4024	4014			
MAXIMUM PARAMETER CHANGE (PERCENT OF STANDARD DEVIATION	--	--	20%	20%	5%	1.25%			
CASE B WITH FIRST ORDER CORRECTION; ESTIMATE DIAGONAL PLUS FIRST OFF-DIAGONAL TERMS OF [m] & [k]									
OBJECT FUNCTION	3954	2554	2068	1813	1720	1682	1658	1659	
RMS DIFFERENCE (ALL E-2)	.8445	.4558	4305	.4183	.4089	.4020	.3952	--	CONVERGED, STEP SIZE SMALLER THAN CUTOFF
MEAN DIFFERENCE (ALL E-2)	.5719	.3012	.2780	.2701	.2670	.2665	.2659	--	
MAXIMUM PARAMETER CHANGE (PERCENT OF STANDARD DEVIATION)	--	--	20%	5%	5%	5%	5%	.078%	
CASE C WITH FIRST ORDER CORRECTION; ESTIMATE DIAGONAL PLUS FIRST AND SECOND OFF-DIAGONAL TERMS OF [m] & [k]									
OBJECT FUNCTION	3954	2554	2131	2035	2006	1995	1995		
RMS DIFFERENCE (ALL E-2)	.8445	.4558	4259	4129	.4107	4019	4014		CONVERGED, STEP SIZE SMALLER THAN CUTOFF
MEAN DIFFERENCE (ALL E-2)	.5719	.3012	.2808	2775	2766	.2749	.2749		
MAXIMUM PARAMETER CHANGE (PERCENT OF STANDARD DEVIATION)	--	--	30%	7.5%	1 875%	7 5%	.47%		

*E-2 means $\times 10^{-2}$

Table 3-10. Modal Frequencies for Quarter-Scale SRB Parameter Identification Using 4 Test Data-Sets

MODE* INDEX	FREQUENCY (Hz)					
	PRIOR MODEL	A EXAMPLE WITHOUT FIRST ORDER CORRECTION: DIAGONAL & FIRST	WITH FIRST ORDER CORRECTION	B EXAMPLE WITH FIRST ORDER CORRECTION: DIAGONAL & FIRST	C EXAMPLE WITH FIRST ORDER CORRECTION: DIAGONAL & FIRST & SECOND	TEST MODES
(1)	38.32	37.23	37.03	36.97	36.97	36.95
(2)	38.14	38.09	37.50	37.54	37.54	37.32
3	81.22	81.19	81.22	81.21	81.21	--
4	82.91	82.76	82.91	82.94	82.86	--
5	85.50	85.51	85.50	85.50	85.49	--
6	87.45	86.33	87.45	87.38	87.29	--
7	90.77	88.64	90.77	89.83	89.22	--
(8)	92.69	95.30	93.53 (MODE 9)	91.04	90.48	97.46
9	93.53	98.26	95.23 (MODE 8)	97.42	97.81	
(10)	96.59	99.47	98.60	99.85	100.36	99.02
11	115.40	115.35	115.40	115.40	115.41	--
12	129.78	129.82	129.78	129.63	129.69	--

*Only circled modes used in First Order Correction.

points were selected to span the length of the vehicle and give the maximum signal-to-noise ratio (as measured by the coefficient of variation).

The object function (Table 3-9) is the function which the estimator is minimizing. It is defined as

$$F = \sum_{j=1}^{n} \frac{\left(u_{o_j} - u_j\right)^2}{S_{\varepsilon\varepsilon_j}} + \sum_{i=1}^{p} \frac{\left(r_{o_i} - r_i\right)^2}{S_{rr_i}} \qquad (25)$$

which is just a simplification of Equation 1 given that $S_{\varepsilon\varepsilon}$ and S_{rr} are diagonal matrices.

For two of the runs, the diagonal plus the first off-diagonal terms of the [m] and [k] matrices were estimated; in the third run the second off-diagonal terms were also estimated. For these examples the object function is dominated by the response because the S_{rr} were assigned large values indicative of a prior model with low confidence.

As shown in Table 3-9, the object function is reduced by 34 percent when the First Order Correction is not used and by 58 percent when it is. The First Order Correction alone provides a 36 percent reduction. The addition of the second off-diagonal terms did not improve the convergence; in fact, it made it slightly worse.

When the First Order Correction methodology is applied, a one-to-one correspondence must be assumed between a test mode and an analytic mode. This correspondence is sometimes not clear, particularly when the analytic model has modes which

do not appear in the test or are not measured during the test. This was the case here because the eight pad modes (Table 3, Reference [1]) were not recorded during the test. Since some of these pad modes are highly coupled with the second vehicle bending modes, it is not clear which analytic modes correspond to the measured second-bending modes. We chose modes 8 and 10 (as defined in Table 3-2) to perform the First Order Correction. In both cases described here, however, the estimator converged modes 9 and 10 to the test modes. The fact that the FOC may have been based on the wrong mode does not seem to have affected this result.

In the first two runs, the Estimator provides about a 35 percent reduction in the object function. The difference in the final result is the 35 percent improvement provided by the FOC. The modal frequencies are shown in Table 3-10. Notice that since only modes 1, 2, 8, and 10 are included in the FOC, only these modes are perturbed by the FOC. Notice also that the FOC frequencies are not the same as in the subsequent example (Section 3.6). Although the same FOC elements are used in both cases, only those related to the four selected prior-model modes are used in the perturbed [m] and [k] matrices.

Application of the FOC provides a much improved frequency match, for the modes selected, but the mode shapes are degraded:

MODE INDEX	$\frac{f_i - f_{test}}{f_{test}} \times 100\%$				
	PRIOR	FOC	W/O FOC	B	C
1	+3.72	+ .22	+ .76	+.05	+ .05
2	+1.92	+ .21	+1.79	+.30	+ .30
8/9	-4.89	-2.29	+ .82	-.04	+ .36
10	-2.46	-0.42	+ .45	+.84	+1.35

Application of the Estimator without the FOC results in an even greater improvement in the frequency match with significantly less degradation in the mode shape (i.e., G_1 closer to 1.0). Application of the Estimator following the FOC improves upon the FOC frequency match for most of the modes (but not always) and also brings the modal mass back toward 1.0. Application of both procedures results in a better fit than application of either individually. It is unclear, however, what effect the known problem with the test modes (i.e., momentum not conserved) has on the final result. The next two sections discuss in more detail the resulting mode shapes for Cases A and B.

First Y- and Z-Bending Modes

See Figure 3-3 for plots of the Z-mode and Figure 3-4 for the Y-mode. Figure 3-15 shows the modal orientation, and Figures 3-16A and B provide additional information.

The first Y-bending mode is at 38.32 Hz in the prior model and 36.95 Hz in the test. The analytic mode lies almost entirely in the Y-plane while the test mode has 10 percent component in +Z (Figure 3-15). When the Estimator is executed without the FOC, significant improvement is obtained in the frequency match with very little change in the mode shape. The FOC improves the frequency match (37.03 Hz) significantly, but rotates the mode in the wrong direction (Figure 3-15). Applying the Estimator further improves the frequency match (36.97 Hz) and rotates the mode back toward the test mode.

The first Z-bending mode is at 38.14 Hz in the prior model and 37.42 Hz in the test. The analytical mode lies almost

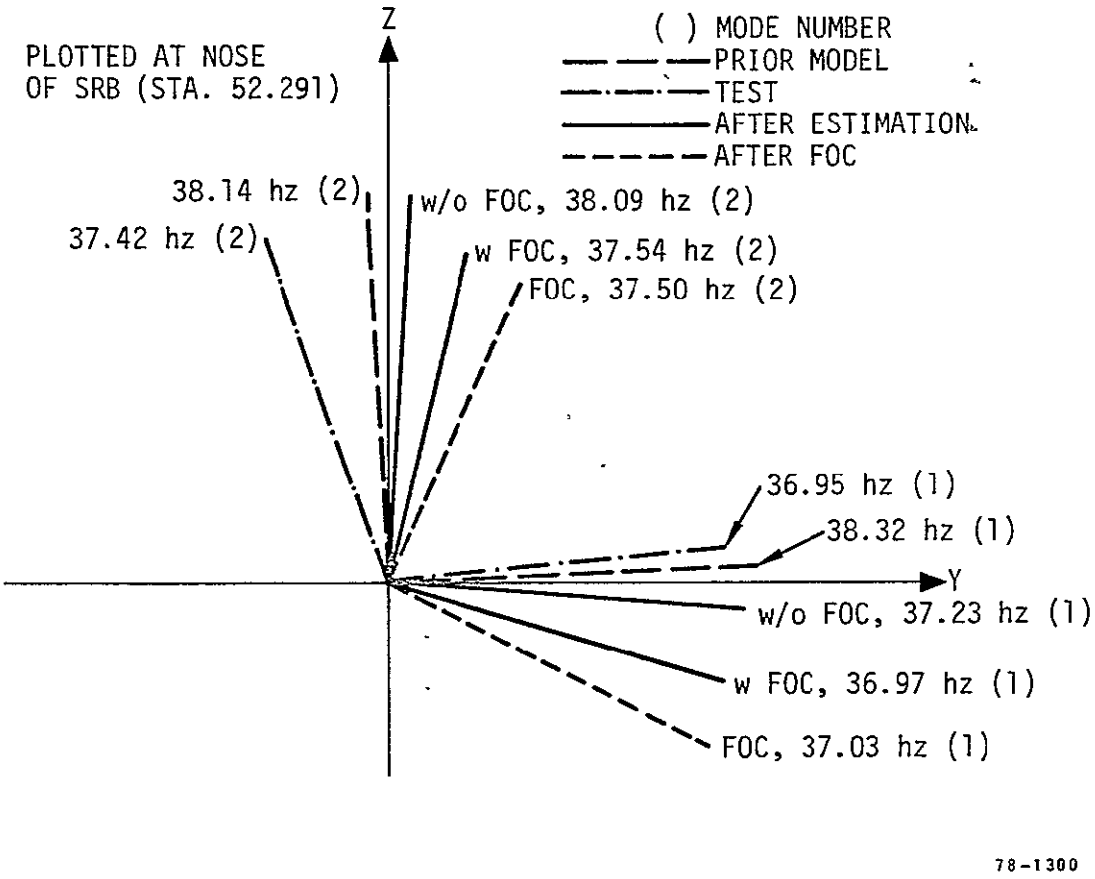

Figure 3-15. Modal Orientation with and without FOC, First Vehicle Bending Modes (Y- and Z-Planes)

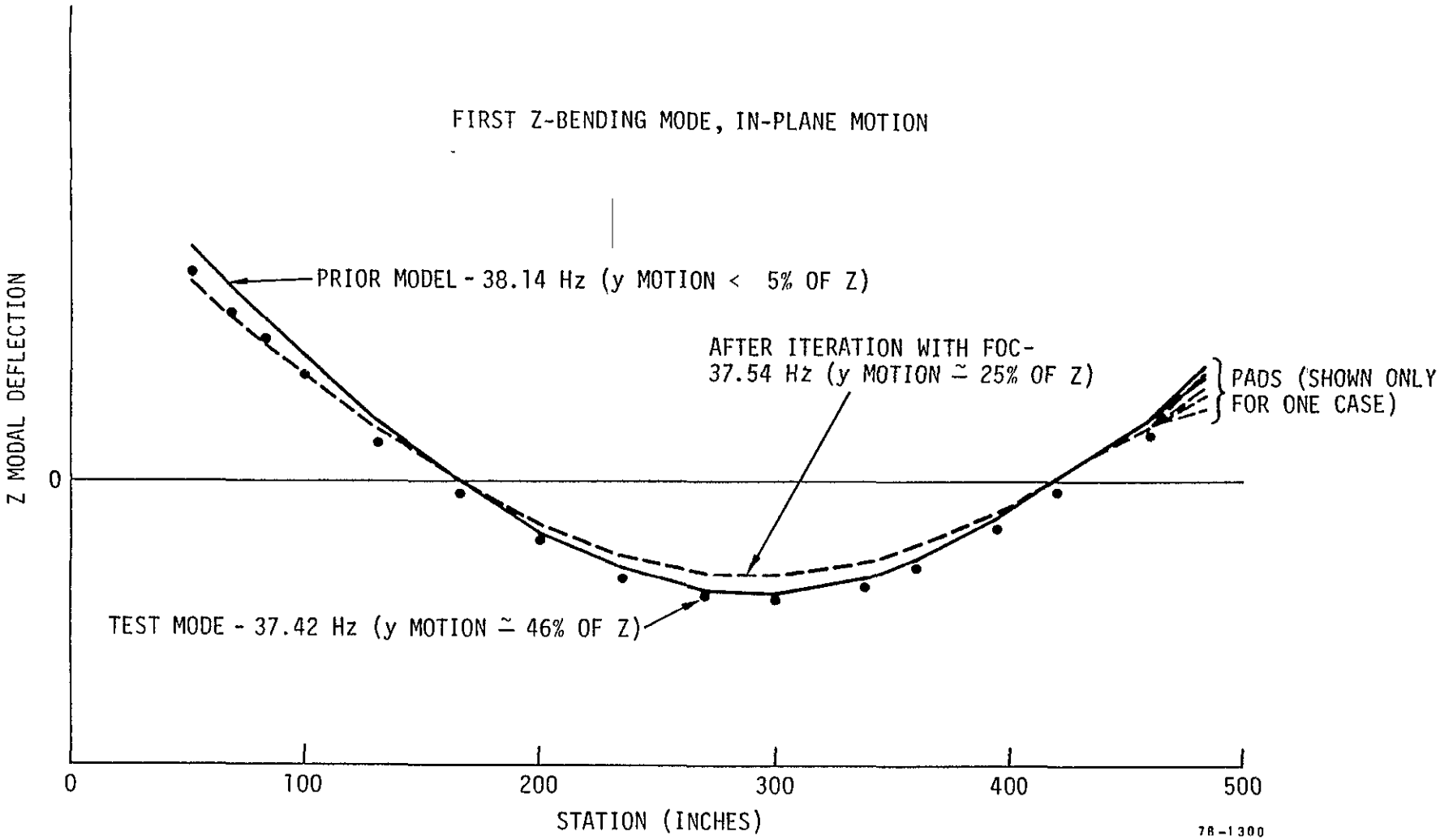

Figure 3-16A. Quarter-Scale SRB: System Identification with First Order Correction

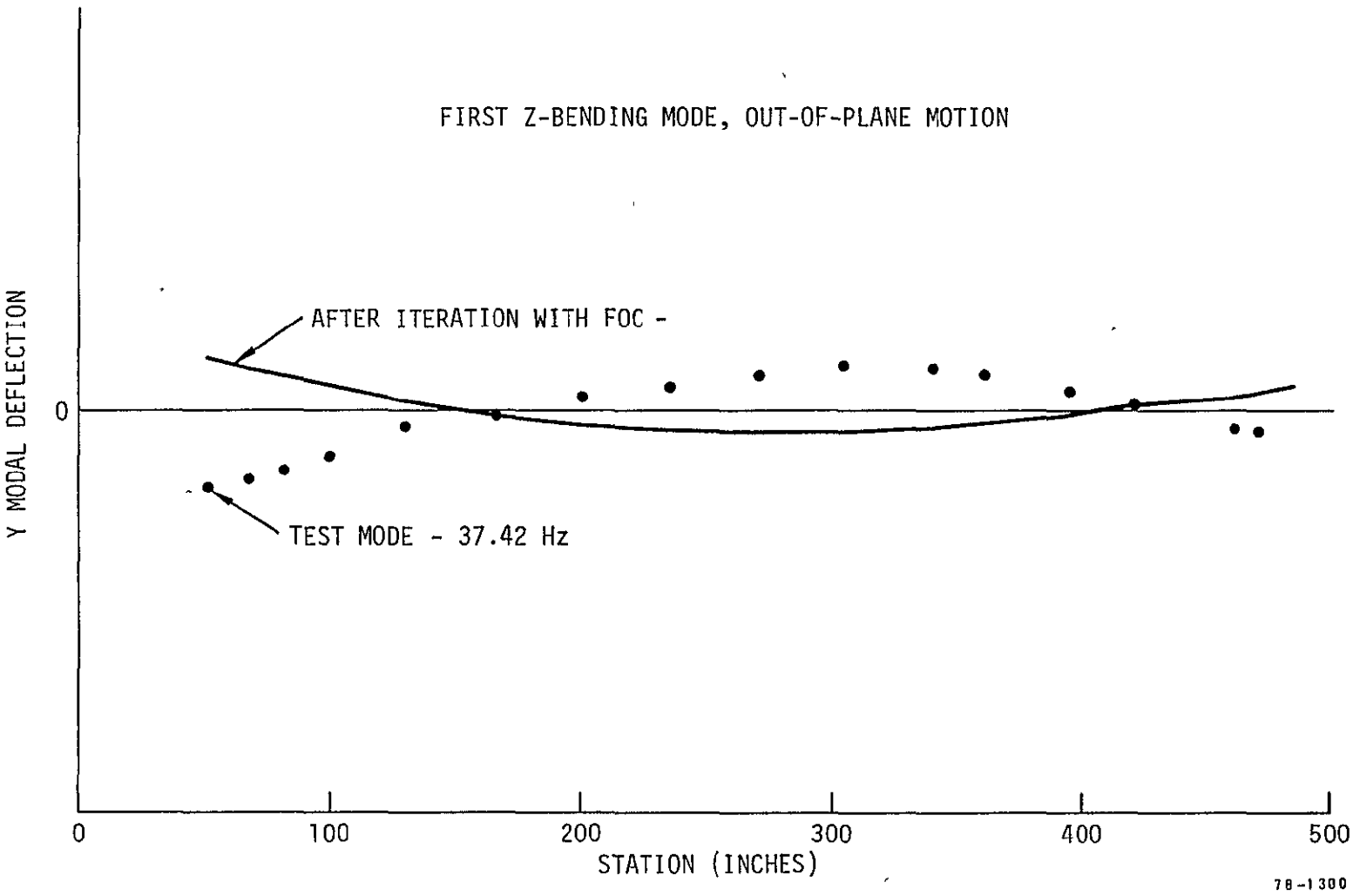

Figure 3-16B. Quarter-Scale SRB: System Identification with First Order Correction

entirely in the Z-plane while the test mode is slightly skewed, having 35 percent as much motion in the Y-plane as it does in Z. When the Estimator is executed without the FOC, very little change is made in the analytic frequency or mode. The FOC improves the frequency match (37.50 Hz) but rotates the mode towards plus Y instead of minus Y. The subsequently executed Estimator made very little change in the frequency (37.54 Hz), but it improved the mode shape by improving the Z-deflection match and decreasing the Y-deflection.

In the analytic model and all of the estimated models, the Y and Z modes lie in perpendicular planes. The test modes, however, do not exhibit such perfect perpendicularity.

Second Y- and Z-Bending Modes

The behavior of the Estimator and the model in this frequency regime is quite involved because of the large number of appendage modes coupled with the two vehicle modes. Perhaps the clearest picture is obtained if the behavior with and without the FOC are separately described. Remember that only two sets of test data are available to experimentally describe this frequency regime: one at 97.46 Hz (Z-bending) and one at 99.02 Hz (Y-bending). Figures 3-9 and 3-10 provide modal plots.

The prior analytical model has two vehicle "YZ-bending" modes at 92.69 and 93.53 Hz and one "Y-bending" mode at 96.59 Hz (Figure 3-17). The test modes are at 97.46 (Z-bending) and 99.03 Hz (Y-bending). The Estimator converges to modes at 95.30, 98.26, and 99.47 Hz. Unexpectedly, the mode closest in frequency to the test Y-mode is oriented most closely with the test Z-mode. Mode 9, the +Z-Y mode, has a significant

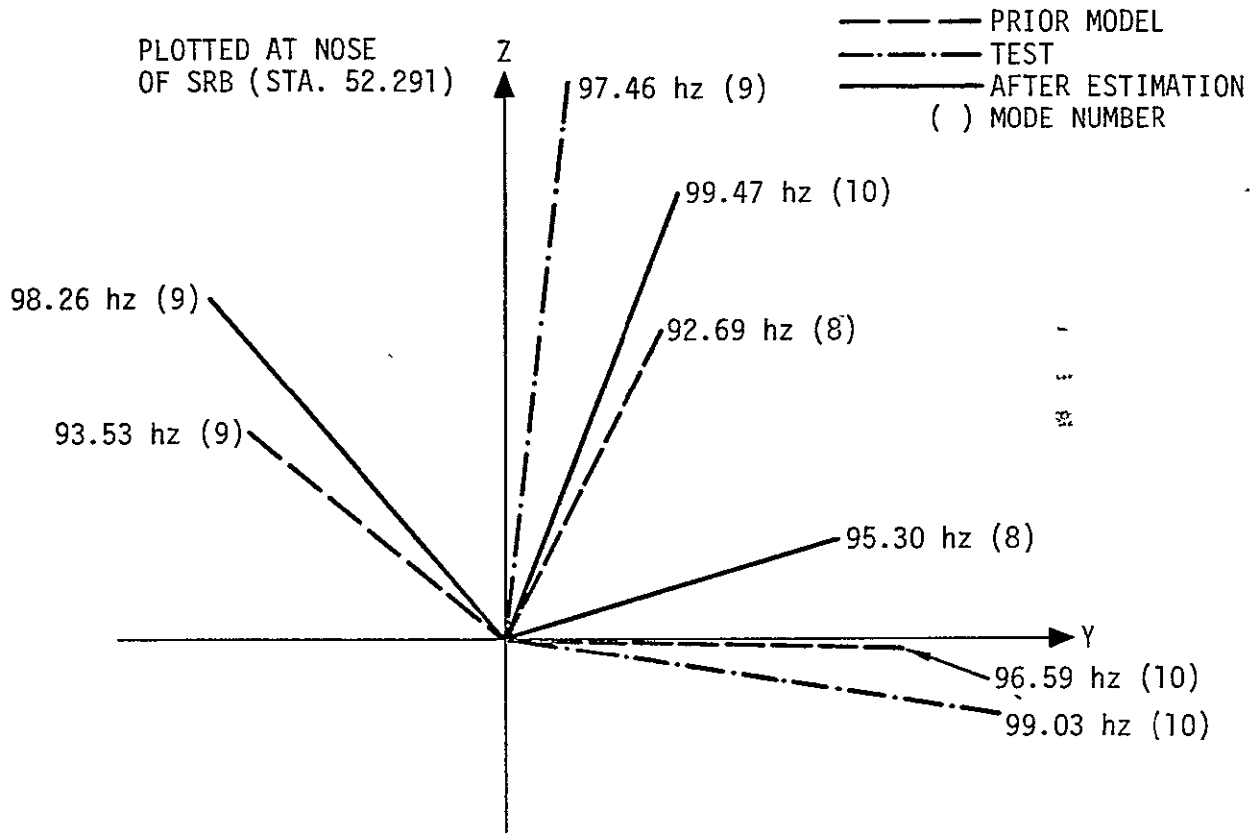

Figure 3-17. Modal Orientation without FOC, Second Vehicle Bending Modes (Y- and Z-Planes)

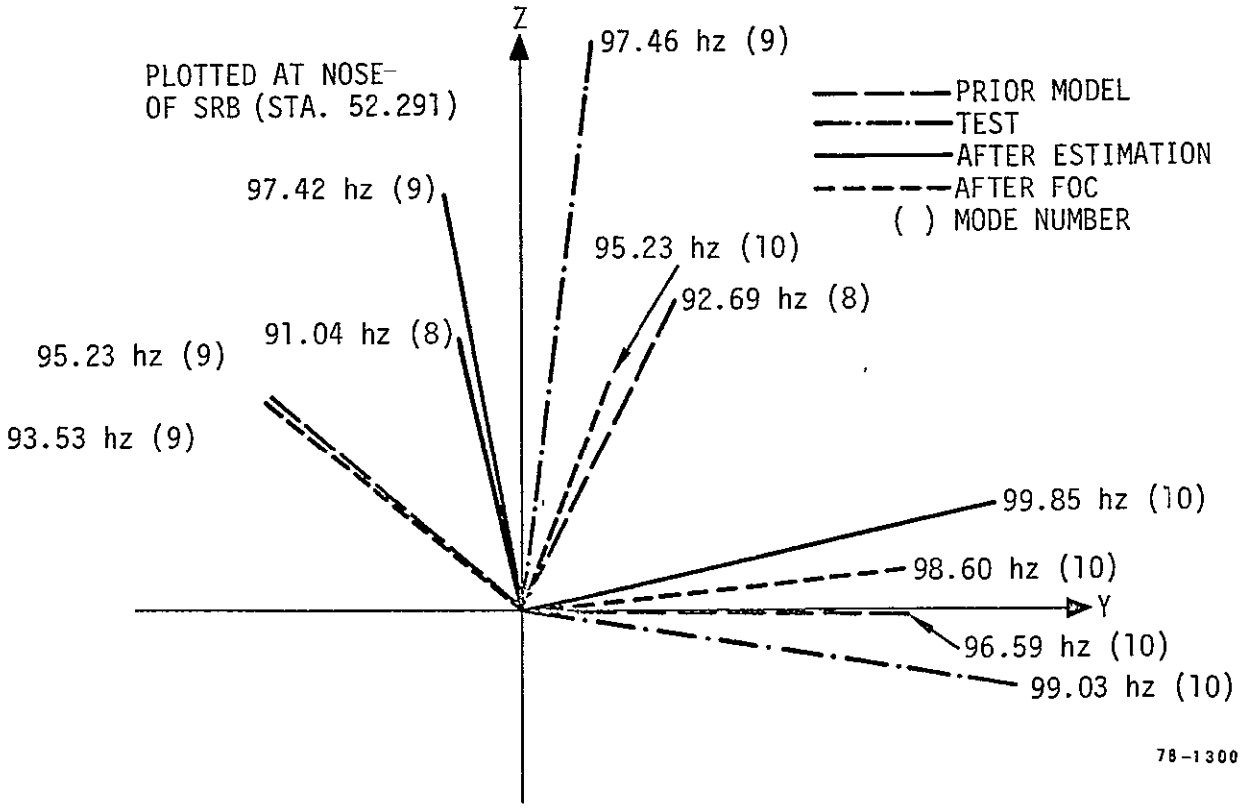

Figure 3-18. Modal Orientation with FOC, Second Vehicle Bending Modes (Y- and Z-Planes)

frequency shift (from 93.53 to 98.26 Hz) but relatively small shape changes. The other two modes have the same degree of change in shape but have reversed position with the 92.69 Hz mode going up to 99.47 Hz and the 96.59 Hz mode going down to 95.30 Hz.

The FOC has a relatively small effect on the mode shapes but its effect on frequency is sufficient to change the modal sequence. Applying the Estimator results in modes of considerably different orientation than obtained without the FOC (Figure 3-18).

3.6 Model Estimation - Example Two

This example used the eight test modes identified as beam modes for the observations and the eight analytic modes selected for use as the analytic model in the first order correction. As was discussed earlier, however, the best set of test modes may not have been selected. Be that as it may, we tested the Estimator using only these eight modes to represent the prior model. In addition, the procedure described in Section 4.2 of Reference [2] was used to select specific elements of the [m] and [k] matrices for perturbation.

The element selection procedure involves calculating the elements

$$\left| \frac{\Delta k_{ij}}{\omega_i^2} - \Delta m_{ij} \right| \left(\frac{Q_i}{(\beta_{ij}^2 - 1)} \right)^{1/2} \qquad (26)$$

where

$\left.\begin{matrix}\Delta k_{ij} \\ \Delta m_{ij}\end{matrix}\right\}$ elements of [Δk] and [Δm] produced by FOC (see Tables 3-5 and 3-6)

$Q_i = 1/2\zeta_i$ = modal amplification factor (see Appendix 2)

$\beta_{ij} = \omega_j/\omega_i$

All of the resulting 36 elements are shown in Table 3-11. The 16 elements corresponding to the 16 largest values were selected for perturbation.

Three runs were conducted using various parameter change limits. The First Order Correction was applied in all runs and the same 64 test data points were used each time. These data points consisted of the 32 points used in the previous example plus 8 more for each additional test data-set (Appendix 2). The results of the three runs are summarized in Tables 3-12, 3-13, and 3-14.

The FOC produced a significant improvement in the natural frequencies (Table 3-13), but the mode shapes themselves diverged from the desired shapes as illustrated by the modal kinetic energy (Table 3-14). Applying the Phase I Estimator to the FOC models generally resulted in some further improvement in the frequencies and tended to bring the modes back toward the desired shape. The best results were obtained for mode 6, the axial mode which has measured frequency of 150.29 Hz and a model frequency of 177.03 Hz (17.8% error). Applying the FOC results in a frequency of 153.46 Hz (2.1% error); after

Table 3-11. Element ij, From Equation 26

	Y 1	Z 2	Z 3	Y 4	θ_x 5	X 6	Z 7	Y 8
1 Y	4.22	.16	.20	.39	.04	.23	.62	.70
2 Z		3.01	.18	1.11	.52	.11	2.44	.15
3 Z			10.14	.21	.20	.06	.39	.30
4 Y				3.70	.00	.09	.43	.24
5 θ_x					5.07	.15	.28	.16
7 X						8.68	.14	.07
7 Z							1.84	.05
8 Y								6.28

Table 3-12. Goodness of Fit for Quarter-Scale SRB Parameter Identification Using 8 Test Data Sets (16 Specified Parameters in both [k] and [m] Allowed to Change)

PARAMETER	PRIOR MODEL	WITH FIRST ORDER CORREC-TION	ITER-ATION ONE	ITER-ATION TWO	ITER-ATION THREE	ITER-ATION FOUR	ITER-ATION FIVE	ITER-ATION SIX
CASE A MAXIMUM CHANGE LIMITED TO 50% OF STANDARD DEVIATION OF ELEMENT								
OBJECT FUNCTION	9288	7404	.7366	7328	7244	7174	7133	
RMS DIFFERENCE (ALL E-2)*	--	.5703	.5650	.5567	.5429	.5329	.5284	
MEAN DIFFERENCE (ALL E-2)	--	.2705	.2686	.2655	.2600	.2556	.2535	TIME LIMITED
MAXIMUM PARAMETER CHANGE (PERCENT OF STANDARD DEVIATION)	--	--	50.0%	50 0%	50.0%	50.0%	50.0%	
CASE B MAXIMUM CHANGE LIMITED TO 100% OF PARAMETER								
OBJECT FUNCTION	9288	7404	7344	7189	7111	7111	CONVERGED - CHANGE PRODUCED BY 100 % PARAMETER CHANGE LESS THAN CONVERGENCE CRITERIA	
RMS DIFFERENCE (ALL E-2)	--	.5703	.5592	.5339	.5252	.5252		
MEAN DIFFERENCE (ALL E-2)	--	.2705	.2665	.2562	2521	.2521		
MAXIMUM PARAMETER CHANGE (PERCENT OF STANDARD DEVIATION)	--	--	100 0%	100.0%	100.0%	100 0%		
CASE C MAXIMUM CHANGE SET SO LESS THAN OR EQUAL TO 200% OF PARAMETER								
OBJECT FUNCTION	9288	7404	7292	7149	7026	6918	6818	
RMS DIFFERENCE (ALL E-2)	--	.5703	.5499	.5284	.5171	5100	.5046	
MEAN DIFFERENCE (ALL E-2)	--	.2705	.2630	.2538	2481	2440	.2404	TIME LIMITED
MAXIMUM PARAMETER CHANGE (PERCENT OF STANDARD DEVIATION)	--	--	172 0%	170 7%	176.2%	161.9	122.6%	

*E-2 means $\times 10^{-2}$

Table 3-13. Model Frequencies for Quarter-Scale SRB Parameter Identificatio
Using 8 Test Data Sets and 8 Analytic Modes

MODE INDEX	FREQUENCY~HERTZ					
	PRIOR MODEL	WITH FIRST ORDER CORREC-TIONS	[A] CHANGE LIMITED TO 50% OF STANDARD DEVIATION	[B] CHANGE LIMITED TO 100% OF PARAMETER	[C] CHANGE LIMITED TO 200% OF PARAMETER	TEST MODE
1	38.32	36.30	36.23	36.22	36.12	36.95
2	38.14	37.24	37.18	37.17	37.14	37.42
3	92.69	95.18	95.84	95.88	96.25	97.46
4	96.59	98.56	98.66	98.67	98.79	99.02
5	121.02	123.28	123.25	123.26	123.25	123.99
6	177.03	153.46	153.34	153.33	153.15	150.29
7	158.63	158.40	158.36	158.38	158.31	157.04
8	155.94	164.18	163.92	163.91	163.59	163.21

Table 3-14. Comparison of Modal Kinetic Energy (Case C)

$KE_i = \omega_i^2 G_i$ where $\omega_i = i^{th}$ modal frequency (rad/sec)

$$G_i = \sum_i m_i \phi_i^2$$

MODE	DESCRIPTION	KINETIC ENERGY (10^4)			
		PRIOR MODEL	FIRST ORDER CORRECTION	AFTER 5 ESTIMA ITER.	TEST
1	FIRST Y-BENDING	5.798	4.486	4.274	5 389
2	FIRST Z-BENDING	5.742	4.116	4.302	5.527
3	SECOND Z-BENDING	33.92	18.35	18.46	37.50
4	SECOND Y-BENDING	36.83	28.08	28.83	38.71
5	FIRST TORSION	57.82	44.50	44.81	60.69
6	FIRST AXIAL	123.7	75.03	85.24	89.17
7	THIRD Z-BENDING	99.34	65.94	66.27	97.37
8	THIRD Y-BENDING	95.99	87.65	91.67	105.2

5 iterations of ESTIMA the frequency dropped slightly to 153.15 Hz (Case C, 1.9% error). The corresponding modal energies show even a more dramatic improvement:

- Test 89.17×10^4
- Prior model 123.7×10^4 (38.7% error)
- FOC 75.03×10^4 (15.9% error)
- 5th Iteration 85.24×10^4 (4.5% error)

Five iterations of the Phase I Estimator produced measurable improvements on four frequencies and four mode shapes, negligible change on two frequencies and three shapes, and slightly degraded two frequencies and one shape.

It must be emphasized that for Cases A and C the Phase I Estimator was arbitrarily terminated after five iterations to conserve computer costs. At this time, we have no idea how much further improvement it might have produced had it been allowed to run to completion. The FOC produced a 20% reduction in the object function. The Estimator produced another 6% reduction (Case C) before time limiting.

The primary conclusion to be drawn from this example is that the choice of the step limiting technique affects the amount of improvement obtained and the rapidity of convergence. Prior experience has demonstrated the need for a step limiter. However, this selection of a step limit must be made judiciously. The calculated responses have different sensitivities to each element of the [m] and [k] matrices. But an element that is initially small may show large percentage changes from step to step with but negligible change in the calculated response. This is what happened in Case B. A

change in one parameter was limited to 100% with all other parameters changing a smaller percentage. The limited parameter had such a small effect on the calculated response, however, that the program convergence criteria was satisifed. When the step limit was increased to 200% (Case C) a better set of modes was obtained.

3.7 Estimation of Scaling Parameters

To demonstrate the Phase II Estimator on the SRB problem, the Phase I results of Case C of Example One were selected. The diagonal mass matrix (Table 3-2) was divided in five submatrices and four (the maximum possible) mass scaling parameters were estimated using ESTIMB. The resulting scaling parameters are shown in Table 3-15.

The five submatrices consisted of

(1) the nose and frustum (nodes 400-404),
(2) the forward half of the motor (nodes 411-424),
(3) the aft half of the motor (nodes 429-442),
(4) the skirt (i.e., launch pads, nodes 446-449), and
(5) the nozzle (nodes 450 and 452).

If the maximum number of submatrices, five, is desired, one of them has be be non-varying. In the absence of any definitive information, we felt that the weight of a forward end of the motor case was probably the most accurate and, therefore, chose that submatrix to be non-varying.

Two cases were run, one with equally large uncertainty (all $\sigma_p^2 = 1.0$) for the prior estimate of the scaling parameters (Case A) and one with varying small uncertainties (Case B).

Table 3-15. Quarter-Scale SRB: Mass Scaling Parameters

	Ⓐ NOSE AND FRUSTUM	Ⓑ MOTOR-FORWARD	Ⓒ MOTOR-AFT	Ⓓ SKIRT	Ⓔ NOZZLE	TOTAL
CASE A						
PRIOR MASS*	.58549	2.81021	2.31981	.20230	1.09654	7.01435
PRIOR SCALING PARAMETER	1.0	none	1.0	1.0	1.0	1.0
ADJUSTED SCALING PARAMETER	.8232	none	.6951	1.0166	1.8121	1.0118
ADJUSTED MASS*	.48197	2.81021	1.61250	.20566	1.98704	7.09738
PRIOR σ_p^2	1.0	none	1.0	1.0	1.0	--
ADJUSTED σ_p^2 (DIAGONAL ELEMENTS OF $[S_{r_p r_p}]$)	1.37×10^{-4}	none	20.1×10^{-4}	7.65×10^{-4}	41.7×10^{-4}	--
DECREASE IN OBJECT FUNCTION = 6080.						
CASE B						
PRIOR MASS*	.58549	2.81021	2.31981	.20230	1.09654	7.01435
PRIOR SCALING PARAMETER	1.0	none	1.0	1.0	1.0	1.0
ADJUSTED SCALING PARAMETER	.8551	none	.8238	.9556	1.6258	1.0262
ADJUSTED MASS*	.50065	2.81021	1.91106	.19332	1.78275	7.19799
PRIOR σ_p^2	.01	none	.01	.04	.02	--
ADJUSTED σ_p^2 (DIAGONAL ELEMENTS OF $[S_{r_p r_p}]$)	1.00×10^{-4}	none	14.15×10^{-4}	6.19×10^{-4}	29.44×10^{-4}	--
DECREASE IN OBJECT FUNCTION = 6148						

MASS UNITS = lb-sec^2/in

In the first case, relatively large changes were produced for the aft motor-case (minus 273 lb) and the nozzle (plus 344 lb) but the net weight change was only 32 lb, a 1.2 percent change. In the second case, the parameter changes are somewhat smaller except for the aft skirt. The largest weight changes occurred on the aft motor-case (minus 158 lb) and on the nozzle (plus 265 lb) with a net vehicle weight increase of 2.6 percent.

Mass Scaling	Prior Parameter	Case A Parameter	σ	Case B Parameter	σ
Nose and Frustum	1.0	.8232	.0117	.8551	.0100
Motor-Aft	1.0	.6951	.0448	.8238	.0376
Skirt	1.0	1.0166	.0277	.9556	.0249
Nozzle	1.0	1.8121	.0646	1.6258	.0543

- Nose and Frustum. In both cases, the adjusted parameter and its standard deviation are about the same with the parameter change many times larger than the standard deviation. Thus, resulting mass/inertia decrease of about 15 percent is statistically significant.

- Motor-Aft. The difference between the two cases is relatively large but both are in the same direction and statistically significant. They show a 20 to 30 percent mass/inertia reduction.

- Skirt. In Case A the change is small compared to the standard deviation. This confirms the original value with a greatly improved confidence (i.e., σ reduced from 1.0 to .03). In Case B the change

4. DEMONSTRATION PROBLEM: QUARTER-SCALE ORBITER

4.1 Background and Conclusions

The Orbiter and its modal tests are more complex than those associated with the SRB. The fact that fewer data problems were encountered is, therefore, probably due to the fact that much less time was spent checking the data. Project constraints required that the Orbiter data be accepted as presented, converted to usable forms, and processed. The problems that were encountered, such as the lack of a compatible set of analytic modes, were addressed in as simple a manner as possible. When information was lacking, "reasonable" values were assumed and the analysis continued.

A number of potential difficulties, such as assumption of vehicle symmetry, were not addressed. Only the symmetric modes of an assumed symmetric vehicle were analyzed. Since most of the effort was concentrated in the low frequency range covering the first seven flexible-body, symmetric modes, the effects of vehicle asymmetry should be minimal. The use of only the symmetric modes simplified the problem by removing many possible closely spaced modes such as were present in the SRB problem. Also characteristic of the data is that the momentum of the test modes is not always conserved even in those instances where it should be.

The following conclusions, which are similar to those found on the SRB, can be drawn from our experience with the estimators on this problem:

First Order Correction

- The FOC consistently improves the frequency match. Disregarding the mode shape contributions to the FOC produces better frequency matches.

- The FOC appears to consistently worsen the mode shapes, but it always provides an improved starting point for the Phase I Estimator.

- The usefulness of the FOC is degraded whenever there are analytic modes for which a companion test mode cannot be readily identified.

Phase I Estimator

- Unless the analytic/test frequency match is very good at the start, the application of the FOC enables the Phase I Estimator to do a better job.

- The Estimator consistently improves the analytic/test correlation, both in frequency and mode shape, when it is working with high-confidence test data.

- The end result is unpredictable when and where the test data has low confidence, as measured by its coefficient of variation or variance.

- The selection of the step limit is very important. Too large a limit may cause divergence by allowing the estimator to overshoot its mark. Too small a limit causes slow convergence and may result in a model with less improvement.

- The Estimator can be successfully applied even when data is available only at resonant frequencies. Estimating higher frequency modes from lower frequency data is not possible.

Phase II Estimator

- The Phase II Estimator can successfully produce mass and stiffness scaling parameters that improve the model/Phase I results correlation.

4.2 Analytic Model

Detailed analytic models of the Quarter-Scale Orbiter were prepared by NASA and/or Rockwell-International. In these models the Orbiter was assumed to be symmetric about the vehicle centerline so that only half of the structure needed to be modeled. The model used for the symmetric modes has 357 dynamic degrees-of-freedom (DOF), while the anti-symmetric version has 340. These models were not examined during the performance of this work, nor were they directly used in any of the operations performed.

The accelerometer/model transformation equations [9] that were made available convert the 240 potential accelerometer readings to a dynamic model coordinate system with only 124 dynamic DOF. Since the test modes, therefore, are expressed in a 124 DOF system, it is imperative that analytic modes be obtained for the same coordinate system and be based on the mass matrix used to normalize the test modes. We requested,

and were supplied with, reduced mass and stiffness matrices for the 124 DOF system. These two matrices were accepted as provided without any study of how they were developed and reduced from 357 to 124 dynamic DOF. Only the symmetric model with payload was used here. A description of the model coordinates and a degree-of-freedom schedule are provided in Appendix 3.

Rockwell did all of their test correlation [8] with modes generated directly from the 357 DOF model from which only the desired DOF were selected. When we attempted to use these modes for the first order correction, we found that they were not sufficiently orthogonal with respect to the 124 DOF mass matrix to yield meaningful off-diagonal terms. We, therefore, generated our own symmetric orbiter modes using the 124 DOF mass and stiffness matrices. A description of the lowest 14 modes is provided in Table 4-1. Table 4-1 also provides a list of the first 14 frequencies from the 357 DOF Rockwell model. These frequencies are generally lower and differ by up to ten percent. The degree of modal similarity is not known.

4.3 Test Data

The quarter-scale ground vibration tests of the Orbiter were conducted during April and May of 1977. The Orbiter was soft-suspended in the horizontal attitude and contained a rigid 500-pound payload that simulated a full-scale 32,000-pound payload. Both symmetric and anti-symmetric modes were excited and several major components were also studied. Data were recorded only at resonant dwells, although some of these

Table 4-1. Quarter-Scale Orbiter with Payload: Description of JHW Generated Analytic Modes (124 DOF System)

INDEX*	FREQUENCY (Hz)	DESCRIPTION	FREQUENCY OF FIRST 14 ROCKWELL ANALYTIC MODES (Hz)
4	18.314	FIRST FUSELAGE Z-BENDING, VERTICAL TAIL X-Z ROCKING	18.247
5	19.617	PAYLOAD PITCH COUPLED WITH FUSELAGE Z-BENDING	19.609
6	28.138	WING-ELEVON Z-BENDING COUPLED WITH VERTICAL TAIL PITCH, ENGINE PITCH, AND FUSELAGE Z-BENDING	27.892
7	30.073	VERTICAL TAIL - RUDDER PITCH (I.E., ROCKING ABOUT Y-AXIS)	29.545
8	32.477	LOWER ENGINE AND OMS FUEL TANK ROCKING	30.886
9	35.395	WING-ELEVON TORSION COUPLED WITH OMS FUEL TANK AND ENGINE YAW	34.835
10	37.767	LOWER ENGINE YAW COUPLED WITH WING-ELEVON TORSION	35.210
11	40.321	SECOND FUSELAGE Z-BENDING COUPLED WITH WIND-ELEVON TORSION AND RCS MOTION	37.612
12	40.439	RCS TANKS AND STRUCTURE MOTION	37.832
13	42.479	UPPER ENGINE Z-MOTION COUPLED WITH ELEVON ROLL	40.213
14	43.724	ELEVEN ROLL, INBOARD ELEVON OUT-OF-PHASE WITH OUTBOARD ELEVON	40.314

*Mode 1 to 3 are rigid body modes (f ≅ 0. Hz).

dwells were later determined not to be "good" modes [7, 8]. Test data were provided to us on disk files on the Rockwell Cyber 177 computer [9] at Seal Beach, California.

There were 240 accelerometers mounted on the test article, a few of which were not applicable to the symmetric modes of the overall vehicle [10]. At each dwell, five pieces of information were recorded:

Peak Acceleration (G)
Coincident Response (G/lb)
Quadrature Response (G/lb)
Phase (degrees)
Reference Shaker

The applicable accelerometers are numbered consecutively from 1 to 227. Twenty-four shakers, located on both the +Y and -Y sides of the centerline, were used to excite the vehicle. Only the total concident and quadrature responses (G) were provided on disk files. The transformation from accelerometers to dynamic model DOF was provided by Rockwell [9]. A catalog of the 42 test data-sets is provided in Appendix 3.

A transformation for the shaker forces was not available, so one was developed (Appendix 3). The 24 shakers provide a maximum of 17 generalized forces. No data anomalies were found during our work with this data, but then none were looked for.

4.4 First Order Correction

The first step in performing the first order correction(FOC) is to correlate the analytic modes with the test modes. This was done here by calculating the cross-orthogonality between all 124 analytic modes and all 42 test data-sets and then searching the resulting matrix for the largest values. Whenever a value of 1.0, or nearly so, is found we have good agreement between the analytic mode and the test mode. All analytic modes for which a test/model cross-orthogonality is greater than 0.30 are summarized in Table 4-2. Only about half, 22, of the first 41 flexible body modes were found to have a test data-set meeting this condition. These 22 modal pairs were used for the first order correction calculation.

The new generalized mass and stiffness matrices for the 22 analytic modes being perturbed are similar to those reported earlier for the Quarter-Scale SRB. Their size (22 x 22) prevents their inclusion in this report. The use of all 41 analytic modes covering the frequency range of the test would result in an intractable problem. Therefore, a reduced set, consisting of the first seven analytic modes, was selected for further processing. The perturbed matrices for this reduced system are shown in Tables 4-3 and 4-4. The original matrices were diagonal with the diagonal terms unity for the mass and ω^2 for the stiffness. Notice that mode 8 is not perturbed--no test mode could be found with which to perturb it.

Table 4-2. Quarter-Scale Orbiter: Analytic/Test Correlation (6 to 130 Hz)

	ANALYTIC MODE		CORRESPONDING TEST DATA SET		$\{^{o}\phi\}_j^T[^{o}M]\{\hat{\Phi}\}_j$
	INDEX*	FREQUENCY Hz	INDEX	FREQUENCY Hz	
MODES USED FOR PARAMETER IDENTIFICATION	4	18.314	4	19.384	.939
	5	19.617	13	21.546	.942
	6	28.138	5	26.614	.866
	7	30.073	35	25.597	.539
	9	35.395	27	31.409	.304
	10	37.767	23	29.980	.869
	13	42.479	20	62.234	.496
	14	43.724	17	41.237	.770
	15	46.352	12	52.893	.663
	16	48.856	16	39.178	.482
	20	59.929	7	50.246	.474
	23	64.159	41	78.397	.315
	24	67.821	15	40.161	.532
	26	72.093	10	77.615	.605
	27	75.891	36	47.192	.552
	31	82.155	18	82.625	.616
	32	82.600	19	83.656	.514
	35	88.764	37	91.496	.295
	39	102.209	8	95.816	.634
	41	113.817	42	93.724	.672
	43	121.473	32	118.768	.313
	44	125.434	26	138.299	.608

TOTAL NUMBER OF MODES = 22

*MODES 1 TO 3 ARE RIGID BODY MODES NOT CONSIDERED IN COMPARISON.

Table 4-3. Quarter-Scale Orbiter, Symmetric Modes: FOC Generalized Stiffness Matrix for 7 Mode Model

DESCRIPTION	INDEX	GENERALIZED STIFFNESS MATRIX						
FIRST FUSELAGE Z	4	16449.						
PAYLOAD PITCH	5	3915.	20102.					
FIRST WING BENDING	6	925.	-847.	36318.		SYMMETRIC		
TAIL PITCH	7	-2291.	4315.	-25063.	58753.			
LOWER ENGINE	8	0	0	0	0	41640.		
WING TORSION	9	-3691.	7068.	-8007.	964.	0	107825	
LOWER ENGINE YAW	10	-5184.	-828.	-6599.	-12380.	0	-14617.	50218.

Table 4-4. Quarter-Scale Orbiter, Symmetric Modes: FOC Generalized Mass Matrix for 7 Mode Model

DESCRIPTION	INDEX	GENERALIZED MASS MATRIX						
FIRST FUSELAGE Z	4	1.1221						
PAYLOAD PITCH	5	.2681	1.1168					
FIRST WING BENDING	6	-.1011	.0373	1.2673		SYMMETRIC		
TAIL PITCH	7	-.1675	.1873	-.7594	1.9211			
LOWER ENGINE	8	0	0	0	0	1.0000		
WING TORSION	9	.0190	.0961	-.1344	-.0865	0	2.3926	
LOWER ENGINE YAW	10	.1268	-.0253	-.2067	-.2231	0	-.2837	1.2617

4.5 Phase I Model Estimation - Example One

The first Quarter-Scale Orbiter problem investigated with the Phase I Estimator was based on the seven flexible-mode model described in the preceding section. The prior model consisted of the lowest seven flexible-body modes including the fundamental modes for

a) fuselage bending,
b) payload pitch,
c) wing-elevon bending and torsion,
d) tail-rudder pitch, and
e) lower engine yaw.

Four of the analytic mode shapes agree very well with a test mode, having a cross-correlation coefficient greater than 0.86, although some of the frequency matches are not nearly as good. These modes are

a) fuselage bending (mode correlation = .939, frequency ratio = .94),

b) payload pitch (mode correlation = .942, frequency ratio = .91),

c) wing-elevon bending (mode correlation = .866, frequency ratio = 1.06),

d) lower engine yaw (mode correlation = .869, frequency ratio = 1.26).

The other three analytic modes could not be paired nearly as easily with a test data-set, having cross-correlation coefficients less than about 0.5.

Three cases were investigated using different approaches for the first order correction (FOC). These runs are summarized in Tables 4-5 and 4-6. The same 150 test data points were used for all cases. These data consist of the 15 largest responses (deflections) measured at 10 different dwells. Since only 7 of the dwells provided good test modes, we have a little inter-resonance information here. All of the test-data points used for the Phase I estimation are provided in Appendix 3. The 10 test data-sets are:

Frequency	Good Mode	Approximate Coef. of Variation of Response Data
19.384	Yes	.3
21.546	Yes	2.0
25.597	Yes	.05
26.614	Yes	.06
27.476	No	.07
29.980	Yes	.2
31.409	Yes	.3
34.247	No	.2
34.344	Yes	.3
35.225	No	.7

Damping was not estimated with the Phase I Estimator. Instead, the modal damping values were optimized beforehand using the technique described in Appendix 3 and also used on the SRB.

Table 4-5. Goodness of Fit for Quarter-Scale Orbiter Parameter Identification Using 7 Analytic Modes and 10 Test Data-Sets

PARAMETER	PRIOR MODEL	FIRST ORDER CORRECTION	ITERATION ONE	ITERATION TWO	ITERATION THREE	
CASE A WITH STANDARD FOC, 50 PERCENT CHANGE LIMIT, LARGE UNCERTAINTY ON PRIOR						
OBJECT FUNCTION (E+6)*	16.82	150.26	20.94	2.13	2.05	CONVERGED, STEP SIZE SMALLER THAN CUTOFF
RMS DIFFERENCE (ALL E-2)	3.08	9.46	3.50	1.13	1.11	
MEAN DIFFERENCE (ALL E-2)	-.527	-2.62	-.845	-.142	-.148	
MAXIMUM PARAMETER CHANGE (PERCENT OF STANDARD DEVIATION)	--	--	50%	50%	12.5%	
CASE B WITH LIMITED FOC, 50 PERCENT CHANGE LIMIT, LARGE UNCERTAINTY ON PRIOR						
OBJECT FUNCTION (E+6)	16.82	23.70	15.11	14.52		CONVERGED, STEP SIZE SMALLER THAN CUTOFF
RMS DIFFERENCE (ALL E-2)	3.08	3.61	2.90	2.90		
MEAN DIFFERENCE (ALL E-2)	-.527	-.596	-.528	-.569		
MAXIMUM PARAMETER CHANGE (PERCENT OF STANDARD DEVIATION)	--	--	50%	50%		
CASE C WITH MODIFIED FOC, 50 PERCENT CHANGE LIMIT, LARGE UNCERTAINTY ON PRIOR						
OBJECT FUNCITON (E+6)	16.82	7.99	6.14			CONVERGED, STEP SIZE SMALLER THAN CUTOFF
RMS DIFFERENCE (ALL E-2)	3.08	2.18	1.93			
MEAN DIFFERENCE (ALL E-2)	-.527	-.602	-.482			
MAXIMUM PARAMETER CHANGE (PERCENT OF STANDARD DEVIATION)	--	--	50%			

Table 4-6. Modal Frequencies for Quarter-Scale Orbiter Parameter Identification Using 7 Analytic Modes and 10 Test Data-Sets

MODE* INDEX	FREQUENCY (Hz)							
	PRIOR MODEL	CASE A		CASE B		CASE C		TEST** MODE
		STANDARD FOC	FINAL ITERATION	LIMITED FOC	FINAL ITERATION	MODIFIED FOC	FINAL ITERATION	
4	18.314	18.425	18.119	18.790	18.509	19.384	18.380	19.384
5	19.617	21.082	19.454	21.281	20.417	21.546	19.345	21.546
6	28.138	26.030	26.036	27.529	27.103	26.614	26.525	26.614
7	30.073	27.664	27.529	30.073	30.524	25.597	25.027	25.597(?)
8	32.477	32.477	33.291	32.477	36.352	32.477	32.506	NO MATCH
9	35.395	34.125	35.011	35.395	34.085	31.409	31.543	31.409(?)
10	37.767	31.675	31.897	31.820	31.686	29.980	29.847	29.980

*Modes 1-3 are rigid-body suspension modes.
**The only test data significantly more accurate than the prior model is around the blocked frequency, 26. Hz.

To estimate the accuracy of the test data we assumed that the accelerometer measurements had a standard deviation of .01 g (1 percent of full scale) and that the transformation coefficients had a coefficient of variation of 5 percent. Even with this very tight accelerometer tolerance (.05 g was used for the SRB data), much of the test data have large coefficients of variation indicating that the accelerometers were over-ranged or that the shakers were under-driven. The degree of uncertainty on the prior model was set arbitrarily large to give maximum weight to the test data. Initially, the standard deviations were arbitrarily set to 25 percent of the value of the corresponding diagonal terms. Even so, this is considerably less than the values for some of the test data. As became apparent later, the low confidence in much of the test data probably had important effects on the outcome. In retrospect, a better demonstration would have been obtained if the uncertainty in the prior model had been made larger.

The parameters presented in Table 4-5 have been defined in Section 3.5. All elements of the generalized mass and stiffness matrices were estimated. A run was attempted without any kind of first order correction but without success (i.e., the object function was not decreased). The three runs presented in Table 4-5 differ only in the type of FOC used.

The FOC has been previously described in Reference [2]. We found, for this vehicle, that the off-diagonal elements of the FOC involve small differences of large numbers. Since the

numbers, in turn, depend on test data with questionable accuracy, the off-diagonal FOC terms may not be meaningful. The three cases were formulated to investigate this question.

Case A used the standard FOC, as presented in Section 4.4, for six of the seven analytic modes. Application of the standard FOC produced a significant improvement in the frequency match but so degraded the mode shapes that the object function increased from 16×10^6 to 150×10^6. Having a much better frequency match to start, however, the Phase I Estimator was now able to produce significant improvement. It decreased the object function to 2×10^6 and the RMS difference to .01 inch.

Case B used an FOC with only those terms corresponding to the four analytic/test modes with a good cross-correlation coefficient. Here the FOC did not increase the object function as much but the Phase I Estimator was not nearly as successful as in Case A. Consequently, the final result is not nearly as "good" as Case A (i.e., the final object function is not as small).

For Case C, all of the FOC information based on mode shape was discarded leaving only the diagonal stiffness terms given by $\Delta k_{ii} = \omega^2_{ii}(\text{test}) - \omega^2_{ii}(\text{anal})$. The resulting FOC model has a perfect frequency match with unchanged analytic modes. Consequently, both the FOC and the Phase I Estimator decrease the object function but the final result is not as good as Case A.

The first conclusion evident here is that the FOC provides a very useful model adjustment, even though the mode shapes are

degraded, the object function increased drastically, and the off-diagonal terms are questionable. When the standard FOC is applied, the Phase I Estimator is able to significantly improve the model. Without any FOC, the Estimator was unsuccessful, and with a modified FOC, less successful.

The second result is the importance of the confidence assigned to test data. All of the high-confidence (relative to the prior model) test data were found to be the three data sets between 25 and 28 Hz. The test mode located in this region is the only one for which the Phase I Estimator consistently provides a good frequency match. In retrospect, the Estimator seems to be dramatically saying

> If you say the test data are good and the model poor, a model to match the test data will be generated; but if you say both are bad, who can predict what will happen?

4.6 Phase I Model Estimation - Example Two

The second Quarter-Scale Orbiter problem investigated with the Phase I Estimator is a simplified version of Example One. The first four analytic modes are retained together with the three test data-sets corresponding to the first three analytic modes. The cross-correlation for all three of these modal pairs is greater than 0.86. The fact that there is very good agreement between the analytic and test modes for the three test data-sets makes this problem behave quite differently from Example One. The three test data-sets consist of:

(a) the fundamental fuselage bending mode (19.384 Hz),
(b) the payload pitch mode (21.546 Hz),
and (c) the fundamental wing-elevon bending mode (26.614 Hz).

Test data sensitive to the fourth analytic mode (30.073 Hz) were not used for either the FOC or Phase I, thus allowing this mode significant leeway to drift. The three cases investigated were

- No FOC
- Standard FOC on 3 modes
- Modified FOC on 3 modes

The same 45 test data points were used for all three cases. They are a subset of the data used in Example One and tabulated in Appendix 3. They do not provide any inter-resonance information. All elements of the generalized mass and stiffness matrices were estimated, a total of 20 elements. Damping was not estimated with the Phase I Estimator, although the modal damping values were optimized beforehand using the technique described in Appendix 3.

For the case without the FOC, the Estimator was able to generate an improved model, i.e., the object function was reduced from 1180 to 223 in six iterations (Table 4-7). This was expected for two reasons: 1) the analytic mode shapes are already very close to the test modes, and 2) no test data are provided for the fourth mode for which there is not a good match. What was not expected was the frequency divergence. At convergence, the first two model frequencies (Table 4-8) are farther from the test frequencies than at the start, even though the object function has decreased drastically. This seemingly anomalous behavior is probably due to the low confidence assigned to the test data for these modes, which reduces the influence of the data on the final outcome and on the object function itself. Nevertheless, this divergence makes the no-FOC case unacceptable just as it was in Example One.

Table 4-7. Goodness of Fit for Quarter-Scale Orbiter Parameter Identification Using 4 Analytic Modes and 3 Test Data-Sets

PARAMETER	PRIOR MODEL	FIRST ORDER CORREC-TION	ITER-ATION ONE	ITER-ATION TWO	ITER-ATION THREE	ITER-ATION FOUR	ITER-ATION FIVE	ITER-ATION SIX	
CASE A NO FOC, 50 PERCENT CHANGE LIMIT									
OBJECT FUNCTION	1180.	--	919.3	690.8	543.3	299.2	252.3	228.0	
RMS DIFFERENCE (ALL E-2)*	.1414	--	.1195	.0925	.0745	.0574	.0548	.0533	
MEAN DIFFERENCE (ALL E-2)	.0918	--	.0795	.0653	.0528	.0399	.0404	.0399	CONVERGED
MAXIMUM PARAMETER CHANGE (PERCENT OF STANDARD DEVIATION)	--	--	50%	50%	50%	12.5%	12.5%	12.5%	
CASE B STANDARD FOC, 50 PERCENT CHANGE LIMIT ON 3 MODES									
OBJECT FUNCTION	1180.	1043.3	705.0	315.0	202.7	147.8	108.5		
RMS DIFFERENCE (ALL E-2)	.1414	.1301	.1212	.0794	.0597	.0420	.0428		
MEAN IDFFERENCE (ALL E-2)	.0918	.0656	.0614	.0508	.0412	.0263	.0267	CONVERGED	
MAXIMUM PARAMETER CHANGE (PERCENT OF STANDARD DEVIATION)	--	--	50%	50%	12.5%	50%	50%		
CASE C MODIFIED FOC ON 3 MODES, 50 PERCENT CHANGE LIMIT									
OBJECT FUNCTION	1180.	90.0	71.5	57.7	53.9	23.2	22.7		
RMS DIFFERENCE (ALL E-2)	.1414	.0294	.0356	.0324	.0316	.0184	.0181		
MEAN DIFFERENCE (ALL E-2)	.0918	-.0032	.0073	.0044	.0051	.0020	.0019	CONVERGED	
MAXIMUM PARAMETER CHANGE (PERCENT OF STANDARD DEVIATION)	--	--	12.5%	8.1%	10.5%	11.0%	0.45%		

Table 4-8. Modal Parameters for Quarter-Scale Orbiter Parameter Identification Using 4 Analytic Modes and 3 Test Data-Sets

MODE* INDEX	FREQUENCY (Hz)							
	PRIOR MODEL	CASE A		CASE B		CASE C		TEST MODE
		NO FOC	FINAL ITERATION	STANDARD FOC ON 3 MODES	FINAL ITERATION	MODIFIED FOC ON 3 MODES	FINAL ITERATION	
4	18.314	--	16.954	19.077	17.472	19.384	19.459	19.384
5	19.617	--	19.513	21.306	21.458	21.546	20.890	21.546
6	28.138	--	27.255	27.529	26.443	26.614	26.761	26.614
7	30.073	--	32.937	30.073	39.447	30.073	31.672	--
	MODAL GENERALIZED MASS							
4	1.0	--	1.106	.893	2.756	1.000	.922	1.0
5	1.0	--	1.082	.942	.851	1.000	.966	1.0
6	1.0	--	1.322	.869	1.148	1.000	1.107	1.0
7	1.0	--	1.132	1.000	1.675	1.000	1.045	1.0

*Modes 1-3 are rigid-body suspension modes.

For the case with the standard FOC on three modes, both the FOC and the Phase I Estimator decreased the object function. The FOC reduced it from 1180 to 1043, while the Phase I Estimator further reduced it to 108. The RMS differences were, likewise, reduced significantly. Here the frequency match is better, although the first mode frequency still diverged, dropping to 17.5 Hz instead of increasing to 19.4 Hz. The FOC was applied here only to analytic modes 4, 5, and 6; the modes with a very good shape match with a test mode. Because the modes are so well matched, most of the effect of the FOC is probably due to the improved frequency match. The striking facet of this case is on mode 4. The Estimator allowed the frequency to diverge, which would be expected to degrade the test-model match. But it compensated by increasing the modal deflections, as demonstrated by the increase in the generalized mass from .893 to 2.756 (Table 4-8), thus producing a much "better" model. Just as in Case A, this behavior is probably due to the relatively low confidence in the test data for this mode.

The third case is similar to Case C of Example One. The only FOC applied was to the diagonal elements of the generalized stiffness matrix for modes 4, 5, and 6. This produces an FOC model with "perfect" frequency match on three modes and the original analytic mode shapes (Table 4-8). Since the analytic modes were already very close to the test modes for which test data is provided, the "perfect" frequency match provides a drastic reduction in the object function, from 1180 to 90. Nevertheless, the Phase I Estimator still provides further improvement.

C-2

Just as in Example One, convergence is obtained when any further decrease in the object function by producing a better match with test data is counteracted by an increase caused by the greater differences between the prior and estimated parameters (see Section 3.5). Thus, the final point of convergence would be changed by decreasing the confidence of the prior model with respect to the test data. Of the three data-sets used here (Sets 4, 5, and 13), only Set 5 at 26.614 Hz has a confidence level significantly better than the prior-model parameters.

	Approx. Coef. of Var.	
Prior Model	.25	
Test Data		
Set 4 (19.384 Hz)	.30	(Mode 4)
Set 13 (21.546 Hz)	2.00	(Mode 5)
Set 5 (26.614 Hz)	.06	(Mode 6)

When evaluated in this light, the results of the Phase I Estimator make more sense. In each case, a good frequency match is generated for mode 6, the only one for which the test data have a significantly higher confidence.

4.7 Estimation of Scaling Parameters

To demonstrate the Phase II Estimator on the Orbiter problem, the Phase I results of Case C of Example Two were selected as "test" data. Developing the component submatrices is more involved than for the SRB, however. Having the vehicle mass and stiffness matrices but not having access to any of the component submatrices, recourse was made to the alternate substructuring approach described in Reference [2] (Section 5.2).

The substructuring approach uses a set of "orthogonal" displacement vectors to define submatrices associated with different components of a structure. Force vectors are first defined such that the virtual work done by one set of forces on the displacements caused by another is zero. Since the force sets are still somewhat arbitrary, the component substructures so derived are not unique to the component. Consequently, the meaning of the adjustments made to the elements of [M] and [K] is not as clear as if the actual component matrices were available.

The test data chosen for this demonstration has four modes:

(a) a fuselage bending mode,
(b) a payload pitch mode,
(c) a wing-elevon bending mode, and
(d) a tail rocking mode.

It seems consistent, therefore, to define submatrices for the forward fuselage, the payload, the wing and elevon, and the tail to match the modes of Phase I; plus everything else.

The procedure used to generate the substructures is as follows:

(a) Select a limited number of nodes on the component to which external loads will be applied.

(b) Constrain all of the degrees-of-freedom not associated with the component.

(c) Generate the constrained stiffness matrix, invert it, and calculate the deflections due to the external loads.

(d) Apply the deflections to the unconstrained stiffness matrix to generate the constraint forces. The desired force vector is the vector of the external forces plus the vector of the constraint forces. The loads, and constraints, for each load case are defined in Appendix 3.

(e) Generate the submatrices using the following equation:

$$[K]_i = \frac{1}{K_1^*} \{f\}_i \{f\}_i^t \qquad (27a)$$

$$[M]_i = \frac{1}{M_1^*} \{\delta\}_i \{\delta\}_1^t \qquad (27b)$$

where $\{f\}_i$ = force vector

$\{\delta\}_i$ = deflection vector

$$K_i^* = \{\delta\}_i^t [K] \{\delta\}_1$$

$$M_i^* = \{\delta\}_i^t [M] \{\delta\}_1$$

A check of the orthogonality of the four deflection sets produced the following values (normalized to unity on the diagonal), thus verifying that these load cases satisfy our orthogonality requirement.

for $[K]_1$

$$\begin{bmatrix} 1.000 & & & \text{symmetric} \\ 0 & 1.000 & & \\ 1.50E\text{-}2 & 0 & 1.000 & \\ 2.78E\text{-}5 & 0 & 3.92E\text{-}3 & 1.000 \end{bmatrix}$$

for $[M]_1$

$$\begin{bmatrix} 1.000 & & & \text{symmetric} \\ 0 & 1.000 & & \\ 4.47E\text{-}4 & 0 & 1.000 & \\ 2.39E\text{-}6 & 0 & -1.12E\text{-}4 & 1.000 \end{bmatrix}$$

The results of the Phase II estimation are summarized in Table 4-9. Two cases were run: one with equally large uncertainty for all of the prior estimates (α(prior) = 1.0, σ^2 = 1.0), and one with reduced uncertainties giving more confidence to the mass parameters (α(prior) = 1.0, σ^2 = .0025 for mass; α(prior) = 1.0, σ^2 = .5 for stiffness). In the first case, four characteristics immediately stand out:

- The largest changes occurred on the mass scaling parameters.
- The uncertainty, σ_p, in the scaling parameters decreased considerably for both mass and stiffness, but generally about one order of magnitude more for stiffness.
- The uncertainty in the payload stiffness was not decreased (i.e., σ_p was not reduced).
- The object function was improved drastically from 666 to 4.7.

Table 4-9. Quarter-Scale Orbiter: Scaling Parameters

	FUSELAGE	PAYLOAD	WING-ELEVON	TAIL
CASE A				
MASS				
PRIOR PARAMETER	1.000	1.000	1.000	1.000
PRIOR σ_p^2	1.000	1.000	1.000	1.000
ADJUSTED PARAMETER	1.6648	0.7803	1.0526	0.8340
ADJUSTED σ_p^2	0.1412	0.4813×10^{-2}	0.200×10^{-2}	$.5303 \times 10^{-1}$
STIFFNESS				
PRIOR PARAMETER	1.000	1.000	1.000	1.000
PRIOR σ_p^2	1.000	1.000	1.000	1.000
ADJUSTED PARAMETER	1.0412	1.000	0.9836	1.0245
ADJUSTED σ_p^2	0.1903×10^{-3}	1.000	$.1896 \times 10^{-4}$	0.2283×10^{-3}
CASE B				
MASS				
PRIOR PARAMETER	1.000	1.000	1.000	1.000
PRIOR σ_p^2	$.25 \times 10^{-2}$	$.25 \times 10^{-2}$	$.25 \times 10^{-2}$	$.25 \times 10^{-2}$
ADJUSTED PARAMETER	1.0114	0.9209	1.0479	1.0076
ADJUSTED σ_p^2	$.2451 \times 10^{-2}$	$.1608 \times 10^{-2}$	$.7706 \times 10^{-3}$	$.2338 \times 10^{-2}$
STIFFNESS				
PRIOR PARAMETER	1.000	1.000	1.000	1.000
PRIOR σ_p^2	.500	.500	.500	.500
ADJUSTED PARAMETER	1.0207	1.000	0.9852	1.0390
ADJUSTED σ_p^2	$.8728 \times 10^{-5}$	.500	$.8388 \times 10^{-5}$	$.8493 \times 10^{-4}$

Calculation of a new set of analytic modes using the modified mass and stiffness matrices was not attempted.

The size of the parameter changes for the second case are generally smaller than in the first case, demonstrating the importance of the parameter uncertainty and its use to force changes in particular components. Considered alone, Case B has the following characteristics:

- The changes in the parameters are of about equal magnitude for both mass and stiffness, although the uncertainty σ_p was initially set 20 times lower for the mass scaling parameter.
- The uncertainty in the scaling parameters decreased considerably for stiffness but hardly at all for mass.
- The uncertainty in the payload stiffness was not decreased.
- The object function was improved drastically from 666 to 11.7.

The most interesting phenomena appear when the two cases are compared, however. First, consider the mass scaling parameters.

		Case A		Case B	
Mass Scaling	Parameter	Parameter	σ	Parameter	σ
fuselage	1.000	1.6648	.3758	1.0114	.0495
payload	1.000	.7803	.0694	.9209	.0401
wing-elevon	1.000	1.0526	.0447	1.0479	.02776
tail	1.000	.8340	.2302	1.0076	.04835

- First, we see that the parameters estimated in Case B are within the 2σ range of the parameters estimated in Case A. Although the differences appear large, the two cases are statistically consistent with each other.

- For the fuselage, the standard deviation is large compared to the change in the parameter, particularly in Case B. Consequently, the parameter change is probably not meaningful.

- For the payload and wing-elevon, however, the changes are consistently large compared to the standard deviation. Thus, we conclude that a reduction in payload mass and an increase in wing-elevon mass are meaningful changes.

- The changes to the tail-mass scaling parameter are small compared to σ, thus the changes to the scaling parameter are not meaningful.

For the payload, the size of the mass change is sensitive to the prior model uncertainty, σ. Thus, the change to be incorporated into the model must be made with this in mind. If a good estimate of the prior σ is not available, the analyst should examine his model carefully and obtain new weight data for the test article. With only one set of sub-matrices examined and with little basis for selecting σ_p (prior) the important result is where to look and not the actual values themselves.

Now consider the stiffness scaling parameters.

Stiffness Scaling	Prior Parameter	Case A Parameter	Case A σ	Case B Parameter	Case B σ
fuselage	1.000	1.0412	0.0138	1.0207	.0030
payload	1.000	1.0	1.0	1.0	.707
wing-elevon	1.000	0.9836	0.0044	0.9852	.0029
tail	1.000	1.0245	0.0151	1.0390	.0092

- Again we see that the two cases are statistically consistent, with Case B being within two standard deviations of Case A.

- The payload stiffness parameter was not changed in either case, neither was the standard deviation changed. This implies that the data we are using provide no information on the payload stiffness.

- The changes to the other three components (fuselage, wing-elevon, tail) are all small but statistically meaningful. The reductions in uncertainty are large, approximately two orders of magnitude.

That the three statistically significant changes are small confirms the prior model. That the changes are significant and reduce the object function suggests that possibly they should be incorporated into the model, or at least investigated further.

5. SUMMARY OF EXPERIENCE TO DATE

5.1 Parameter Estimation Algorithms

The three-phase estimation procedure developed under this project shows great promise. For each example investigated, it has generated revised models with greatly improved object functions. The importance of the First Order Correction (FOC) has been verified again and again. Since the entire approach is based on linear perturbation theory or the iterative application of a linear estimator to a highly non-linear problem, the prior model is critical. The FOC itself has been found to be fundamentally identical to the perturbation method developed by J. C. Chen [11, 12], although the present application and interpretation are significantly different.

The Phase I Estimator is quite stable but it is sensitive to both its prior model and the step limit. The sensitivity matrix is a highly non-linear function of the analytical eigenvalues. Consequently, the capability of the Phase I Estimator to generate an improved analytic model is increased the better the frequency match between analysis and test. The test/model frequencies must be fairly well aligned or this estimator will diverge. Thus, the frequency improvement provided by the FOC greatly enhances the performance of the Phase I Estimator.

The new model generated by the procedure is not unique. The selection of the prior, the observations, the variances, and the step limit all influence the outcome. The selection of these interrelated parameters is still a trial and error approach. When the model developers begin to provide more

information about the uncertainties assigned to various components and to the modal characteristics, the whole procedure will become more effective.

Much remains to be learned, however. Foremost among the unanswered questions are:

- Why does the First Order Correction often produce modes less representative of test? How meaningful are the off-diagonal elements of the FOC?
- What are the implications of the fact that, in Phase II, the magnitude of object function appears to be predominately controlled by the generalized stiffness matrix?
- How should the step limit be set?

5.2 Proper Models

The initial dynamic model of the Quarter-Scale orbiter had approximately 350 dynamic degrees-of-freedom (DOF). For comparison with test data Rockwell collapsed the 350 DOF mass matrix to 124 DOF using a Guyan reduction. The analytic modes were not recalculated for the reduced system but were obtained by selecting the appropriate modal deflections from the original set of 350-DOF modes. This approach provides the maximum fidelity of the mode shape, but it introduces mathematical error because the orthogonality of the original modes (350 DOF) with the reduced mass matrix (124 DOF) is no longer exactly identical. In fact, the introduced error may be quite large when the mode is characterized by large motion on the deleted degrees-of-freedom (Table 5-1). When we tried

Table 5-1. Auto-Orthogonality of Analytic Modes for Quarter-Scale Orbiter

$$[\phi_o]^t[M][\phi_o]$$

Using Rockwell modes

off-diagonal terms with magnitudes exceeding 0.10

MODE I	MODE J	VALUE
3	18	.13
32	37	-.33
49	44	.11
49	70	-.25
37	18	.18
37	29	-.13
14	18	.10
18	29	.57
18	44	.28
15	70	.15
29	44	.17
29	53	.15

to perform the First Order Correction with these modes, the mathematical error swamped the off-diagonal terms. Therefore, whenever the First Order Correction is applied, the analytic modes and analytic mass matrix must be perfectly compatible so that $[\phi_o]^t[M][\phi_o] = [I]$.

In the initial SRB example, analytic modes known to be unrepresentative of the test article were excluded. The results were not as successful as when all of the analytic modes in the frequency band of interest were retained (Example Two). This is probably because some of the deleted modes had significant deflection on the structure being estimated. The resulting incompleteness of the analytic model was probably more detrimental than the inaccuracy introduced by the undesired modes. The estimated model retains many characteristics of the prior model, particularly for those modes for which there is no test data. Structure not present in the test article should, therefore, not be included in the analytic model. Every effort should be made to model the test article, including all known differences between it and flight hardware.

5.3 Test Data

A perfect match between the estimated model and the test data means that applying the test forces to the analytic modes yields the measured responses. This is, of course, an ideal which can never be obtained but it also has other implications.

If the forces applied to the analytic modes are not the actual forces used, either no solution or the wrong solution will be obtained. Particularly critical is the phasing of the test forces. If the shaker polarity is recorded incorrectly, substantial errors can be introduced. Our experience with the SRB indicates that this might be a common occurrence. Great care must be exercised to insure that the proper polarity is recorded. The best check might be to calculate the test responses using the test modes. Once the proper damping is found, all of the measured responses should match the calculated ones.

Also inherent in the approach is the assumption that the measured responses are accurate to within the specified uncertainty. The Bayesian estimator is generally insensitive to erroneous information. But this is not necessarily true when incomplete information is used. When only a few response points are being used to represent a very complex mode, the points selected for use have an influence far greater than their contribution to the total picture. One bad reading out of 124 DOF is insignificant, but one out of 10 selected for use is not.

The Bayesian estimator weighs the test data according to the assigned variances. If a particular measurement is assigned a standard deviation of, for example, .05 G, its weighting factor is 1/(.0025). If ten measurements are being used, nine of which read 0.1 G and the tenth 1.0 G when it should read 0.1, the erroneous measurement will have more influence on the result than all nine of the valid measurements together:

$$\text{Obj. Fn.} \propto \frac{1.0}{.0025} + \sum_{1}^{9} \frac{0.1}{.0025}$$

$$\propto \frac{1.0}{.0025} + \frac{.9}{.0025}$$

This effect was also observed on the SRB demonstration problem. Care must be exercised in the selection of the data to insure that erroneous data is culled out when only a few points are being used.

The Bayesian estimator weighs both the prior model and the test data. The greater the relative uncertainty a parameter or measurement has, the less its influence on the final result. Consequently, if the test data-sets are to have equal weight, they must have similar variances. To accomplish this, the test dwells should be taken at similar response levels. Care must be taken to insure that the important response measurements are well above the noise level or the uncertainty levels assigned to the measurement. The results of the Quarter-Scale Orbiter problem demonstrate clearly the preference of the estimators for the high confidence data and their disregard for model parameters or data assigned low relative confidence.

All of our experience with real test data indicates the importance of the analyst's involvement during the performance of the test. Questions continually arise which would be simple if asked during the test but whose answers fade quickly after its completion. Many steps and operations which took us considerable time will become trivial when the modal tests are conducted with the needs of the estimators in mind. Things as simple as putting the test forces on magnetic tape or deleting erroneous accelerometer readings will greatly simplify the development of improved analytic models.

6. CONCLUSIONS AND RECOMMENDATIONS

6.1 Conclusions

The formulation originally proposed for the estimation procedure has been extended in two ways. First, a linear perturbation technique was implemented to provide a better match between the "prior" model and the test results. Early in the project [2] it was found that the Phase I estimation procedure would not converge properly when the differences between the calculated and measured frequency response were excessive. A Phase 0 perturbation, using measured modal data not otherwise used explicitly, was implemented to provide an improved starting point for Phase I. The use of Phase 0 is optional.

Second, a procedure was developed for automatically generating mass and stiffness submatrices, given only the total mass and stiffness matrices themselves. This procedure offers an expedient alternative to acquiring component submatrices when the latter are not available. Limited application of the procedure to the Orbiter demonstration problem showed promising results.

Based on the extended formulation, a triad of computer codes has been developed, one for each phase of the estimation procedure. The first, FOCOR, calculates the Phase 0 first order correction and prepares input data files for the second. The second, ESTIMA, performs the Phase I estimation wherein the modal representation of the test article is adjusted to best fit the measured response. The third program, ESTIMB, uses the refined modal representation from Phase I to revise the dynamic model mass and stiffness matrices. The programs may be linked through computer data files but are otherwise executed individually.

Numerous examples have been run. These include the one, two, and three degree-of-freedom problems previously described in the interim report [2]. All of these used artifically generated "test" data and were somewhat unrealistic. They were primarily intended to provide independently verifiable check cases and to test the methodology under some extreme conditions. A fourth artificial example, a two degree-of-freedom close-mode problem, was also worked. When previously reported [2], the results were unsatisfactory. Subsequently, however, several input-data errors were discovered. When these were corrected, the estimators were able to find the correct solution. The revised results of this example are presented in Appendix 1.

In addition to the artificial problems, two real problems have been studied: the Quarter-Scale SRB and the Quarter-Scale Orbiter. All aspects of the methodology have been exercised and the results demonstrate the potential of this approach. The SRB problem provided good experience with real data and identified many of the difficulties one should anticipate, such as erroneous response readings, incorrect shaker polarity, incompatible analytic models, etc. One particularly important discovery was the need to retain all analytic modes in the frequency range of study.

Although the lack of a proper stiffness matrix for the SRB precluded the complete modification of the dynamic model, an incomplete modification was performed using the mass matrix only. The new model should provide a better fit of the test data, even though its physical significance remains questionable. The lack of a stiffness matrix to be scaled implies a high degree of confidence in the stiffness matrix, when in reality

this is not the case. Unrealistically high confidence in one part of the model may generate unrealistically large changes elsewhere. But the procedures did accomplish the objective of improving the match between model and test within the constraints applied. The resulting changes were a 15 percent reduction in the nose and frustum mass/inertia, a 20 to 30 percent reduction in the aft-motor mass/inertia, and a 60 to 80 percent increase in the nozzle mass/inertia.

The Quarter-Scale Orbiter problem was also studied with success. New analytic models were developed, using the first four to seven flexible body modes. From these, new mass and stiffness matrices were generated for one possible set of sub-matrices. The sub-matrices were developed using a modal technique developed for the project [2]. Although probably not as meaningful as the original component sub-matrices, this approach is a quick practical alternative. In each step and for almost every case, an improved model, as measured by the object function, was obtained.

The resulting Orbiter changes are a reduction in payload mass/inertia and an increase in wing-elevon mass/inertia. The payload change is in the range of 10 to 20 percent and the wing-elevon change is about 5 percent. Along with these mass changes are stiffness changes of about +2 to +4 percent for the fuselage, -2 percent for the wing-elevon, and +2 to +4 percent for the tail. Other sets of sub-matrices might produce other kinds of changes.

6.2 Recommendations

Upon reflection, all of our recommendations concerning the procedures and methodology described herein fall into three

categories: recommendations related to the operational use of the program, recommendations for further study using the programs as they presently stand, and recommendations for future expansion. Before addressing any of the recommendations in detail, it must be emphasized that the number one priority is to obtain more operational experience on a variety of problems. If the bulk of the operational-use recommendations are followed during the acquisition of this experience, a much better picture of the methodology and its potential for further development will be obtained. Based on our experience, we feel that the methodology shows significant promise, but this conclusion can only be verified with further operational use. Indeed, as more experience is obtained, many of the questions addressed in the Category II recommendations may be answered.

Category I - Recommendations for Current Operational Use

A complete and consistent analytic model should be available. First and foremost, both the prior model mass and stiffness matrices should be available including, whenever possible, the component sub-matrices. As discussed in Section 3, the results obtained on an incomplete model may be misleading since this implies perfection in the missing parts. Second, the analytic modes must be based on exactly the same mass matrix as is used for normalizing and calculating the orthogonality of the test modes. If the two sets of modes, model and test, are not based on exactly the same mass matrix the off-diagonal terms of the cross-orthogonality matrix are meaningless. Third, the analytic model should be a model of the test article and not a model of flight hardware which might be only approximated by the test article. Because we are

using test data to modify a mathematical model, the existence of known differences only clouds the issue. Fourth, the component sub-matrices should be made available for Phase II. The procedure described herein for generating component sub-matrices may have merit. It will, however, probably never provide as definitive a set of sub-matrices as provided by the finite-element model of the component.

The second set of Category I recommendations addresses the test data. The important aspect here is that the test data be complete and accurate. In most modal tests that we have been associated with, the emphasis has been on the mode shape. Once a nice clean mode is obtained, the rest of the test information is often forgotten. But for parameter identification just as much care must be given to recording the shaker forces, the shaker polarity, the shaker phases, and the shaker locations. Second, all of the test data (frequencies, forces, responses, phases, etc.) should be recorded on a common location. This will help insure that all of it is saved and that data from different surveys and dwells does not get mixed. Third, as discovered in the Orbiter example, the response data should have a large signal to noise ratio if the test data are to be useful. Unless the recorded levels are large compared to the assigned noise level, the test results will have little influence, even though the data may look good.

Another aspect of the test also requires mention. If a particular range of frequencies, say 1 to 100 Hz, is of interest, then all resonances within this frequency band should be investigated. Data germane to every test resonance discovered in this frequency band should be recorded. Likewise, an

experimental mode analogous to every analytic mode in this frequency band should be sought even if the experimental resonance is found outside the specified frequency band.

Finally a word about the First Order Correction. Two different methods were described (Section 4) for calculating the FOC perturbations. One uses frequency information only, and the other both frequency and mode information. Which approach to use depends on the accuracy of the mode shapes. If the mode data are good, use them; otherwise, use only the resonant frequency data to perturb the prior model.

Category II - Recommendations for Further Study Using the Existing Programs

Much has been learned about the methodology during the present study, but many new questions have also appeared (for examples, see Section 6). Many of these questions can be addressed using the programs as they now exist, or with very minor changes in the output.

Foremost, among the questions needing further study is the use of frequency-response data versus resonant-dwell data. The methodology has been formulated and structured to use frequency-response data but, to date, essentially only resonant-dwell data have been available. Experience with frequency-response data is needed since this approach might provide better estimates with less computer cost.

Many of the questions which have arisen relate to convergence: How should convergence be defined? How can convergence be accelerated? How sensitive is the result to the starting

point? Consequently, work should be performed to further investigate the step limit, the starting parameter values, the variance of the data, the variance of the parameters, and the effect of sequential estimation.

Another set of questions relates to the object function. In Phase II, it is dominated by the generalized-stiffness-matrix observations. Do these facts have implications which we are not presently aware of? Is it possible to normalize the object function so that different examples can be compared to a common standard?

Much attention has been given to the First Order Correction and the mode and frequency perturbation it produces. Nevertheless, further study should be made to establish more rigorously the meaning and accuracy of the changes produced and why the FOC modes seem to be degraded.

Further experience also needs to be obtained in using this methodology to estimate elements of the damping matrix and to develop criteria by which the important elements of [k] and [m] can be identified.

Category III - Recommendations for Further Development

When working with the Quarter-Scale SRB and Orbiter models, and the simple models too, there were a number of additional capabilities which would have been very helpful. Foremost among them would be the capability to plot the transfer functions, the frequency response functions, and the mode shapes. In addition, it would be helpful if the computation of the final set of modes based on the revised [M] and [K] matrices from Phase II was automatically performed by ESTIMB.

Should the additional experience obtained from Categories I and II substantiate our conclusions, the basic program constraints should be expanded. This would include enlarging the size of the models (degrees-of-freedom) that can be handled, adding the capability to sweep through the frequency band, adding the capability to apply linear constraints such as holding the total mass constant, and providing more interpretive output.

REFERENCES

1) J.D. Collins, G.C. Hart, T.K. Hasselman, B. Kennedy, "Statistical Identification of Structures," AIAA Journal, Vol. 12, No. 2, Feb. 1974.

2) L.T. Lee and T.K. Hasselman, "Model Verification of Large Structural Systems, Interim Report," J.H. Wiggins Company Report TR77-1267, June 1977.

3) J. Isenberg, "Generalization of Automated Data Analysis Application of Statistical Estimation of Geological Material Model Parameters," J.H. Wiggins Company Report 78-1319, submitted to Air Force Weapons Laboratory, July 1978.

4) Frank Bugg, "Vibration Analysis Math Model of the 1/4 Scale SRB Test Article," NASA-MSFC Report ED23-76-289, 17 Sept. 1976.

5) D.S. Levine, "Test Measurement List, Shuttle, One-Quarter Scale Ground Vibration Test," Rockwell International Report SD76-SH-0187, Nov. 1976.

6) Rockwell International - Space Division, "Quarter-Scale SRB, Modal Test, Data Sheets," Nov. 1976 to Jan. 1977.

7) Rockwell International - Space Division, "Quarter-Scale Orbiter Post Test Report," SSP-VSD-77-38.

8) J.A. Barrett and B.H. Ujihara, "Verification Analysis Report of Quarter-Scale Ground Vibration Test, Orbiter Element Soft Mounted," Rockwell International Report SD77-SH-0244, Oct. 1977.

9) Rockwell International - Space Division, "Quarter-Scale Orbiter, Modal Test, Data Files for Symmetric Modes: 124 DOF Stiffness Matrix, 124 DOF Mass Matrix, Accelerometer Model Transformation Matrix, Test Quadrature Response, Test Coincident Response, Test Frequencies (70 data sets)," 1978.

10) Rockwell International - Space Division, "Test Measurement List, Quarter-Scale Orbiter, Test Configuration 8, Soft Suspension, Ground Vibration Test," SD76-SH-0187.

11) J.C. Chen and B.K. Wada, "Matrix Perturbation for Structural Dynamic Analysis," 17th AIAA/ASME/SAE Structures, Structural Dynamics, and Materials Conference, May 1976.

12) J.A. Garba and B.K. Wada, "Application of Perturbation Methods to Improve Analytic Model Correlation with Test Data," 1977 SAE Aerospace meeting, 1977.

APPENDIX 1

Demonstration Problem

Two Degrees-of-Freedom

Close Modes

(Previously reported in a 1976 progress report)

Two Degree-of-Freedom Problem - Close Modes

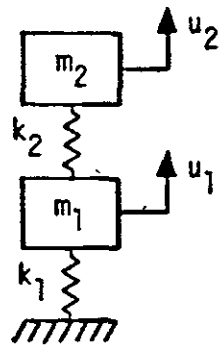

To investigate the effects of close modes on the estimator performance, the two degree-of-freedom model was adjusted to yield two resonant frequencies within 20 percent of each other (Figures 1 and 2).

The artficially generated "test" data is based on the following parameters:

$k_1 = 33.333$ $\quad k_2 = 1.0$

$m_1 = 28.83$ $\quad m_2 = .8649$

$\zeta_1 = .05$ $\quad \zeta_2 = .10$

The resulting frequencies and modes are:

$$\omega_1 = .98617 \text{ rad/sec}$$

$$\omega_2 = 1.17214$$

$$[\phi] = \begin{bmatrix} .12588 & .13726 \\ .79246 & -.72677 \end{bmatrix}$$

The sinusoidal forcing function was applied at node 1 with a magnitude of 1 pound. The prior model used here had these characteristics:

$$k_1 = 86.715 \qquad k_2 = 1.00$$

$$m_1 = 75.00 \qquad m_2 = .8649$$

$$\zeta_1 = .05 \qquad \zeta_2 = .10$$

$$[^{\circ}\phi] = \begin{bmatrix} .07943 & .08381 \\ .78044 & -.73967 \end{bmatrix}$$

which yields natural frequencies of 1.1091 and 1.1346 rad/sec.

Six different runs have been made to date of which three were previously described in the interim report (Reference [4]). At that time the estimator had not been able to effectively improve the model and our tentative conclusion was that the:

> prior model is so far off in its mass and stiffness that the sensitivity matrix elements are not representative of the true model. This is true even though the frequencies are well matched.

A recent review of that model in conjunction with the modifications that have been made to MOUSE and to ESTIMA uncovered a misapplication of the input data being used. This mistake resulted in (1) the actual prior model which the program was using being substantially different from what we thought it was, and (2) the observation data being totally unrepresentative of the "exact" model. This problem has been corrected and successful estimations have been accomplished using both the original MOUSE algorithm and the modified version.

RUN NO.	NO. TEST FREQ.	RANGE OF TEST FREQ. (RAD/SEC)	NO. TEST POINTS PER FREQUENCY	σ^2 FOR [K]	σ^2 FOR [M]	RESULTS
4A	10	.9-1.25	2	ALL .25	ALL .25	CONVERGED TO IMPROVED, STABLE MODEL IN 16 ITERATIONS
4B	10	.9-1.25	2	ALL .25	ALL .25	CONVERGED TO IMPROVED, STABLE MODEL IN 15 ITERATIONS

Variance of Data = .0016

The estimator now incorporates both a two-way step retarder and a maximum-change step ratarder. The first prevents increases in the RMS difference between the calculated and measured response. The second limits the amount which any parameter can change on any one iteration. Run 4A used the original MOUSE algorithm. The RMS difference was reduced from .215 at the start to .015 at the end. Run 4B was identical to run 4A except that the modified MOUSE algorithm was used. On this run the RMS error was reduced to .016. The difference in the two runs is accounted for by the fact that the modified algorithm gives slightly greater weight to the prior model.

Phase II of the estimation procedure was not performed on this example.

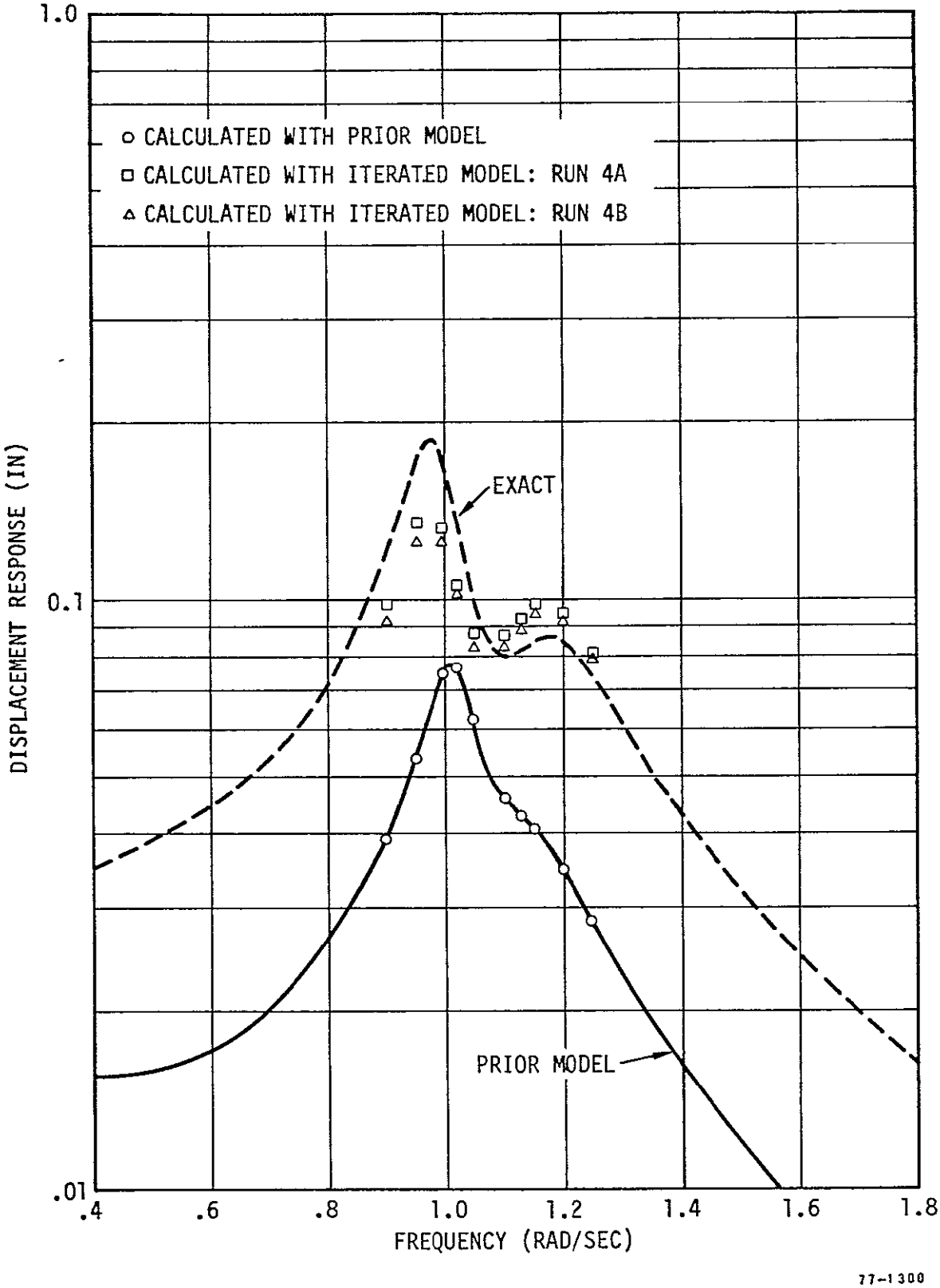

Figure 1. Frequency Response Plots - Example 4 - Close Modes, Node 1

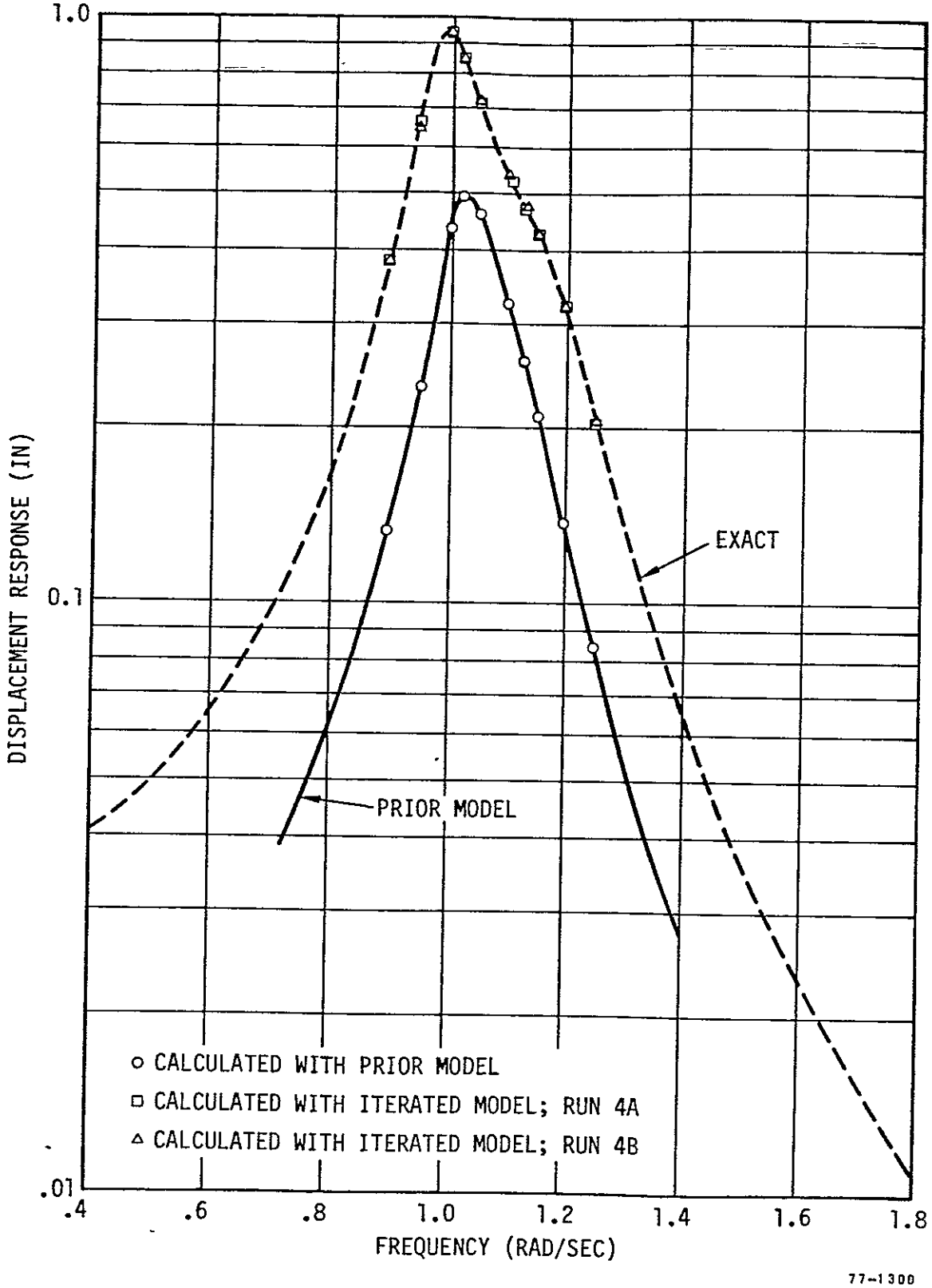

Figure 2. Frequency Response Plots - Example 4 - Close Modes, Node 2

APPENDIX 2

Quarter-Scale SRB

End-of-Action Time

Demonstration Problem

Supporting Data

LIST OF TABLES

Table 1. Quarter-Scale SRB: Accelerometer/Degree-of-Freedom Schedule

ITEM	DYNAMIC D. OF F. MODEL	ORIGINAL D. OF F. MODEL	DYNAMIC D. OF F. TEST	MODEL STATION X	DIRECTION	*NODE NO.	COEF.	ACCEL.	COEF.	ACCEL.	COEF.	ACCEL.	COEF.	ACCEL.	COEF.	ACCEL.	COEF.	ACCEL.
NOSE CAP	1	1	1	52.291	X	0	1.0	1X										
	2	2	2	52.291	Y	0	1.0	2Y										
	3	3	3	52.291	Z	0	1.0	3Z										
	4	4	-	52.291	θ_x	0	.0561	4Z	-.0561	6Z								
NOSE-FRUSTUM INTERFACE	5	7	-	68.750	X	1	.500	1X	.250	7X	.250	11X						
	6	8	4	68.750	Y	1	-.500	4Z	1.0	5Y	.500	6Z						
	7	9	5	68.750	Z	1	.500	4Z	.500	6Z								
	8	10	6	68.750	θ_x	1	.0561	4Z	-.0561	6Z								
FRUSTUM	9	13	-	82.500	X	2	.350	1X	.325	7X	.325	11X						
	10	14	-	82.500	Y	2	-.270	4Z	.54	5Y	.270	6Z	-.230	8Z	.230	12Z	460	10Y
	11	15	-	82.500	Z	2	.270	4Z	.270	6Z	.230	8Z	.230	12Z				
	12	16	-	82.500	θ_x	2	.0303	4Z	-.0303	6Z	.0123	8Z	-.0123	12Z				
	13	17	-	82.500	θ_y	2	.0268	7X	-.0536	9X	.0268	11X						
	14	18	-	82.500	θ_z	2	-.0268	7X	.0268	11X								
FRUSTUM-SEP. RING INTERFACE	15	19	7	98.750	X	3	.500	7X	.500	11X								
	16	20	8	98.750	Y	3	-.500	8Z	.500	12Z	1.0	10Y						
	17	21	9	98.750	Z	3	.500	8Z	.500	12Z								
	18	22	10	98.750	θ_x	3	.0268	8Z	-.0268	12Z								
	19	23	11	98.750	θ_y	3	.0268	7X	-.0536	9X	.0268	11X						
	20	24	12	98.750	θ_z	3	-.0268	7X	.0268	11X								
SEP. RING-FWD SKIRT INTERFACE	21	25	-	100.250	X	4	.500	7X	.500	11X								
	22	26	-	100.250	Y	4	-.500	8Z	.500	12Z	1.0	10Y						
	23	27	-	100.250	Z	4	.500	8Z	.500	12Z								
	24	28	-	100.250	θ_x	4	.0268	8Z	-.0268	12Z								
	25	30	-	100.250	θ_z	4	-.0268	7X	.0268	11X								
FWD SKIRT MOTOR INTERFACE	26	67	13	130.957	X	11	.500	16X	.500	18X								
	27	68	14	130.957	Y	11	1.0	15Y	-.500	17Z	.500	19Z						
	28	69	15	130.957	Z	11	.500	17Z	.500	19Z								
	29	70	16	130.957	θ_x	11	.0268	17Z	-.0268	19Z								
	--	71	17	130.957	θ_y	11	-.0536	14X	.0268	16X	.0268	18X						
	--	72	18	130.957	θ_z	11	-.0268	16X	.0268	18X								
MOTOR	30	73	--	166.250	X	12	.250	16X	.250	18X	.250	23X	.250	27X				
	31	74	19	166.250	Y	12	-.500	20Z	1.0	21Y	.500	22Z						
	32	75	20	166.250	Z	12	.500	20Z	.500	22Z								
	33	76	21	166.250	θ_x	12	.0268	20Z	-.0268	22Z								
	34	77	--	166.250	θ_y	12	-.0768	14X	.0134	16X	.0134	18X	.0134	23X	-0268	25X	.0134	27X
	35	78	--	166.250	θ_z	12	-.0134	16X	.0134	18X	.0134	23X	.0134	27X				
	36	85	22	201.500	X	17	.500	23X	.500	27X								
	37	86	23	201.500	Y	17	-.500	24Z	1.0	26Y	.500	28Z						
	38	87	24	201.500	Z	17	.500	24Z	.500	28Z								
	39	88	25	201.500	θ_x	17	.0268	24Z	-.0268	28Z								
	40	89	26	201.500	θ_y	17	.0268	23X	-.0536	25X	.0268	27X						
	41	90	27	201.500	θ_z	17	-.0268	23X	.0268	27X								

*In some tables the node number is added to 400.

Table 1. Quarter-Scale SRB: Accelerometer/Degree-of-Freedom Schedule (continued)

ITEM	DYNAMIC D. OF F. MODEL	ORIGINAL D. OF F. MODEL	DYNAMIC D OF F. TEST	MODEL STATION X	DIRECTION	NODE NO.	COEF.	ACCEL.	COEF.	ACCEL.	COEF.	ACCEL.	COEF.	ACCEL.	COEF.	ACCEL.	COEF.	ACCEL.
MOTOR (CON'T)	42	91	28	235.750	X	18	.500	31X	.500	33X								
	43	92	29	235.750	Y	18	1.0	30Y	-.500	32Z	.500	34Z						
	44	93	30	235.750	Z	18	.500	32Z	.500	34Z								
	45	94	31	235.750	θ_x	18	.0268	32Z	-.0268	34Z								
	46	95	32	235.750	θ_y	18	-.0536	29X	.0268	31X	.0268	33X						
	47	96	33	235.750	θ_z	18	-.0268	31X	.0268	33X								
	48	103	34	270.000	X	23	.500	35X	.500	39X								
	49	104	35	270.000	Y	23	-.500	36Z	1.0	38Y	.500	40Z						
	50	105	36	270.000	Z	23	.500	36Z	.500	40Z								
	51	106	37	270.000	θ_x	23	.0268	36Z	-.0268	40Z								
	52	107	38	270.000	θ_y	23	.0268	35X	-.0536	37X	.0268	39X						
	53	108	39	270.000	θ_z	23	-.0268	35X	.0268	39X								
	54	109	--	304.250	X	24	.250	35X	.250	39X	.250	46X	.250	48Z				
	55	110	40	304 250	Y	24	-.500	41Z	1 0	42Y	.500	43Z						
	56	111	41	304.250	Z	24	.500	41Z	.500	43Z								
	57	112	42	304.250	θ_x	24	.0268	41Z	-.0268	43Z								
	58	113	--	304.250	θ_y	24	0134	35X	-.0268	37X	.0134	39X	-.0268	44Z	.0134	46Z	.0134	48Z
	59	114	--	304.250	θ_z	24	-.0134	35X	.0134	39X	-.0134	46X	.0134	48X				
	60	121	43	338.500	X	29	.500	46X	.500	48X								
	61	122	44	338.500	Y	29	1.0	45Y	-.500	47Z	.500	49Z						
	62	123	45	338.500	Z	29	.500	47Z	.500	49Z								
	63	124	46	338.500	θ_x	29	-.0268	47Z	-.0268	49Z								
	64	125	47	338.500	θ_y	29	-.0536	44X	.0268	46X	.0268	48X						
	65	126	48	338.500	θ_z	29	-.0268	46X	.0268	48X								
	66	127	--	361.130	X	30	.250	46X	.250	48X	.250	59X	.250	63X				
	67	128	49	361.130	Y	30	-.500	50Z	1.0	51Y	.500	52Z						
	68	129	50	361.130	Z	30	.500	50Z	500	52Z								
	69	130	51	361.130	θ_x	30	.0268	50Z	-.0268	52Z								
	70	131	--	361.130	θ_y	30	-.0268	44Z	.0134	46Z	.0134	48X	.0134	59X	-.0268	61X	.0134	63X
	71	132	--	361.130	θ_z	30	-.0134	46X	.0134	48X	.0134	59X	.0134	63X				
	72	163	52	394.370	X	36	.500	59X	.500	63X								
	73	164	53	394.370	Y	36	-.500	60Z	1.0	62Y	.500	64Z						
	74	165	54	394.370	Z	36	.500	60Z	.500	64Z								
	75	166	55	394.370	θ_x	36	.0268	60Z	-.0268	64Z								
	76	167	56	394.370	θ_y	36	.0268	59X	-.0536	61X	.0268	63X						
	77	168	57	394.370	θ_z	36	-.0268	59X	.0268	63X								
	78	175	--	420.500	X	41	.300	59X	.300	63X	.200	68X	.200	70X				
	79	176	58	420.500	Y	41	-.500	65Z	1.0	66Y	.500	67Z						
	80	177	59	420.500	Z	41	.500	65Z	.500	67Z								
	81	178	60	420.500	θ_x	41	.0268	65Z	-.0268	67Z								
	82	179	--	420.500	θ_y	41	.01608	59X	-.03216	61X	.01608	63X	.01072	68X	.01072	70X	-.02144	72X
	83	180	--	420 500	θ_z	41	-.01608	59X	.01608	63X	-.01608	68X	01608	70X				

Table 1. Quarter-Scale SRB: Accelerometer/Degree-of-Freedom Schedule (continued)

ITEM	DYNAMIC D. OF F. MODEL	ORIGINAL D. OF F. MODEL	DYNAMIC D. OF F. TEST	MODEL STATION X	DIRECTION	NODE NO.	COEF.	ACCEL.	COEF.	ACCEL.	COEF.	ACCEL.	COEF.	ACCEL.	COEF.	ACCEL.	COEF.	ACCEL.
MOTOR (CON'T)	84	181	61	459.272	X	42	.500	68X	.500	70X								
	85	182	62	459.272	Y	42	-.500	69Z	.500	71Z	1.0	73Y						
	86	183	63	459.272	Z	42	.500	69Z	.500	71Z								
	87	184	64	459.272	θ_x	42	.0268	69Z	-.0268	71Z								
	88	185	65	459.272	θ_y	42	.0268	68X	.0268	70X	-.0536	72X						
	89	186	66	459.272	θ_z	42	-.0268	68X	.0268	70X								
LAUNCH PAD NODES	90	193	--	483.988	X	46	.3061	80X	.9178	82X	-.2239	84						
	91	194	--	483.988	Y	46	.7650	81Z	.235	85Z								
	92	195	--	483.988	Z	46	-.9589	81Z	1.0	83Y	.9589	85Z						
	93	196	--	483.988	θ_x	46	.0197	81Z	-.0197	85Z								
	94	198	--	483.988	θ_z	46	-.0197	80X	.0197	84X								
	95	199	--	483.988	X	47	-.2239	80X	.9178	82X	.3061	84X						
	96	200	--	483.988	Y	47	.2350	81Z	.7650	85Z								
	97	201	--	483.988	Z	47	-.9589	81Z	1.0	83Y	.9589	85Z						
	98	202	--	483.988	θ_x	47	.0197	81Z	-.0197	85Z								
	99	204	--	483.988	θ_z	47	.0197	80X	-.0197	84X								
	100	205	--	483.988	X	48	.6939	80X	-.9178	82X	1.2239	84X						
	101	206	--	483.988	Y	48	.2350	81Z	.765	85Z								
	102	207	--	483.988	Z	48	-.0411	81Z	1.0	83Y	.0411	85Z						
	103	208	--	483.988	θ_x	48	.0197	81Z	-.0197	85Z								
	104	210	--	483.988	θ_z	48	-.0197	80X	.0197	84X								
	105	211	--	483.988	X	49	1.2239	80X	-.9178	82X	.6939	84X						
	106	212	--	483.988	Y	49	.7650	81Z	.2350	85Z								
	107	213	--	483.988	Z	49	-.0411	81Z	1.0	83Y	.0411	85Z						
	108	214	--	483.988	θ_x	49	.0197	81Z	-.0197	85Z								
	109	216	--	483.988	θ_z	49	-.0197	80X	.0197	84X								
---	---	---	67	479.280	X	--	.500	80X	.500	84X								
	---	---	68	479.280	Y	--	-.500	81Z	1.0	83Y	.500	85Z						
	---	---	69	479.280	Z	--	.500	81Z	.500	85Z								
	---	---	70	479.280	θ_x	--	.0197	81Z	-.0197	85Z								
	---	---	71	479.280	θ_y	--	.0197	80X	-.0394	82X	.0197	84X						
	---	---	72	479.280	θ_z	--	-.0197	80X	.0197	84X								
AFT DOME	110	217	73	468.800	X	50	.500	74X	.500	78X								
	111	218	74	468.800	Y	50	-.500	75Z	1.0	77Y	.500	79Z						
	112	219	75	468.800	Z	50	.500	75Z	.500	79Z								
	113	220	76	468.800	θ_x	50	.0403	75Z	-.0403	79Z								
	114	221	77	468.800	θ_y	50	.0403	74X	-.0806	76X	.0403	78X						
	115	222	78	468.800	θ_z	50	-.0403	74X	.0403	78X								
NOZZLE c.g.	116	229	--	468.722	X	52	.500	74X	.500	78X								
	117	230	--	468.722	Y	52	-.500	75Z	1.0	77Y	.500	79Z						
	118	231	--	468.722	Z	52	.500	75Z	.500	79Z								
	119	232	--	468.722	θ_x	52	.0403	75Z	-.0403	79Z								
	120	233	--	468.722	θ_y	52	.0403	74X	-.0806	76X	.0403	78X						
	121	234	--	468.722	θ_z	52	-.0403	74X	.0403	78X								

Table 2. Quarter-Scale SRB: Shaker Catalog

$$F_i = \sum_{j=1}^{N} \text{COEF}(j) * \text{Shaker Force } j$$

DYNAMIC D. OF F. MODEL	ORIGINAL D. OF F. MODEL	DYNAMIC D. OF F. TEST	MODEL STATION X	DIRECTION	NODE NO.	COEF.	SHAKER	COEF.	SHAKER	COEF.	SHAKER	COEF.	SHAKER
27	68	14	130.957	Y	11	1.0	BT02Y	-1.0	BB02Y				
28	69	15	130.957	Z	11	-1.0	BR04Z	1.0	BL04Z				
29	70	16	130.957	θ_x	11	-18.25	BT02Y	-18.25	BB02Y	-18.25	BR04Z	-18.25	BL04Z
43	92	29	235.750	Y	18	1.0	BT06Y	-1.0	BB06Y				
44	93	30	235.750	Z	18	-1.0	BR08Z	1.0	BL08Z	1.0	BB10Z		
45	94	31	235.750	θ_x	18	-18.25	BT06Y	-18.25	BB06Y	18.25	BR08Z	18.25	BL08Z
61	122	44	338.500	Y	29	1.0	BT12Y	-1.0	BB12Y	1.0	BL14Y		
62	123	45	338.500	Z	29	-1.0	BR16Z	1.0	BL16Z				
63	124	46	338.500	θ_x	29	-18.25	BT12Y	-18.25	BB12Y	18.25	BR16Z	18.25	BL16Z
85	182	62	459.272	Y	42	1.0	BB20Y	-1.0	BB20Y				
86	183	63	459.272	Z	42	-1.0	BR18Z	1.0	BL18Z				
87	184	64	459.272	θ_x	42	18.25	BR18Z	18.25	BL18Z	-18.25	BT20Y	-18.25	BB20Y
116	229	--	468.722	X	52	-1.0	BT22X	-1.0	BB22X				
120	233	--	468.722	θ_y	52	-10.0	BT22X	10.0	BB22X				

Calculated Test Response and System Damping

The test modes are obtained using the accelerometer transformation matrix and the measured quadrature response:

$$\left\{\phi_{test}\right\} = [T] \left\{\begin{matrix}\text{quadrature} \\ \text{acceleration}\end{matrix}\right\}$$

where [T] = defined in Table 1

$\{acc\}$ = defined in Reference [6] for 85 accelerometers

The response that should have been measured at each coordinate during the test can be calculated using the "measured" modes, frequency, damping, and force vector. This was done for eight coordinates and the results are summarized in Table 3. The most prominent discovery from this comparison is that the measured damping values are usually inadequate to describe the vehicle response under the test excitation levels. The small scatter in X(measured)/X(calculated) for the in-line coordinates indicates that by adjusting ζ a very good match can be obtained. The adjusted values for ζ, as shown in Table 4, were taken as input values for our identification procedure.

$$(\text{adjusted } \zeta) = (1/\rho)(\text{measured } \zeta)$$

Table 3. Quarter-Scale SRB: Estimate of Modal Damping for Analytic Modes

COORDINATE NO	COORDINATE DIR.	MEASURED A (IN)	CALCULATED B (IN)	RATIO $\rho = A/B$	AVERAGE RATIO $(\bar{\rho})$
MODE 1 - FIRST Y-BENDING					
2	Y	.03319	.01533	2.165	
3	Z	.00545	.00507	-----	
27	Y	.00741	.00342	2.167	
37	Y	.01087	.00483	2.251	2.177
49	Y	.02053	00932	2 203	
67	Y	.01321	.00615	2.148	
73	Y	00709	.00334	2.123	
85	Y	.00874	.00401	2.180	
MODE 2 - FIRST Z-BENDING					
2	Y	.01056	01076	-----	
3	Z	.03005	.02518	1.193	
28	Z	.00551	.00459	1.200	
38	Z	.00858	.00719	1.193	1.197
50	Z	.01623	.01358	1.195	
68	Z	.01216	.01015	1.198	
74	Z	.00661	.00552	1.197	
86	Z	.00687	.00572	1.201	
MODE 3 - SECOND Z-BENDING					
2	Y	.00081	.00126	-----	
3	Z	.00633	.00975	0 649	
28	Z	.00136	.00210	0.648	
38	Z	00191	00294	0.650	
50	Z	.00041	00062	0.661	0.649
68	Z	.00207	.00321	0.645	
74	Z	00178	.00275	0.647	
112	Z	.00070	00109	0.642	
MODE 4 - SECOND Y-BENDING					
2	Y	.00510	.00486	1 049	
3	Z	.00078	.00066	-----	
27	Y	.00095	.00092	1.033	
37	Y	.00191	.00183	1.043	1.044
49	Y	.00038	00036	1.056	
67	Y	.00180	00172	1.047	
73	Y	.00169	.00162	1.043	
85	Y	.00026	.00025	1 040	

Table 3. Quarter-Scale SRB: Estimate of Modal Damping for Analytic Modes (continued)

COORDINATE NO.	COORDINATE DIR	MEASURED A (IN)	CALCULATED B (IN)	RATIO ρ = A/B	AVERAGE RATIO ($\bar{\rho}$)
MODE 5 - FIRST TORSION					
4	θ_x	.7539 E-4	.5331 E-4	1.414	
12	θ_x	.7049 E-4	.4981 E-4	1.415	
29	θ_x	.5422 E-4	.3850 E-4	1.408	
39	θ_x	.3761 E-4	.2652 E-4	1.418	1.420
51	θ_x	.2144 E-4	.1522 E-4	1.409	
63	θ_x	.0695 E-4	.0485 E-4	1.433	
75	θ_x	.2621 E-4	.1845 E-4	1.421	
87	θ_x	.5730 E-4	.3978 E-4	1.440	
MODE 6 - FIRST AXIAL					
1	X	.002378	.002322	1.0241	
9	X	.002041	.001994	1.0235	
26	X	.001173	.001148	1.0218	
36	X	.000768	.000751	1.0226	1.0241
48	X	.000205	.000199	1.0302	
60	X	.000444	.000433	1.0254	
72	X	.000747	.000730	1.0233	
84	X	.001283	.001255	1.0223	
MODE 7 - THIRD Z-BENDING					
2	Y	.000046	.000047	-----	
3	Z	.002254	.001569	1.437	
28	Z	.000586	.000408	1.436	
38	Z	.000140	.000100	1.400	1.429
50	Z	.000430	.000301	1 429	
68	Z	.000277	.000195	1.421	
74	Z	.000398	.000280	1.421	
86	Z	.000051	.000035	1.457	
MODE 8 - THIRD Y-BENDING					
2	Y	.002221	.001367	1.624	
3	Z	.000157	.000093	-----	
27	Y	.000647	.000399	1.621	
37	Y	.000118	.000035	DISREGARD	1.653
49	Y	.000708	.000426	1.662	
67	Y	.000292	.000180	1.622	
73	Y	.000476	.000294	1.619	
85	Y	.000023	.000013	1.769	

Table 4. Quarter-Scale SRB: Modal Damping Factors

MODE NO.		MODE DESCRIPTION	DAMPING RATIO (ζ)	
ANAL.	TEST		TEST (FROM REF.[3])	ADJUSTED (USED IN ESTIMA)
10	12	FIRST Y-BENDING	.0168	.0077
9	14	FIRST Z-BENDING	.0074	.0062
11	NA	LAUNCH PADS MODE	NA*	(.0050)#
12	NA	LAUNCH PADS MODE COUPLED WITH SECOND Y-BENDING	NA	(.0070)
13	NA	LAUNCH PADS MODE COUPLED WITH SECOND Z-BENDING	NA	(.0050)
14	NA	LAUNCH PADS MODE COUPLED WITH SECOND Y-BENDING	NA	(.0070)
15	NA	LAUNCH PADS MODE COUPLED WITH SECOND Z-BENDING	NA	(.0050)
16	7	SECOND Z-BENDING COUPLED WITH LAUNCH PADS	.0034	.0052
17	NA	LAUNCH PADS MODE COUPLED WITH SECOND BENDING	NA	(.0070)
18	6	SECOND Y-BENDING COUPLED WITH LAUNCH PADS	.0072	.0069
19	NA	LAUNCH PADS MODE	NA	(.0050)
20	8	FIRST TORSION	.0070	.0049
21	NA	LAUNCH PADS MODE COUPLED WITH THIRD Z-BENDING	NA	(.0070)
22	11	THIRD Y-BENDING	.0125	.0076
23	10	THIRD Z-BENDING	.0077	.0054
24	9	FIRST AXIAL	.0079	.0077

* NA = NOT AVAILABLE
\# ( ) = ESTIMATED FROM SECOND BENDING MODE WITH DATA

Table 5. Quarter-Scale SRB: Test Data Used for Parameter Identification

NODE	X-STATION	D. OF F.	DIRECTION	VALUE (INCH)	COEFFICIENT OF VARIATION %
TEST MODE 1					
400	52.291	2	Y	.03319	5 4
400	-------	3	Z	.00545	14.1
411	130.957	27	Y	.00741	12.9
417	201.500	37	Y	.01087	9 4
423	270.000	49	Y	.02053	6 5
430	361.130	67	Y	.01321	8 4
436	394.370	73	Y	.00709	13.4
442	459.272	85	Y	.00874	11.3
TEST MODE 2					
400	52.291	2	Y	.01056	8.3
400	-------	3	Z	.03005	5.5
411	130.957	28	Z	.00551	9.6
417	201.500	38	Z	.00858	6.8
423	270.000	50	Z	.01623	4.7
430	361.130	68	Z	.01216	5.4
436	394.370	74	Z	.00661	8.3
442	459.272	86	Z	.00687	8.0
TEST MODE 3					
400	52.291	2	Y	.00081	13.7
400	-------	3	Z	.00633	5 3
411	130 957	28	Z	.00136	6.4
417	201.500	38	Z	.00191	5 2
423	270.000	50	Z	.00041	18.3
430	361.130	68	Z	.00207	5.0
436	394.370	74	Z	.00178	5 4
450	468.800	112	Z	.00070	11 0
TEST MODE 4					
400	52 291	2	Y	.00509	5.4
400	-------	3	Z	.00078	13.8
411	130.957	27	Y	.00095	13.7
417	201.500	37	Y	.00191	8.2
423	270.000	49	Y	.00038	32 5
430	361.130	67	Y	.00180	8 5
436	394.370	73	Y	.00169	8 8
442	459.272	85	Y	.00026	47.3

Table 5. Quarter-Scale SRB: Test Data Used for Parameter Identification (continued)

NODE	X-STATION	D OF F.	DIRECTION	VALUE (INCH)	COEFFICIENT OF VARIATION %
TEST MODE 5					
400	52.291	4	θ_x	.00008	7.6
402	82.500	12	θ_x	.00007	4.9
411	130.957	29	θ_x	00005	5.7
417	201.500	39	θ_x	.00004	7.3
423	270.000	51	θ_x	.00002	11 8
429		63	θ_x	00001	34.9
436	394.370	75	θ_x	.00003	9.9
442	459 272	87	θ_x	.00006	5.5
TEST MODE 6					
400	52.291	1	X	.00238	5.3
402	82.500	9	X	.00204	3.2
411	130.957	26	X	.00012	4.3
417	201.500	36	X	.00077	5.3
423	270.000	48	X	.00020	15.4
429		60	X	.00044	7 8
436	394.370	72	X	.00075	5.4
442	459 272	84	X	.00128	4 3
TEST MODE 7					
400	52.291	2	Y	.00005	85.5
400	-------	3	Z	.00225	5.3
411	130.957	28	Z	.00059	6.0
417	201.500	38	Z	.00014	20.4
423	270.000	50	Z	.00043	7.4
430	361.130	68	Z	.00028	10.8
436	394.370	74	Z	.00040	7.9
442	459.272	86	Z	.00005	54 7
TEST MODE 8					
400	52.291	2	Y	.00222	5.3
400	-------	3	Z	.00016	24.0
411	130.957	27	Y	.00065	8.3
417	201.500	37	Y	.00012	38.4
423	270.000	49	Y	.00071	8.0
430	361.130	67	Y	.00029	16.3
436	394.370	73	Y	.00048	10.8
442	459.272	85	Y	.00002	193 3

APPENDIX 3

Quarter-Scale Orbiter

Symmetric Modes

Demonstration Problem

Supporting Data

LIST OF TABLES

Table 1. Quarter-Scale Orbiter: Degree-of-Freedom Schedule

NODE	DESCRIPTION	COORDINATES			SYMMETRIC MODES					
		X	Y	Z	X	Y	Z	θ_x	θ_y	θ_z
1	FUSELAGE ORB	270 0	0.	346 0	1	---	2	---	---	---
2	FWD LANDING GEAR, DRAG	327 84	21 0	329 34	---	---	---	---	---	---
3	FWD RCS MODULE	317.7	24 2	365.3	3	---	4	---	---	---
4	FWD LANDING GEAR, MAIN	375 5	21.0	298 0	---	---	---	---	---	---
5	FUSELAGE ORB	378 09	0	353 2	5	---	6	---	7	---
6	LUMPED CABIN	497 0	0	395 0	8	---	9	---	10	---
7	FUSELAGE ORB	447.39	0.	363 74	---	---	---	---	---	---
8	FUSELAGE ORB	582.0	0.	340 0	11	---	12	---	13	---
9	FUSELAGE ORB	750 0	0	310.0	14	---	15	---	16	---
10	FUSELAGE ORB	979 5	0	310 0	18	---	19	---	20	---
13	FUSELAGE ORB	1140 0	0	310 0	30	---	31	---	32	---
16	WING TIE	807.0	105.	308 549	---	---	---	---	---	---
17	WING	835 0	141 16	305.891	---	---	---	---	---	---
18	WING	949 25	159 649	303.386	---	---	---	---	---	---
19	WING	1050 346	201 59	300 029	---	---	---	---	---	---
20	WING	1040 0	167.0	303 965	---	---	---	---	---	---
21	WING TIE	1040 0	105 0	306 909	---	---	---	---	---	---
22	WING	1071.299	195 022	302.927	---	---	---	---	---	---
23	LANDING GEAR, UPLOCK	1107.5	136.0	336 031	---	---	---	---	---	---
223	MAIN LANDING GEAR, DRAG	1097.5	136.0	321.7	---	---	---	---	---	---
24	WING	1103 45	247 42	299 078	---	---	---	---	---	---
25	WING	1127 272	251.321	302.225	---	---	55	---	---	---
26	WING	1139 33	194.951	303 713	---	---	56	---	---	---
27	WING	1163 299	307 295	301.827	---	---	---	---	---	---
28	LANDING GEAR, MAIN	1180 0	136 0	283 0	---	---	---	---	---	---
29	WING	1191 0	315 099	304 914	---	---	59	---	---	---
30	WING	1191.0	251.093	304 711	---	57	58	---	---	---
31	WING	1191 0	167.0	300.782	---	---	---	---	---	---
32	WING TIE	1191 0	105 0	297.614	---	---	---	---	---	---
33	WING	1222.552	366 56	304.5	---	---	---	---	---	---
34	WING	1252 517	396.564	305 824	---	---	---	---	---	---
35	WING	1249.0	373.154	307.267	---	---	62	---	---	---
36	WING		309 728	305.913	---	---	61	---	---	---
37	WING		251.267	302.815	---	---	---	---	---	---
38	WING		195.373	299 094	---	---	60	---	---	---
39	WING		144 98	295 253	---	---	---	---	---	---
40	WING TIE	1249.0	105 0	292.859	---	---	---	---	---	---
41	WING	1275.702	399 89	308 253	---	---	---	---	---	---
42	WING	1282.198	423 50	307 166	---	---	---	---	---	---
50	WING TIE	1307 0	105 0	288.2	---	---	---	---	---	---
52	WING	1365.0	432 671	306 668	69	---	70	---	---	---
53	WING		400 247	304 347	---	---	---	---	---	---
54	WING		370.317	302 215	---	---	68	---	---	---
55	WING		310 456	297 958	66	---	67	---	---	---
56	WING		252.087	293 848	---	---	65	---	---	---
57	WING		196 204	290 022	63	---	64	---	---	---
58	WING	1365 0	145 806	286 597	---	---	---	---	---	---

Table 1. Quarter-Scale Orbiter: Degree-of-Freedom Schedule (continued)

NODE	DESCRIPTION	COORDINATES			SYMMETRIC MODES					
		X	Y	Z	X	Y	Z	θ_x	θ_y	θ_z
407	ELEVON	1425 0	146.009	284 38	71	---	---	---	---	---
408	ELEVON	1421 905	210.387	288 662	---	---	---	---	---	---
409	ELEVON	1417.95	280 252	293 331	72	---	---	---	---	---
410	ELEVON	1414.53	340.633	297 392	73	---	---	---	---	---
411	ELEVON	1411.986	385 542	300.438	---	---	---	---	---	---
412	ELEVON	1409.3	432.943	303.689	74	---	---	---	---	---
413	ELEVON	1489.2	145 91	285.464	---	---	75	---	---	---
414	ELEVON	1477.499	210.308	289.521	---	76	77	---	---	---
415	ELEVON	1464 8	280.212	293.762	---	---	78	---	---	---
416	ELEVON	1453 65	340.622	297.506	---	---	79	---	---	---
417	ELEVON	1444 979	385.556	300.291	---	80	81	---	---	---
418	ELEVON	1435 825	432.982	303.266	---	---	82	---	---	---
59	FUSELAGE ORB	1438.0	0.	409.5	105	106	107	---	108	109
194	OMS FUEL TANK	1422.301	71.725	501.007	110	111	112	---	113	114
195	OMS OX TANK	1422 301	109.98	461.393	---	---	---	---	---	---
196	RCS FUEL TANK	1340.321	66 953	489.99	103	---	---	---	---	---
197	RCS OX TANK	1340.321	98 838	456 973	104	---	---	---	---	---
198	RCS STRUCTURE	1436.3	89 8	463.2	---	---	---	---	---	---
199	RCS STRUCTURE	1532 6	128 3	463 2	124	---	---	---	---	---
62	UPPER ENGINE C.G	1476.0	0.	453 0	115	---	116	---	117	---
63	UPPER ENGINE GIMBAL	1445 0	0	443.0	---	---	---	---	---	---
64	LOWER ENGINE C G	1503 557	55.167	348 891	118	119	120	121	122	123
918	LOWER PR LOX PUMP	1471 836	31.663	321.202	51	---	---	---	---	---
919	LOWER PR LH2 PUMP	1464.947	73 842	363 621	50	---	---	---	---	---
65	LOWER ENGINE GIMBAL	1468 17	53.0	342.64	---	---	---	---	---	---
66	FUSELAGE ORB	1496 0	0	400 0	52	---	53	---	54	---
67	ORBITER BODY FLAP	1560.35	0	287.081	83	---	84	---	---	---
68	VERTICAL TAIL	1309.5	0.	500.109	---	---	---	---	---	---
69	↓	1392 811	0	593.254	85	---	---	---	---	---
70		1426.517	0.	516.806	---	---	---	---	---	---
71		1449 917	0.	550 62	86	---	87	---	---	---
72		1506.778	0.	626.783	89	---	90	---	---	---
73		1521.23	0.	662.639	88	---	---	---	---	---
74		1533.107	0	550.62	---	---	---	---	---	---
75		1533.107	0	740 884	---	---	---	---	---	---
76		1570 898	0.	712.67	91	---	92	---	---	---
77		1579.783	0	790.0	---	---	---	---	---	---
78		1628 629	0	790 0	93	---	94	---	---	---
79	VERTICAL TAIL	1670 159	0.	790 0	---	---	---	---	---	---
80	LOWER RUDDER	1556 092	0.125	636 787	95	---	96	---	---	---
81	LOWER RUDDER	1564.415	↓	587.137	---	97	---	---	---	---
82	LOWER RUDDER	1597.888		640.596	---	98	---	---	---	---
83	UPPER RUDDER	1614.919		721.324	99	---	100	---	---	---
84	UPPER RUDDER	1622 048		674.027	---	101	---	---	---	---
85	UPPER RUDDER	1656.537	0.125	743 226	---	102	---	---	---	---
90	ORBITER/LT FWD ATTACH PT	388 142	0.0	283.143	---	---	---	---	---	---
91	ORBITER/ET AFT ATTACH PT.	1317 0	96.5	267 556	---	---	---	---	---	---

Table 1. Quarter-Scale Orbiter: Degree-of-Freedom Schedule (continued)

NODE	DESCRIPTION	COORDINATES			SYMMETRIC MODES					
		X	Y	Z	X	Y	Z	θ_x	θ_y	θ_z
95	ORB	1324.0	0.	340 0	34	---	35	---	36	---
650	STA 1307 BLKHD	1307 0	26.25	470.134	---	---	---	---	---	---
651			26 25	456.714	38	---	---	---	---	---
652			52.5	427.16	39	---	---	---	---	---
653			78.75	410 0	42	---	---	---	---	---
654			94 0	368 0	44	---	---	---	---	---
655	STA. 1307 BLKHD		94.0	338 877	46	---	---	---	---	---
656	RT GYRO		26.25	286.375	48	---	---	---	---	---
657	RT. GYRO		0.0	285 375	47	---	---	---	---	---
658	STA. 1307 BLKHD		52 5	286 375	---	---	---	---	---	---
659			0 0	407.0	40	---	---	---	---	---
660			0 0	385.0	43	---	---	---	---	---
662			0 0	470.134	37	---	---	---	---	---
663			26.25	427 16	---	---	---	---	---	---
664	STA 1307 BLKHD		52.5	410.0	---	---	---	---	---	---
665	RT GYRO		100 0	354.0	45	---	---	---	---	---
666	STA. 1307 BLKHD		26 25	410.0	41	---	---	---	---	---
850	AFT BLKHD	1307.0	0.	261.036	49	---	---	---	---	---
86	CARGO	1069 0	0.	400.0	26	---	27	---	28	---
87	LONGERON ATTACH		94.0	414.0	22	23	24	---	---	---
88	KEEL ATTACH		0.	305.0	25	---	---	---	---	---
888	KEEL FITTING 2 (NO TIE)		0	305.0	---	---	---	---	---	---
89	BRIDGE FITTING	1069.0	94 0	410.0	---	---	---	---	---	---
151	CARGO ATTACH - LONG.	582 0	94 0	410 0	---	---	---	---	---	---
152	- KEEL	636.0	0.	305.0	---	---	---	---	---	---
153	- LONG.	636.0	94 0	410.0	---	---	---	---	---	---
154	- KEEL	693.0	0	305 0	---	---	---	---	---	---
155	- LONG.	693.0	94 0	410.0	---	---	---	---	---	---
158	- KEEL	750 0	0	305.0	---	---	---	---	---	---
159	- LONG	750.0	94.0	410.0	---	17	---	---	---	---
160	- KEEL	807.0	0.	305 0	---	---	---	---	---	---
161	- LONG.	807 0	94 0	410 0	---	---	---	---	---	---
162	- KEEL	863 0	0.	305 0	---	---	---	---	---	---
163	- LONG	863 0	94 0	410.0	---	---	---	---	---	---
164	- KEEL	919 0	0.	305.0	---	---	---	---	---	---
165	- LONG.	919.0	94.0	410.0	---	---	---	---	---	---
166	- KEEL	979 0	0.	305 0	---	---	---	---	---	---
167	- LONG.	979.0	94 0	410 0	---	21	---	---	---	---
168	- KEEL	1040.0	0	305 0	---	---	---	---	---	---
169	- LONG	1040 0	94 0	410.0	---	---	---	---	---	---
170	- KEEL	1090 33	0	305.0	---	---	---	---	---	---
171	- LONG	1090.33	94.0	410.0	---	29	---	---	---	---
174	- KEEL	1140 67	0.	305.0	---	---	---	---	---	---
175	- LONG.	1140.67	94 0	410.0	---	33	---	---	---	---
176	- KEEL	1191.0	0	305.0	---	---	---	---	---	---
177	- LONG.	1191.0	94.0	410 0	---	---	---	---	---	---
178	- KEEL	1249 0	0.	305 0	---	---	---	---	---	---
179	- LONG.	1249 0	94 0	410 0	---	---	---	---	---	---
183	- LONG.	1303 0	94 0	410 0	---	---	---	---	---	---
184	- KEEL	1307.0	0.	305 0	---	---	---	---	---	---
185	CARGO ATTACH - LONG	1307 0	94.0	410 0	---	---	---	---	---	---

- ONLY THE +Y HALF OF THE VEHICLE IS REPRESENTED IN THE MODEL DEFINED HERE, THE RIGHT SIDE
- COORDINATE VALUES ARE FOR A FULL SCALE MODEL

Table 2. Quarter-Scale Orbiter: Shaker Catalog - Symmetric Modes

$$F_i = \sum_{j=1}^{N} \text{COEF}(j) * \text{Shaker Force } j$$

DYNAMIC D. OF F. MODEL (i)	LOCATION	DIRECTION	NODE NO.	COEF.	SHAKER	COEF.	SHAKER	COEF.	SHAKER
6	FUSELAGE	Z	5	-0.50	FT60Z				
15	FUSELAGE	Z	9	+0.50	FL62Z	+0.50	FR62Z		
17	CARGO ATTACHMENT	Y	159	-0.50	FL63Y	-0.50	FR63Y		
58	WING	Z	30	-0.50	WL67Z	-0.50	WR67Z		
68	WING	Z	54	-0.50	WL68Z	-0.50	WR68Z		
82	ELEVON	Z	418	+0.50	WL69Z	+0.50	WR69Z		
53	FUSELAGE ORB.	Z	66	+0.50	FL66Z	+0.50	FR66Z		
78	ELEVON	Z	415	+0.50	WL70Z	+0.50	WR70Z		
89	VERTICAL TAIL	X	72	+0.3536	VF71XZ				
90	VERTICAL TAIL	Z	72	-0.3536	VF71XZ				
29	CARGO ATTACHMENT	Y	171	-0.50	FL64Y				
124	RCS STRUCTURE	X	199	-0.50	OE75X				
115	UPPER ENGINE	X	62	-0.3536	MT74XZ				
116	UPPER ENGINE	Z	62	-0.3536	MT74XZ				
118	LOWER ENGINE	X	64	-0.4915	MR73XZ	-0.4915	ML73XZ		
119	LOWER ENGINE	Y	64	-0.0301	MR73XZ	-0.0301	ML73XZ	-0.50	FL65Y
120	LOWER ENGINE	Z	64	-0.0867	MR73XZ	-0.0867	ML73XZ		

Calculated Test Response and System Damping

The test modes are obtained using the accelerometer transformation matrix and the measured quadrature response:

$$\left\{\phi_{Test}\right\} = [T] \left\{\begin{matrix}\text{quadrature} \\ \text{acceleration}\end{matrix}\right\}$$

where $[T]$ = accelerometer transformation matrix, Reference [9]

$\left\{acc\right\}$ = defined in Reference [9] for 240 accelerometers and 42 test data sets

For these data sets corresponding to vehicle modes, the response that should have been measured at each coordinate can be calculated using the "measured" modes, frequency, force vector. This was done for the six lowest flexible modes and the results for the largest ten responses are presented in Table 3. A modal damping of 1% was used to make the calculations. By comparing the calculated responses, based on $\zeta = .01$, to the measured responses one can obtain the actual system modal damping (Table 3).

Table 3. Quarter-Scale Orbiter: Estimate of Modal Damping for Analytic Modes 4,5,6,7,9,10

DEGREE OF FREEDOM	DIRECTION	ⓐ* TOTAL MEASURED RESPONSE (10^{-4}IN)	ⓑ TOTAL CALCULATED RESPONSE (10^{-4}IN)	$\rho = ⓑ/ⓐ$	$\bar{\rho}$
TEST DATA SET 4 = ANALYTIC MODE 4; f = 19.384 hz					
6	FUSELAGE Z	6.8652	106.4067	15.4994	
88	TAIL X	11.3057	175.7258	15.5430	
91	TAIL X	14.1718	220.2382	15.5405	
92	TAIL Z	10.2105	158.8199	15.5546	
93	TAIL X	20.3780	316.6344	15.5381	15.5206
94	TAIL Z	14.2336	221.2987	15.5476	
95	RUDDER X	10.1934	158.2510	15.5248	
99	RUDDER X	13.7917	214.2760	15.5366	
100	RUDDER Z	14.6988	228.3459	15.5350	
120	ENGINE Z	8.5764	131.9626	15.3867	
F_r = REF. FORCE = 12.3195 , C = MODE NORM. CONST. = .04350307					
TEST DATA SET 5 = ANALYTIC MODE 6; F = 26.614 hz					
62	WING Z	22.4302	121.8093	5.4306	
67	WING Z	27.0902	147.9872	5.4628	
68	WING Z	37.1728	202.8551	5.4571	
70	WING Z	51.6911	281.2871	5.4417	
77	ELEVON Z	23.2820	129.2316	5.5507	5.4715
78	ELEVON Z	34.8354	191.8743	5.5080	
79	ELEVON Z	69.5042	379.9528	5.4666	
81	ELEVON Z	71.8284	391.8939	5.4560	
82	ELEVON Z	80.9198	442.6480	5.4702	
93	TAIL X	26.6150	97.5854	3.6665	(?)#
F_r = 1.8575, C = .11966750					

*See note on page 3 of table.
#Inspection of the test data showed that, on all coordinates where the response was inconsistant with the majority of the measurements, these coordinates had very poor phase correlation.

Table 3. Quarter-Scale Orbiter: Estimate of Modal Damping for Analytic Modes 4,5,6,7,9,10 (continued)

TEST DATA SET 13 = ANALYTIC MODE 5; f= 21.546 hz

25	KEEL X	1.9802	35.8454	18.102	(?)
88	TAIL X	1.6891	13.4712	7.975	
91	TAIL X	2.1647	16.9908	7.8490	
92	TAIL Z	1.8225	13.7894	7.5662	7.6606
93	TAIL X	3.2595	25.2309	7.7407	
94	TAIL Z	2.5378	19.0978	7.5253	
96	RUDDER Z	1.6600	12.5595	7.5660	
99	RUDDER X	2.0075	16.4421	8.1903	
100	RUDDER Z	2.7443	19.5667	7.1299	
120	ENGINE Z	1.5859	11.7410	7.4034	

F_r= 5.5694 , C = .0059265

TEST DATA SET 23 = ANALYTIC MODE 10; f = 29.980 hz

68	WING Z	11.4732	8.9416	.7793	
70	WING Z	16.8160	12.0584	.7171	
78	ELEVON Z	9.0406	9.2522	1.0234	(?)
79	ELEVON Z	24.6010	16.7462	.6807	
81	ELEVON Z	25.3274	16.9506	.6693	
82	ELEVON Z	29.0111	19.7227	.6788	.7112
84	FLAP Z	13.7355	10.3268	.7518	
93	TAIL X	9.0735	6.3611	.7011	
102	RUDDER Y	10.0182	0.6298	.06286	(?)
119	ENGINE Y	38.4293	3.1594	.082213	(?)

F_r= .9197, C = .21152960

TEST DATA SET 27 = ANALYTIC MODE 9; f = 31.409 hz

84	FLAP Z	36.0276	26.3858	.7324	(?)
88	TAIL X	5.0118	5.4661	1.0906	
91	TAIL X	7.8615	7.7957	.9916	
92	TAIL Z	6.5983	6.4595	.9789	

Table 3. Quarter-Scale Orbiter: Estimate of Modal Damping for Analytic Modes 4,5,6,7,9,10 (continued)

93	TAIL X	13.9803	13.1506	.9407	
94	TAIL Z	10.8887	10.1804	.9350	
96	RUDDER Z	5.6543	5.5910	.9888	.9817
99	RUDDER X	8.0300	7.8952	.9832	
100	RUDDER Z	10.9401	10.3395	.9451	
119	ENGINE Y	5.0462	2.5751	.5103	(?)

F_r= 2.517 , C = .077733872

TEST DATA SET 35 = ANALYTIC MODE 7; f = 25.597 hz

70	WING Z	164.2394	111.8788	.6812	
78	ELEVON Z	136.0748	93.4633	.6868	
79	ELEVON Z	224.8105	153.1467	.6812	
81	ELEVON Z	218.6414	149.5063	.6838	
82	ELEVON Z	279.3554	191.5261	.6856	.7064
84	FLAP Z	136.2012	97.0242	.7124	
93	TAIL X	187.9309	137.5309	.7318	
94	TAIL Z	152.2787	110.9966	.7289	
100	RUDDER Z	160.4961	117.5643	.7325	
120	ENGINE Z	110.8812	82.0351	.7398	

F_r= .7861 , C = .68008224

DAMPING RATIO $\zeta_a = \zeta_b \left[\frac{b}{a}\right] = \frac{.01}{F_r} \left[\frac{b}{a}\right] = .01 \frac{}{\rho}$

DIVIDE BY F_r BECAUSE FORCING VECTOR HAD ERROR (F_r TOO LARGE)

ANALYTIC MODE	ζ	ζ MEASURED	TEST MODE
4	.0126	.022	4
5	.0138	.011 BEATS	13
6	.0295	.0315/.0221	5
7	.0090	.017	35
8	NO CORRESPONDING TEST MODE		
9	.0039	.0158	27
10	.0077	.020	23

Table 4. Quarter-Scale Orbiter, Symmetric Modes: Test Data Used for Parameter Identification and Calculated Response Using the Prior Model

COORDINATE	DIRECTION	DESCRIPTION	MEASURED RESPONSE (10^{-4}IN)	COEF. OF VAR. (%)	PRIOR MODEL RESPONSE
TEST DATA SET 4; f = 19.384 Hz					
2	Z	FUSELAGE, NOSE	9.7715	27.1	3.5280
6	Z	FUSELAGE, NOSE	6.8652	38.8	2.4431
15	Z	FUSELAGE, NOSE	2.2320	82.6	0.8689
62	Z	WING	5.2500	49.9	1.0289
70	Z	WING	5.1006	51.3	0.3793
82	Z	ELEVON	4.7411	55.2	0.1410
88	X	TAIL	11.3057	23.6	3.2218
91	X	TAIL	14.1718	19.0	4.1916
92	Z	TAIL	10.2105	26.0	3.0390
93	X	TAIL	20.3780	13.7	5.7630
94	Z	TAIL	14.2336	19.0	4.2407
95	X	LOWER RUDDER	10.1934	26.0	2.7813
99	X	LOWER RUDDER	13.7917	19.5	4.3535
100	Z	LOWER RUDDER	14.6988	18.4	3.9747
120	Z	LOWER ENGINE	8.5764	22.6	1.5967
TEST DATA SET 5; f = 26.614 Hz					
2			5.0782	27.7	1.8932
6			3.4194	41.3	1.0540
15			2.8315	34.7	1.1884
62			22.4302	7.9	10.2252
67			27.0902	7.1	12.3276
68			37.1728	6.2	17.6537
70			51.6911	5.7	23.3620
77			23.2820	7.8	11.5546
78			34.8354	6.4	16.7186
79			69.5042	5.4	30.4158
81			71.8284	5.4	33.2315
82			80.9198	5.3	39.0759
93			26.6150	7.2	4.2678
94			21.0172	8.3	4.1400
100			21.3420	8.2	3.9062

Table 4. Quarter-Scale Orbiter, Symmetric Modes: Test Data Used for Parameter Identification and Calculated Response Using the Prior Model (continued)

COORDINATE	DIRECTION DESCRIPTION	MEASURED RESPONSE (10^{-4}IN)	COEF. OF VAR. (%)	PRIOR MODEL RESPONSE
TEST DATA SET 11; f = 35.225 Hz				
2		.7816	101.0	.6356
6		.4382	182.7	.2793
15		1.2764	43.8	.4723
17		3.9749	20.5	.0019
21		1.2848	61.6	.0013
62		.2355	334.9	.7022
70		.6835	115.5	1.7866
75		1.0133	78.0	1.7590
79		1.1321	69.9	2.2712
81		1.2017	65.8	2.6822
82		1.4183	55.8	3.4650
84		6.6644	12.8	1.2155
93		1.4640	54.1	2.0155
94		1.0375	76.2	1.3174
100		1.0077	78.4	1.1754
TEST DATA SET 13; f = 21.546 Hz				
2		.6129	344.0	.7946
15		.1193	1249.5	.1834
25		1.9802	106.6	.4539
28		.0761	88.4	.0172
62		.4592	459.2	.2163
70		.4196	502.5	.0479
82		.3638	579.5	.1935
88		1.6891	124.9	.9754
91		2.1647	97.5	1.3355
92		1.8225	115.8	1.0119
93		3.2595	64.9	1.9300
94		2.5378	83.2	1.4699
99		2.0075	105.1	1.3930
100		2.7443	77.0	1.3733
120		1.5859	97.8	.4595

Table 4. Quarter-Scale Orbiter, Symmetric Modes: Test Data Used for Parameter Identification and Calculated Response Using the Prior Model (continued)

COORDINATE	DIRECTION	DESCRIPTION	MEASURED RESPONSE (10^{-4}IN)	COEF. OF VAR. (%)	PRIOR MODEL RESPONSE
TEST DATA SET 21; f = 34.247 Hz					
2			2.9207	29.0	106.7643
15			2.0035	29.7	187.3897
62			2.5627	32.9	309.0004
70			4.1800	20.6	1129.887
75			8.6480	10.9	1191.421
77			6.4700	13.8	740.6398
81			5.3312	16.4	1825.561
82			6.7082	13.4	2349.541
84			4.7518	5.3	697.1524
91			6.9472	13.0	489.9989
92			4.9137	17.7	136.7189
93			12.6718	8.3	794.7146
94			9.0388	10.5	350.7917
99			6.9504	13.0	524.4679
100			9.0997	10.4	298.4139
TEST DATA SET 23; f = 29.980 Hz					
2			1.5898	68.7	8.7222
15			.9318	82.7	5.9566
62			6.3189	17.9	13.4938
67			7.6150	15.1	12.4006
68			11.4732	10.7	19.1721
70			16.8160	8.2	26.4761
78			9.0406	13.0	12.2908
79			24.6010	6.7	31.5666
81			25.3274	6.6	35.7501
82			29.0111	6.3	43.5930
84			13.7355	9.4	3.9283
93			9.0735	13.0	136.0246
102			10.0182	12.0	.0109
106			7.2114	11.5	7.2760
119			38.4293	4.4	.8107

Table 4. Quarter-Scale Orbiter, Symmetric Modes: Test Data Used for Parameter Identification and Calculated Response Using the Prior Model (continued)

COORDINATE	DIRECTION	DESCRIPTION	MEASURED RESPONSE (10^{-4}IN)	COEF. OF VAR. (%)	PRIOR MODEL RESPONSE
TEST DATA SET 27; f = 31.409 Hz					
2			2.0157	49.5	.2774
15			1.2507	56.2	.2941
62			1.1260	88.3	1.9361
70			1.6953	58.7	4.1952
82			2.5732	38.9	7.0093
84			36.0276	5.7	.2917
88			5.0119	20.4	3.7021
91			7.8615	13.6	5.9474
92			6.5983	15.8	5.0400
93			13.9803	8.7	9.7785
94			10.8887	10.4	8.0321
96			5.6543	18.2	4.4197
99			8.0300	13.3	6.2711
100			10.9401	10.4	7.4608
119			5.0463	15.5	.1109
TEST DATA SET 28; f = 34.344 Hz					
2			2.2434	37.3	.0451
4			2.0374	41.0	.0349
6			1.2658	66.7	.0327
8			1.7544	34.0	.0033
15			5.2837	11.7	.0210
17			20.3407	6.5	.0000
21			6.2705	14.1	.0002
62			.5392	154.0	.5947
70			.7241	114.7	1.3802
76			2.1357	39.2	.1576
79			1.9072	43.8	1.7927
82			1.9420	43.0	2.3575
84			13.4274	7.9	.1476
93			2.5267	33.2	.1556
94			1.7981	46.4	.0882

Table 4. Quarter-Scale Orbiter, Symmetric Modes: Test Data Used for Parameter Identification and Calculated Response Using the Prior Model (continued)

COORDINATE	DIRECTION	DESCRIPTION	MEASURED RESPONSE (10^{-4}IN)	COEF. OF VAR. (%)	PRIOR MODEL RESPONSE
TEST DATA SET 34 ; f = 27.476 Hz					
2			9.3013	14.8	3.7512
15			5.9046	15.9	2.2585
62			38.7000	6.0	9.7927
68			73.2998	5.3	17.6370
70			94.3870	5.2	23.1454
78			64.5102	5.4	17.9147
79			130.8367	5.1	30.6253
81			143.9423	5.1	33.2379
82			146.4306	5.1	38.8024
91			72.9031	5.3	11.7909
92			60.5433	5.4	10.9123
93			122.3990	5.1	19.6513
94			95.0447	5.2	17.0552
99			71.6008	5.3	12.4357
100			95.9832	5.2	15.9070
TEST DATA SET 35; f = 25.597 Hz					
2			26.9933	7.5	10.9534
15			12.0928	9.4	5.2326
62			63.0654	5.5	9.4231
68			127.3167	5.1	19.3788
70			164.2394	5.1	25.2368
78			136.0748	5.1	21.8609
79			224.8105	5.0	34.8870
81			218.6414	5.0	37.4473
82			279.3554	5.0	43.2455
84			136.2012	5.1	3.1960
93			187.9309	5.1	46.5125
94			152.2787	5.1	40.2299
99			125.2131	5.1	28.6699
100			160.4961	5.1	37.4174
120			110.8812	3.8	5.5655

Table 5. Quarter-Scale Orbiter, Symmetric Modes: Catalogue of Test Data-Sets

TEST DATA-SET NO.	TEST FREQ. (Hz)	DESCRIPTION OF MODE	DAMP. ζ
1	1.2818	DISCARD, SUSPENSION MODE	----
2	1.4188	DISCARD, SUSPENSION MODE	----
3	.425	DISCARD, SUSPENSION MODE	----
4	19.384	FIRST FUSELAGE Z BENDING, VERTICAL TAIL, X-Z ROCKING	.022
5	26.614	WING-ELEVON Z BENDING	----
6	27.211	APPEARS TO BE SAME AS MODE 5	.022
7	50.245	OUTBD ELEVON ROTATION, OUT-OF-PHASE WITH WING BENDING	.027
8	95.816	WING TORSION, INBD AND OUTBD ELEVON ROLL	.018
9	76.246	APPEARS TO BE SAME AS MODE 10	.016
10	77.615	RIGHT OUTBD ELEVON ROLL	.016
11	35.225	APPEARS TO BE SAME AS MODE 27	----
12	52.893	SECOND FUSELAGE Z BENDING, PAYLOAD Z, CREW CABIN Z	.022
13	21.546	PAYLOAD PITCH	.011
14	40.323	APPEARS TO BE SAME AS MODE 15	----
15	40.161	CREW CABIN AXIAL AND PITCH	.012
16	39.178	LEFT INBD. ELEVON ROTATION	.013
17	41.237	RIGHT INBD. ELEVON ROTATION	.018
18	82.625	LEFT INBD. ELEVON ROLL	.018
19	83.856	APPEARS TO BE SAME AS MODE 18	.014
20	62.234	UPPER SSME PITCH, FUSELAGE Z BENDING	.044
21	34.247	APPEARS TO BE SAME AS MODE 11/27	----
22	77.742	ENGINE ONE AXIAL, 1307 BLKHD AND PAYLOAD	.024
23	29.980	LOWER SSME SYM. YAW	.020
24	31.409	DUPLICATE OF MODE 27	----
25	34.247	DUPLICATE OF MODE 21	----
26	138.299	LOW PRESSURE PUMPS AXIAL, LOWER SSME	.020
27	31.409	BODY FLAP ROTATION	.016
28	34.344	MID-FUSELAGE FIRST BREATHING	.028
29	110.274	VERTICAL TAIL X-Z, OMB TANKS X-Z	.031
30	159.116	NO. THREE PUMPS AXIAL, ENGINE ONE AXIAL	.031
31	163.898	NO. THREE PUMPS AXIAL, ENGINE THREE AXIAL	.018
32	118.768	NO. THREE PUMPS AXIAL, WING/ELEVON Z, ENGINE THREE AXIAL	.022
33	288.129	OMS ENGINE AXIAL	----

Table 5. Quarter-Scale Orbiter, Symmetric Modes: Catalogue of Test Data-Sets (continued)

TEST DATA-SET NO.	TEST FREQ. (H_z)	DESCRIPTION OF MODE	DAMP. ζ
34	27.476	APPEARS TO BE SAME AS MODE 5	.016
35	25.597	ENGINE θ_z ROCKING, WING Z BENDING, VERTICAL TAIL ROCKING	.017
36	47.192	1307 BULKHEAD AXIAL, CREW CABIN AXIAL	.0055
37	91.496	ENGINE ONE AXIAL, 1307 BLKHD X	.014
38	20.205	APPEARS TO BE THE SAME AS MODE 4	----
39	19.178	APPEARS TO BE SAME AS MODE 4	
40	78.886	APPEARS TO BE SAME AS MODE 41	----
41	78.397	----	----
42	93.724	----	----

Table 6. Quarter-Scale Orbiter, Symmetric Model: Load Cases to Generate Mass and Stiffness Matrix Submatrices

Fuselage Component

Loads at DOF 2, 6, 9, 12, 15, 19

Free DOF 1, 3, 4, 5, 7, 8, 10, 11, 13, 14, 16, 18, 20

Payload Component

Loads at DOF 28

Free DOF 26, 27

Wing-Eleven Component

Loads at DOF 55, 56, 58, 59, 60, 61, 62, 64, 65, 67, 68, 70

Free DOF 57, 63, 66, 69, 71, 72, 73, 74, 75, 76, 77, 78, 79, 80, 81, 82

Tail Component (± indicate direction)

Loads at DOF 86+, 87-, 88+, 89+, 90-, 91+, 92-, 93+, 94-

Free DOF 85, 95, 96, 97, 98, 99, 100, 101, 102

For each case, all DOF not specified are constrained.

APPENDIX 4

Program FOCOR

USER's Instructions

A - General Description

B - Subroutines

C - Flow Chart

D - Input

E - Job Control Cards

A

General Description of FOCOR

This computer program develops the First Order Correction (FOC) and prepares the input data files for Program ESTIMA. Any or all of these operations may be performed on one run. The program consists of a main routine plus four subroutines (Section B). Three of the subroutines perform simple matrix manipulations. The fourth is a user supplied routine providing the primary data interface between this entire family of computer programs and the raw data. A flow chart of the main routine is provided in Section C.

The program input consists of four data sets described in detail in Section D. Data Set One includes the job title, the program control, and the indices of the modes to be used. These indices are used as follows. The analytic-model data (Data Set Three) and the test data (Data Set Four) must be provided to the main program on disk files 20 and 21. Up to 70 analytic modes and 70 test data sets may be stored on these files. As described in Section D, each mode or data set must be assigned an identification number. These identification numbers, called herein "index" numbers, must be numerical integers, but they need not be contiguous or sequential. Any or all of the modes and data sets can be selected for processing by listing the desired index numbers in Data Set One. The modes and data sets are placed into the modal matrices according to the sequence in which they are listed here.

Data Set Two is the system mass matrix. This data must be

provided to the program on a binary disk (or tape) file according to the specifications described in Section D. The program is dimensioned for 125 dynamic degrees-of-freedom with only the non-constrained, non-reduced coordinates being used here. The mass matrix may be printed if the user so desires.

Data Set Three is the prior-model data and consists of one label card, one dimension card, and as many modal information cards as required. It is a formatted disk-file according to the specifications described in Section D. This data file is set up by subroutine PREPAR. Once created it may be saved for later use thus negating the need to execute PREPAR each time this program is run.

Data Set Four is the test data. It includes frequency, mode shape, total acceleration, variance, and force data. This is also a formatted disk-file according to the specification described in Section D. Each data-set corresponds to one excitation frequency which may or may not be determined to be a system resonance. Any of the data-sets may be used as input to ESTIMA, but only those determined to be at a system resonance should be used when the first order corrections are calculated. When calculating the first order correction (FOC), the mode and data-set indices must be matched so that the equivalent modes appear in the same place in their respective modal matrices.

Normally the analytic modes are assigned to File 21 and the test data to File 20. However, either file can be read as the prior and either can be read as the test. In fact the same file can be both the prior and the test. In the course

of calculating the FOC, the program calculates the cross-orthogonality $[\theta_o]^T[M][\theta_T]$ where $[\theta_o]$ are the prior model modes and $[\theta_T]$ are the test modes. If the same data is read into both matrices, a check of the model orthogonality for either the analytic modes or the test modes can be obtained. The program can also be used to correlate the test data-sets with the analytic modes by using all of the test data-sets and all of the analytic modes and searching the cross-orthogonality matrix for the largest values. A value of 1.0 means the test and analytic modes are identical. To use the program to perform any of these operations set the operations flag (Data Set one) for FOC.

Other tasks performed by FOCOR are to print the 15 largest accelerations in each test data set and to calculate the coefficient of variation for each test response selected for ESTIMA use. These operations are performed only when the operations flag is set to "prepare ESTIMA data files". The program writes the ESTIMA files onto disk files:

22 - First Order Correction data
23 - Prior-Model data
24 - Test data

These files must be saved at the completion of the run if they are to be used later by ESTIMA.

A set of sample job control cards are presented in Section E. The program source code has been designed for easy comprehension. It is extensively annotated and is keyed both to the input description and the flow chart. All of the mnemonics are defined at the beginning of the code.

Two versions of PREPAR were developed: one to process 1/4-scale SRB data and one to process 1/4-scale Orbiter data. The source codes for both are provided.

B

FOCOR Subroutines

PREPAR — PREPAR is a user supplied subroutine to interface with the raw data. It writes the prior-model data on to a disk file using the sequence and formats described under Data Set Three (File No. 21). It also writes the test data on to a disk file using the sequence and format described under Data Set Four (File No. 20).

MATOUT — Prints all non-zero terms of a matrix with titles and paging. It is identical to the MATOUT subroutines used in ESTIMA and ESTIMB.

MATMUL — Multiplies two conformable matrices. The input matrices are destroyed. It is also used in ESTIMA.

TRMUL — Multiplies the transpose of a matrix times another matrix.

C

FOCOR FLOW CHART

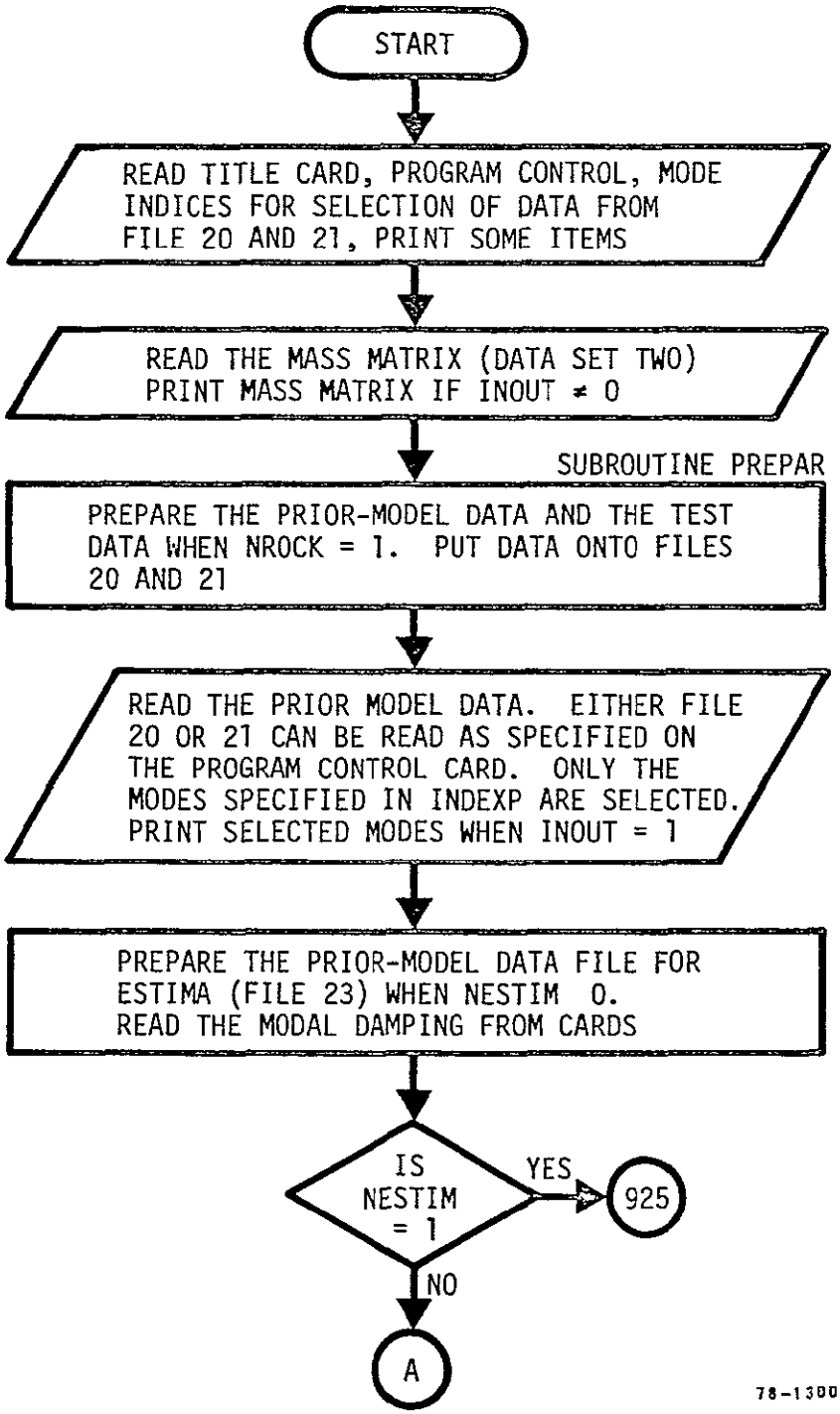

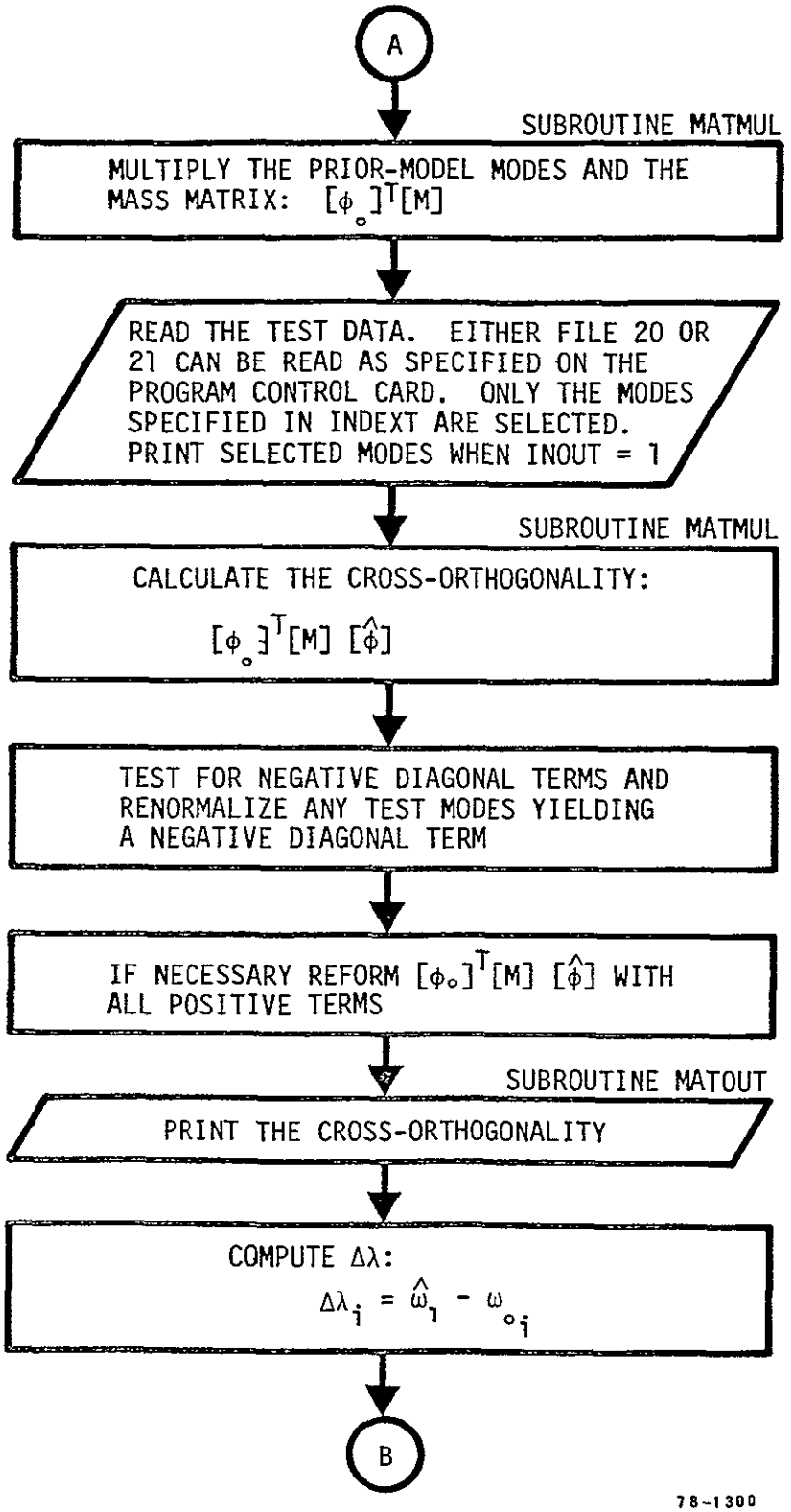
A
SUBROUTINE MATMUL
MULTIPLY THE PRIOR-MODEL MODES AND THE MASS MATRIX: $[\phi_o]^T[M]$
READ THE TEST DATA. EITHER FILE 20 OR 21 CAN BE READ AS SPECIFIED ON THE PROGRAM CONTROL CARD. ONLY THE MODES SPECIFIED IN INDEXT ARE SELECTED. PRINT SELECTED MODES WHEN INOUT = 1
SUBROUTINE MATMUL
CALCULATE THE CROSS-ORTHOGONALITY:
$[\phi_o]^T[M]\ [\hat{\phi}]$
TEST FOR NEGATIVE DIAGONAL TERMS AND RENORMALIZE ANY TEST MODES YIELDING A NEGATIVE DIAGONAL TERM
IF NECESSARY REFORM $[\phi_o]^T[M]\ [\hat{\phi}]$ WITH ALL POSITIVE TERMS
SUBROUTINE MATOUT
PRINT THE CROSS-ORTHOGONALITY
COMPUTE $\Delta\lambda$:
$\Delta\lambda_i = \hat{\omega}_1 - \omega_{o_i}$
B
78-1300

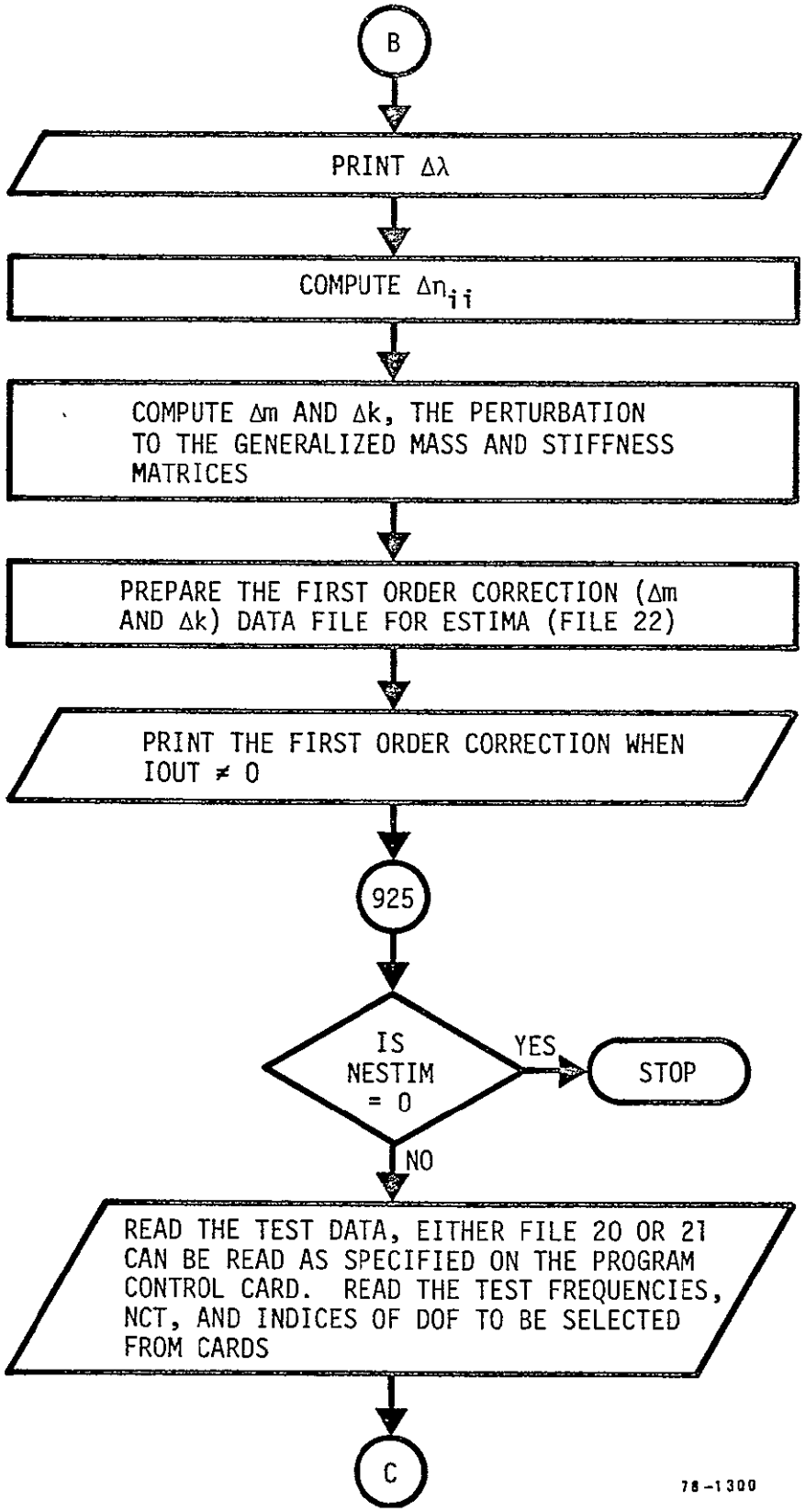
B
PRINT Δλ
COMPUTE Δn_{ii}
COMPUTE Δm AND Δk, THE PERTURBATION TO THE GENERALIZED MASS AND STIFFNESS MATRICES
PREPARE THE FIRST ORDER CORRECTION (Δm AND Δk) DATA FILE FOR ESTIMA (FILE 22)
PRINT THE FIRST ORDER CORRECTION WHEN IOUT ≠ 0
925
IS NESTIM = 0
YES
STOP
NO
READ THE TEST DATA, EITHER FILE 20 OR 21 CAN BE READ AS SPECIFIED ON THE PROGRAM CONTROL CARD. READ THE TEST FREQUENCIES, NCT, AND INDICES OF DOF TO BE SELECTED FROM CARDS
C
78-1300

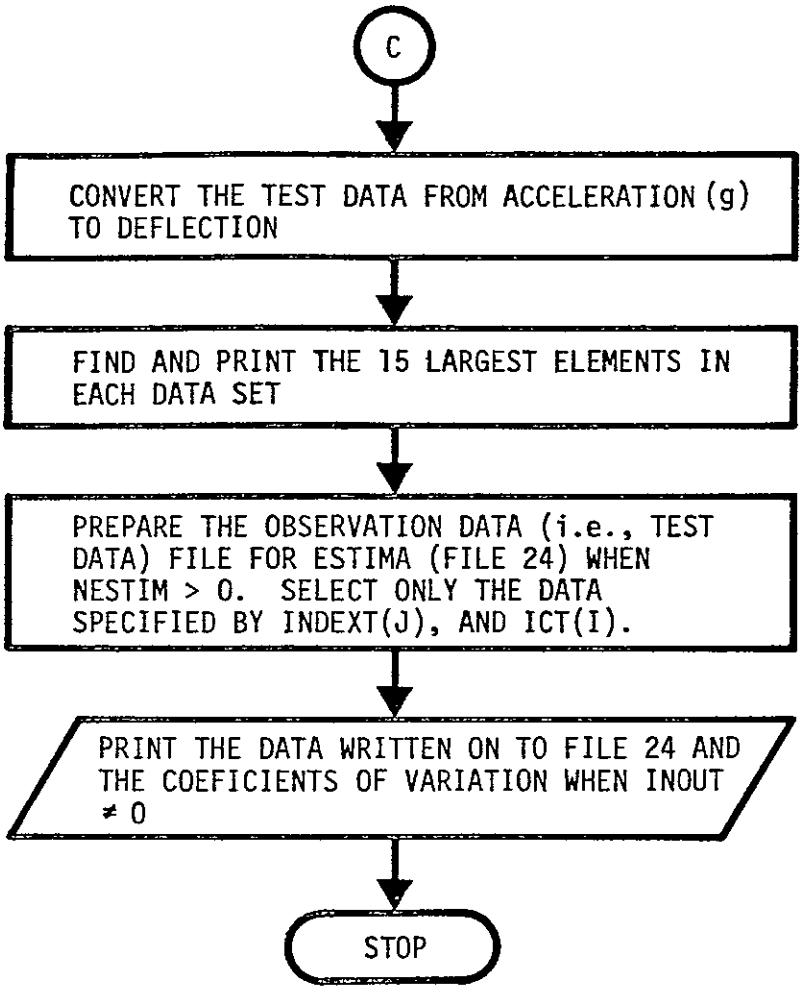
C
CONVERT THE TEST DATA FROM ACCELERATION (g) TO DEFLECTION
FIND AND PRINT THE 15 LARGEST ELEMENTS IN EACH DATA SET
PREPARE THE OBSERVATION DATA (i.e., TEST DATA) FILE FOR ESTIMA (FILE 24) WHEN NESTIM > 0. SELECT ONLY THE DATA SPECIFIED BY INDEXT(J), AND ICT(I).
PRINT THE DATA WRITTEN ON TO FILE 24 AND THE COEFICIENTS OF VARIATION WHEN INOUT ≠ 0
STOP

78-1300

FOCOR INPUT

Data Set One

Data Set One provides the card data required by the main program. The data included here consists of the program control parameters, the damping for the analytic modes, and the indices of the response points to be provided to ESTIMA.

Card One

NAME(I), I = 1, 9
9A8 FORMAT

where

NAME(9) is the job title.

Cards Two

NMP, NMT, NDOF, INOUT, ISAVE, IOUT, PDATA, TDATA,
NROCK, NESTIM
8I10 FORMAT

where

NMP is the number of prior-model modes to be used in the First Order Correction (FOC) or written onto File 23.

NMT	is the number of test data sets to be used in the First Order Correction or written onto File 24.
NDOF	is the number of degrees-of-freedom in the modes.
INOUT	is an output flag. ≠0 print all input data. =0 do not print input data.
ISAVE	is an output flag. ≠0 write FOC on Tape 22. =0 do not write FOC on Tape 22.
IOUT	is an output flag. ≠0 print results. =0 do not print results.
PDATA	is file number where prior-model modal data is to be found. =5 read data from cards, already in desired format. =xx read data from File xx. Data must be placed on File xx with a user supplied subroutine (xx can be 20 or 21).
TDATA	is file number where test data is to be found. =5 read from cards, already in desired format. =xx read data from File xx. Data must be placed on File xx with a user supplied subroutine (xx can be 20 or 21).
NROCK	is an input flag. =0 prior-model data already on File 21 and test data already on File 20.

=1 prior-model and test data must be read from cards and written onto Files 20 and 21. See card sets 3, 4, 5, and 6.

NESTIM is an option flag.

=0 only calculate First Order Correction.

=1 only prepare Files 23 and 24 for input to ESTIMA.

=2 do both of the above.

If both PDATA and TDATA are set to 21, the program will produce the orthogonality of the analytical modes. If they are set to 20, the test orthogonality is produced. INDEXT(NM) and INDEXP (NM) must be set appropriately. Use two cards.

Cards Three

INDEXT(I), I = 1, NMT	
8I10	FORMAT

where

INDEXT(NMT) are the indices of the test modes to be selected for use in model update (FOC).

Cards Four

INDEXP(I), I = 1, NMP	
8I10	FORMAT

where

INDEXP(NMP) are the indices of the prior-model modes to be selected for use in model update (FOC).

Although neither INDEXT or INDEXP need be numbered consecutively or sequentially, the i^{th} value of one must correspond to the i^{th} value of the other. Use as many cards as needed for each.

Insert whatever data is needed by the user supplied subroutine here.

See Data Set Five

Cards Five (use only when NESTIM > 0)

ZET(J), J = 1, NMP	
4E20.14	FORMAT

where

ZET(J)	are the modal damping values to be written onto File 23 for input to ESTIMA.

Cards Six (use only when NESTIM > 0)

WT(J), J = 1, NMT	
4E20.14	FORMAT

where

WT(J)	are the frequencies (Hertz) of the test data sets to be written onto File 24 for input to ESTIMA.

Cards Seven and Eight must be repeated NMT times (once for each test data set to be written onto File 24 for input to ESTIMA).

Card Seven (not required when NESTIM = 0)

NCT	
I10	FORMAT

where

NCT	is the number of response points to be written onto File 24 for this test data set.

Card Eight (not required when NESTIM = 0)

ICT(J), J = 1, NCT	
8I10	FORMAT

where

ICT(J)	are the indices of the response to be written onto File 24 for this test data set.

FOCOR INPUT

Data Set Two (File No. 1)

Data Set Two provides the analytic mass matrix. It is a binary disk or tape file. NR must equal NC for program to run successfully.

Record One

```
NR, NC, LABl(9)
```

where

NR	is the number of rows in the matrix.
NC	is the number of columns in the matrix.
LABl(9)	is a title with up to 72 characters.

Records Two to Two + NC

```
M(J,I), J = 1, NR
```

where

M(J,I)	is I^{th} column of the matrix. Repeat NC times (i.e., one record per column).

FOCOR INPUT

Data Set Three (File No. 21)

Data Set Three is the information about the prior model required by FOCOR to calculate the First Order Correction or prepare the prior-model data file (File No. 23). It is a formatted file which must be provided by the user or generated during the run with a user provided subroutine called PREPAR. It may be saved for later use.

Record One

LABl(I), I = 1,9
9A8 FORMAT

where

LABl(I) is a 72 character label.

Record Two

NMP, NCl
I10, I10 FORMAT

where

NMP is the number of modes on the file.

NC1	is the number of free degrees-of-freedom in the mode.

The NC1 read here must equal the NDOF read from Data Set One for the program to run.

Records three and four must be repeated NMP times (i.e., once for each mode). The modes may be in any sequence.

Record Three

NP, W(NP), ZET(NP)
I10, E20.10, E20.10 FORMAT

where

NP	is the index of the mode (i.e., its identification number).
W(NP)	is the natural frequency (Hertz) of the mode.
ZET(NP)	is the damping assigned to the mode. The damping values read from Data Set One override the values read here.

Record Four

PHIO(J,NP), J = 1, NC1
5E16.8 FORMAT

where

PHIO(J,NP)	are the modal deflections written 5 per "card". The mode must be normalized for a generalized mass of unity.

FOCOR INPUT

Data Set Four (File No. 20)

Data Set Four is the test data required by FOCOR to calculate the First Order Correction (FOC) or prepare the observation data (File 24) for ESTIMA. Only those data sets used in the FOC need be system resonances. The number of data sets stored here need not equal the number of modes on File No. 21. This is a formatted file which must be provided by the user or generated during the run with a user provided subroutine called PREPAR. It may be saved for later use. Records three through ten are repeated for each test frequency.

Record One

LAB3(I), I = 1,9
9A8 FORMAT

where

LAB3(I) is a 72 character label.

Record Two

NMT, NCI
I10, I10 FORMAT

where

NMT	is the number of data sets on the file.
NC1	is the number of free degrees-of-freedom in the mode.

The NC1 read here must equal the NDOF read from Data Set One for the program to run.

Record Three

NP, WT(NP), ZET(NP)
I10, E20.10, E20.10 FORMAT

where

NP	is the index of the data block (i.e., its identification number) with one data block for each test frequency.
WT(NP)	is the frequency (Hertz) of the data block.
ZET(NP)	is the recorded damping of the data block (fraction of critical damping). Not required data.

Record Four

PHIHAT(J,NP), J = 1, NC1
5E16.8 FORMAT

where

PHIHAT(J,NP)	are the normalized quadrature responses recorded at each DOF (Normalized to unit generalized mass).

Use as many cards as necessary.

Record Five

WORK4(J), J = 1, NC1
5E16.8 FORMAT

where

WORK4(J)	are total responses (= modulus of response = $[(\text{quad. resp.})^2 + (\text{co. resp.})^2]^{1/2}$) measured at each DOF. Use as many cards as necessary.

Record Six

WORK5(J), J = 1, NC1
5E16.8 FORMAT

where

WORK5(J)	are the variances of the total responses recorded in Record Five.

Record Seven

NCF	
I10	FORMAT

where

NCC	is the number of coordinates (i.e., DOF) which were forces (i.e., excited) when the data set was obtained.

Record Eight

ICF(J), J = 1, NCF	
8I10	FORMAT

where

ICF(J)	are the indices of the forced coordinates. Forces may be applied at up to 17 different coordinates. Use as many cards as necessary.

Record Nine

WORK1(J), J = 1, NCF	
5E16.8	FORMAT

where

WORK1(J)	are the in-phase (i.e., real component) portions of the excitation forces. Use as many cards as necessary.

Record Ten

WORK2(J), J = 1, NCF
5E16.8 FORMAT

where

WORK2(J)	are the out-of-phase (i.e., imaginary component) portions of the excitation forces. Use as many cards as necessary.

E

FOCOR Job Control Cards

Compile and store relocatable on CDC computer

```
job card
account card
REQUEST, LGO, *PF.
FTN, R = 3.
CATALOG, LGO, FOCOR, ID = xxxxx.
AUDIT, AI = P, ID = xxxxx.
¶ - end of record
source deck
¶ - end of record
¶ - end of information
```

Execute using disk files for all output and for program, and cards for input data

```
job card
account card
REQUEST, TAPE20, prior-model data for FOCOR, *PF.
REQUEST, TAPE21, test data for FOCOR, *PF.
REQUEST, TAPE22, first order correction for ESTIMA, *PF.
REQUEST, TAPE23, prior-model data for ESTIMA, *PF.
REQUEST, TAPE24, test data for ESTIMA, *PF.
ATTACH, OLD, FOCOR, ID = xxxxx.
MAP, OFF.
OLD.
CATALOG, TAPE20, name, ID = xxxxx.
CATALOG, TAPE21, name, ID = xxxxx.
CATALOG, TAPE22, name, ID = xxxxx.
CATALOG, TAPE23, name, ID = xxxxx.
CATALOG, TAPE24, name, ID = xxxxx.
¶ - end of record
card data
¶ - end of record
¶ - end of information
```

APPENDIX 5

Program ESTIMA

USER's Instructions

A - General Description

B - Subroutines

C - Flow Chart

D - Input

E - Job Control Cards

A

General Description of ESTIMA

This program, number two in the family, performs the Phase I estimation: the estimate of elements of the generalized mass and stiffness matrices. The program is sized for 12 modes with 125 degrees-of-freedom and can estimate up to 100 parameters (50 in the generalized mass matrix and 50 in the stiffness matrix). The total number of possible elements in a 12 mode model is 156 (78 in the right-diagonal-half of each matrix) so obviously not all matrix elements can be estimated. The user may specify specific elements to be estimated, or he may specify the number of diagonal rows:

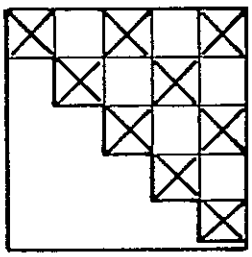

Estimate 9
specific elements
of 5 mode model

or

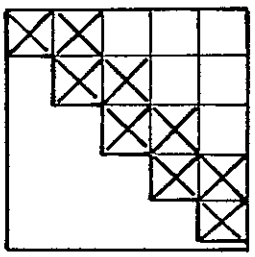

Estimate 2
diagonal rows
of 5 mode model

The diagonal elements must always be included. Since matrix symmetry is assumed, elements below the diagonal must never be specified.

The theoretical basis for all of the operations is described in the interim and final project reports. The program consists

of a main routine plus 16 subroutines (Section B). A flow chart of the main routine is presented in Section C. The program source codes have been designed for easy comprehension. They are extensively annotated. The main routine source code is keyed to both the input description and the flow chart. The mnemonics are defined at the beginning of the source code and, whenever possible, are keyed to the theoretical development symbols.

The Phase I procedures have been divided into two separate operations, one to estimate the generalized mass and stiffness matrices and another to estimate the modal damping matrix. Either one or both can be selected by the user. The program first estimates the generalized mass [m] and the generalized stiffness [k] matrices. After converging on the best model here it then works on the damping matrix. Sequential sets of test data may be used.

Program input is described in detail in Section D. The first three cards provide print control, operations flags, data-source information, and convergence criteria. The next set of data (cards four to nine) provides all of the required information about the prior model. This information may be input from cards in the run stream or from a disk file. Some of the "cards" may consist of many records.

The variances (σ^2) assigned to the prior model must be provided next (cards ten to twelve), always on cards in the run stream. Data for the variances of [m] and [k], and the damping matrix must always be provided even though one or the other is not to be estimated. Zeros (i.e., blank fields) may be used for

the non-estimated parameters.

Cards twelve to sixteen provide the test data. They may be inserted into the run stream or stored previously on a disk file. Some "cards" require several records. The final data set, identified as Card Eighteen, is the First Order Correction information generated by program FOCOR.

B

ESTIMA Subroutines

DCOMP — Performs a Cholesky square root decomposition forming an upper triangular matrix in the inverted form.

DISRES — Computes transfer functions for analytic model coordinates and dynamic model degrees of freedom. Computes frequency response for same two coordinate systems.

FOC — Incorporates the First Order Correction into the analytic model mass and stiffness matrices. Generates a revised set of modes and natural frequencies.

GIVHO — Uses the Householder method to reduce a real symmetric matrix to tridiagonal form. Isolates eigenvalues using Strum sequences and eigenvectors using Wilkinson's Method.

INPUTP — Reads the input data relating to the measured response and forcing vectors and forcing frequencies. Data may be on cards or a tape file.

INVECC — Inverts a complex symmetric matrix.

INVERT — Inverts a real symmetric matrix using a Cholesky SDS decomposition method.

MATMUL	Multiplies two conformable matrices. The input matrices are destroyed. It is also used in FOCOR.
MATOUT	Prints all non-zero elements of a matrix with titles and paging. It is also used in ESTIMB and FOCOR.
MATOUZ	Prints all non-zero elements of a matrix without titles and paging.
MOUSE	Estimates new analytic model mass and stiffness matrices or modal damping matrix. Also develops a new covariance matrix when each set of iteration cycles is complete. It is also used in ESTIMB.
OBJECT	Calculates the value of the object function (i.e., the function which the MOUSE subroutine minimizes). It is also used in ESTIMB.
SENSD	Computes the sensitivity matrix for modal damping matrix.
SENSK	Computes the sensitivity matrix for analytic model mass and stiffness matrices (i.e., the sensitivitiy of the frequency response with respect to variations in the analytical model mass and stiffness matrix).

SYMMT	Prepares the symmetric matrix for GIVHO and calls GIVHO to compute the eigenproperties.
TRMUL	Multiplies the transpose of a matrix times another matrix.

C

ESTIMA FLOW CHART

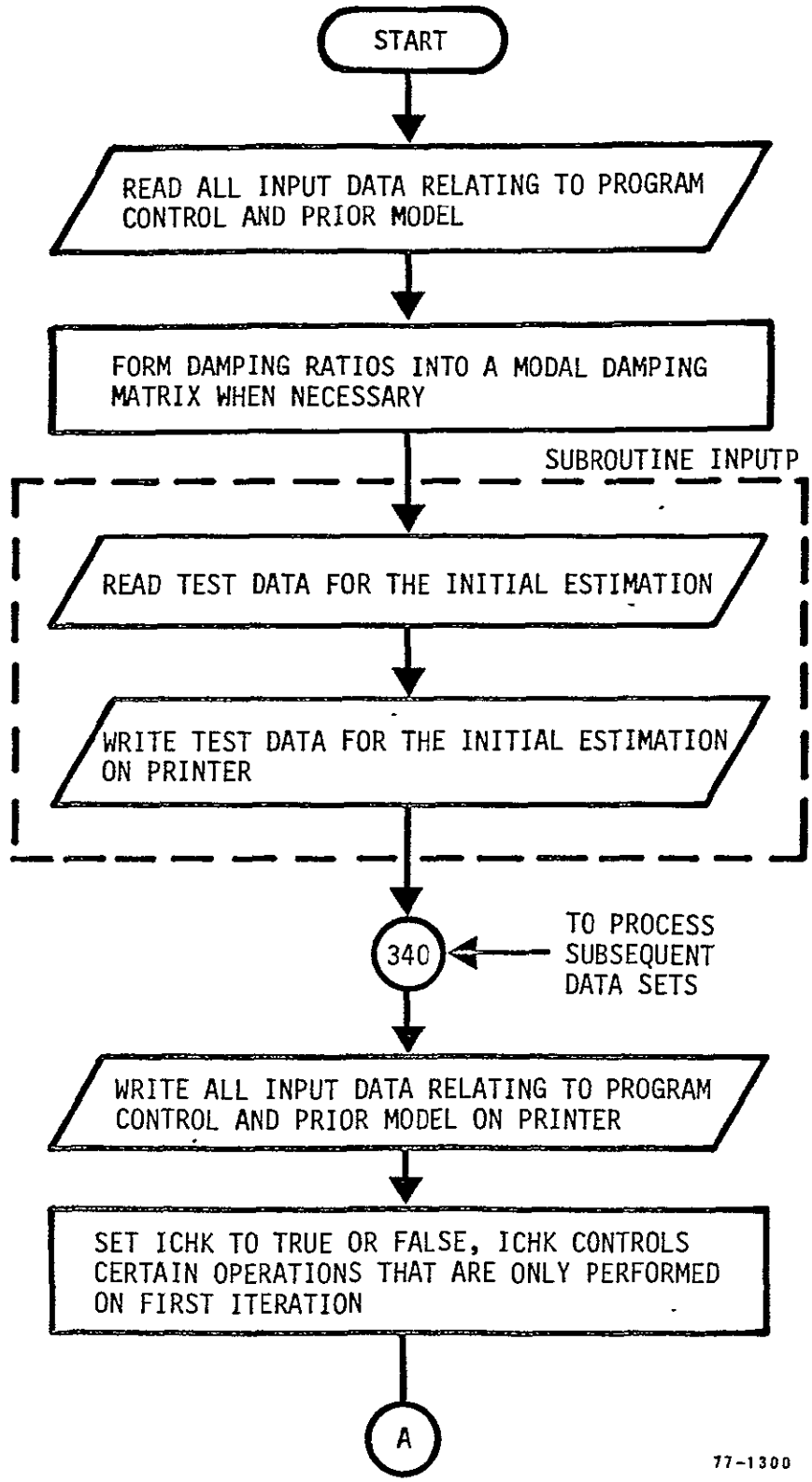

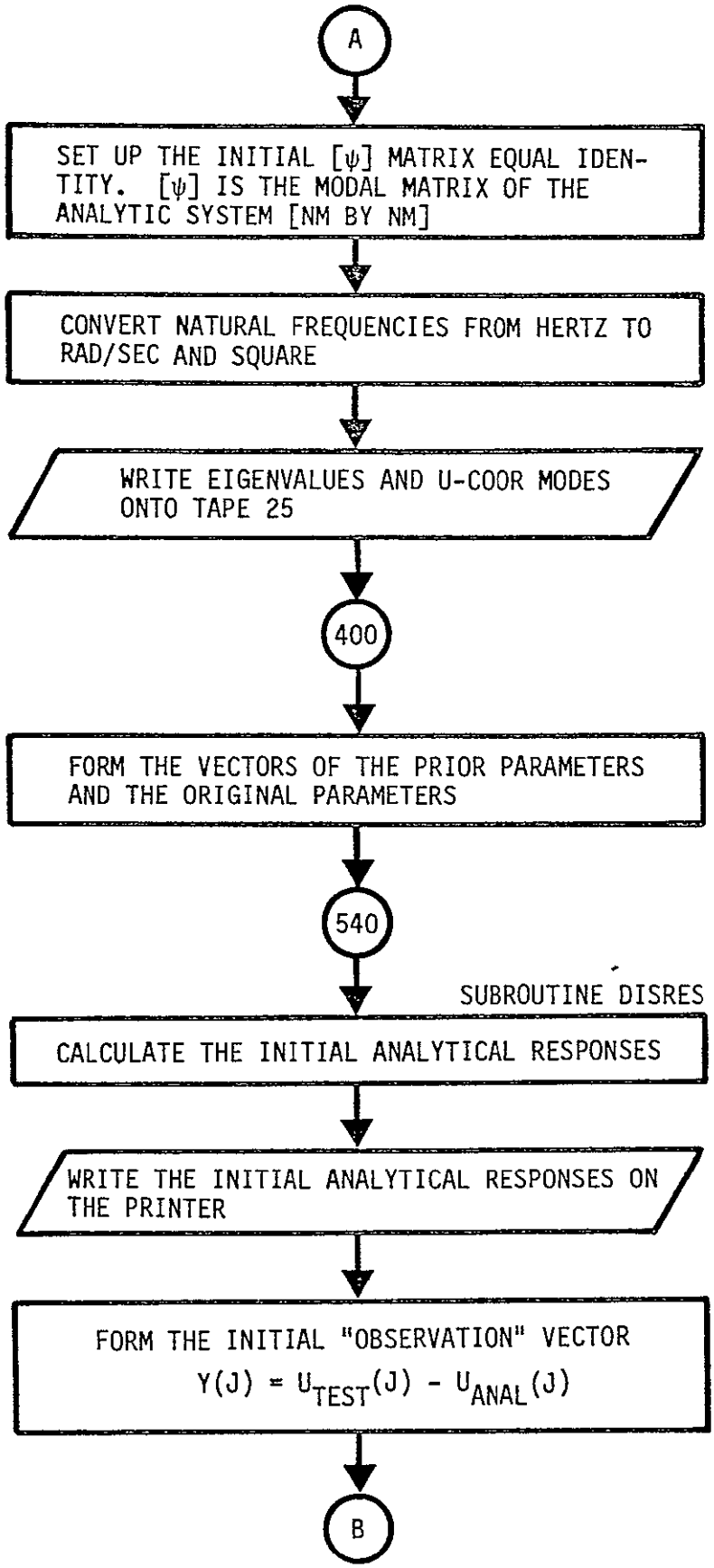
A
SET UP THE INITIAL [ψ] MATRIX EQUAL IDENTITY. [ψ] IS THE MODAL MATRIX OF THE ANALYTIC SYSTEM [NM BY NM]
CONVERT NATURAL FREQUENCIES FROM HERTZ TO RAD/SEC AND SQUARE
WRITE EIGENVALUES AND U-COOR MODES ONTO TAPE 25
400
FORM THE VECTORS OF THE PRIOR PARAMETERS AND THE ORIGINAL PARAMETERS
540
SUBROUTINE DISRES
CALCULATE THE INITIAL ANALYTICAL RESPONSES
WRITE THE INITIAL ANALYTICAL RESPONSES ON THE PRINTER
FORM THE INITIAL "OBSERVATION" VECTOR
Y(J) = U_TEST(J) - U_ANAL(J)
B

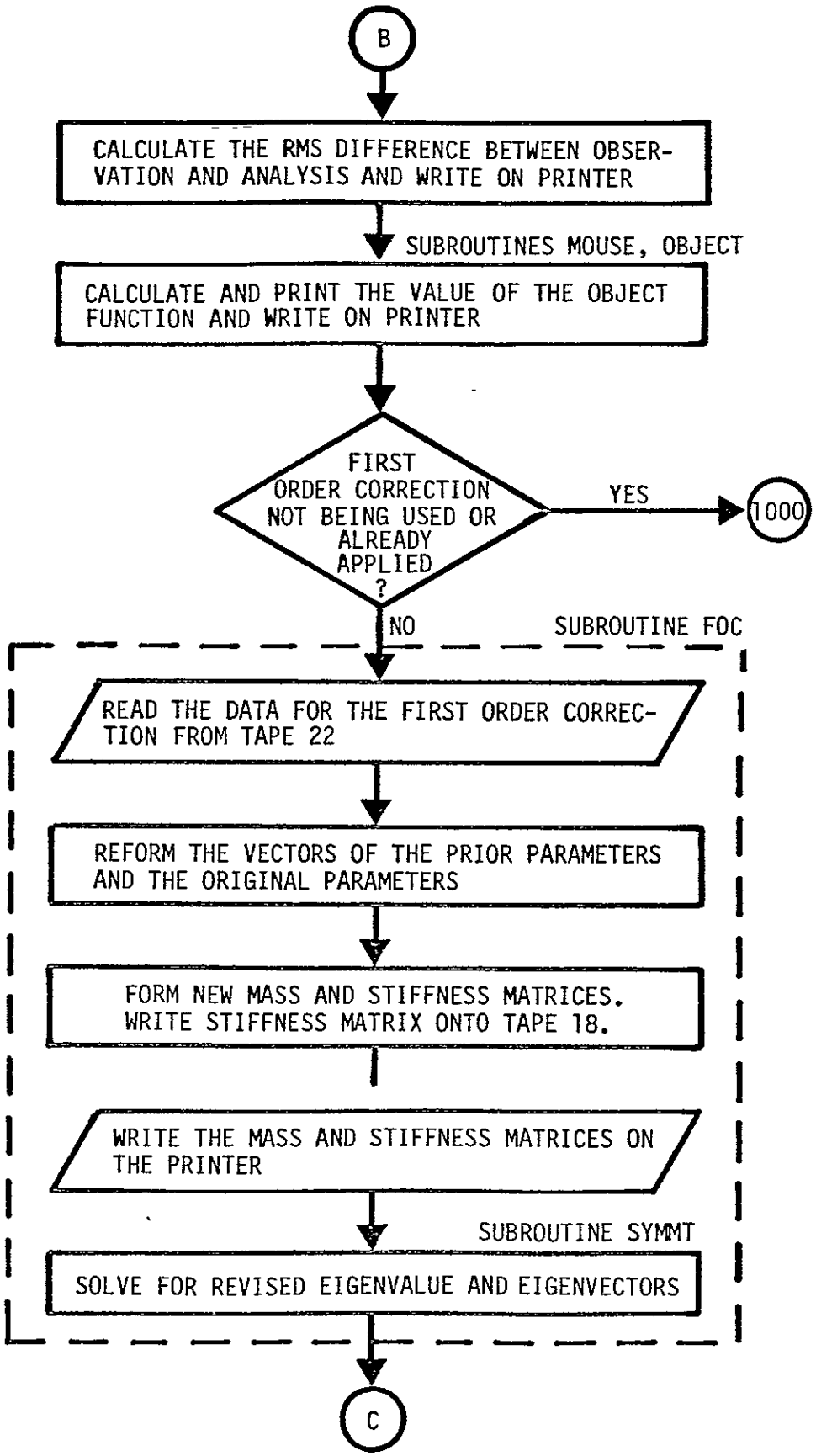
B
CALCULATE THE RMS DIFFERENCE BETWEEN OBSERVATION AND ANALYSIS AND WRITE ON PRINTER
SUBROUTINES MOUSE, OBJECT
CALCULATE AND PRINT THE VALUE OF THE OBJECT FUNCTION AND WRITE ON PRINTER
FIRST ORDER CORRECTION NOT BEING USED OR ALREADY APPLIED ?
YES
1000
NO
SUBROUTINE FOC
READ THE DATA FOR THE FIRST ORDER CORRECTION FROM TAPE 22
REFORM THE VECTORS OF THE PRIOR PARAMETERS AND THE ORIGINAL PARAMETERS
FORM NEW MASS AND STIFFNESS MATRICES. WRITE STIFFNESS MATRIX ONTO TAPE 18.
WRITE THE MASS AND STIFFNESS MATRICES ON THE PRINTER
SUBROUTINE SYMMT
SOLVE FOR REVISED EIGENVALUE AND EIGENVECTORS
C

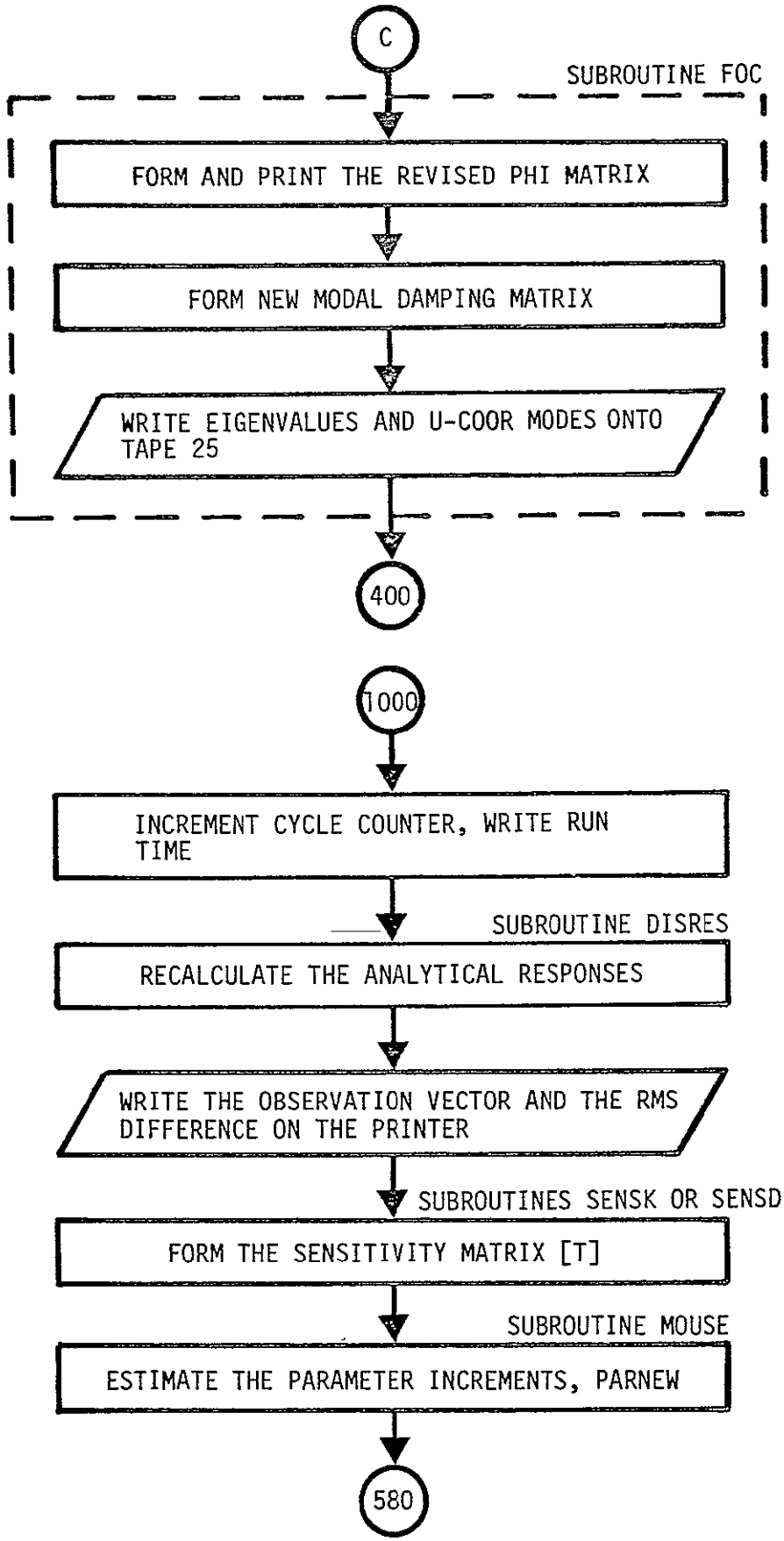
C
SUBROUTINE FOC
FORM AND PRINT THE REVISED PHI MATRIX
FORM NEW MODAL DAMPING MATRIX
WRITE EIGENVALUES AND U-COOR MODES ONTO TAPE 25
400
1000
INCREMENT CYCLE COUNTER, WRITE RUN TIME
SUBROUTINE DISRES
RECALCULATE THE ANALYTICAL RESPONSES
WRITE THE OBSERVATION VECTOR AND THE RMS DIFFERENCE ON THE PRINTER
SUBROUTINES SENSK OR SENSD
FORM THE SENSITIVITY MATRIX [T]
SUBROUTINE MOUSE
ESTIMATE THE PARAMETER INCREMENTS, PARNEW
580

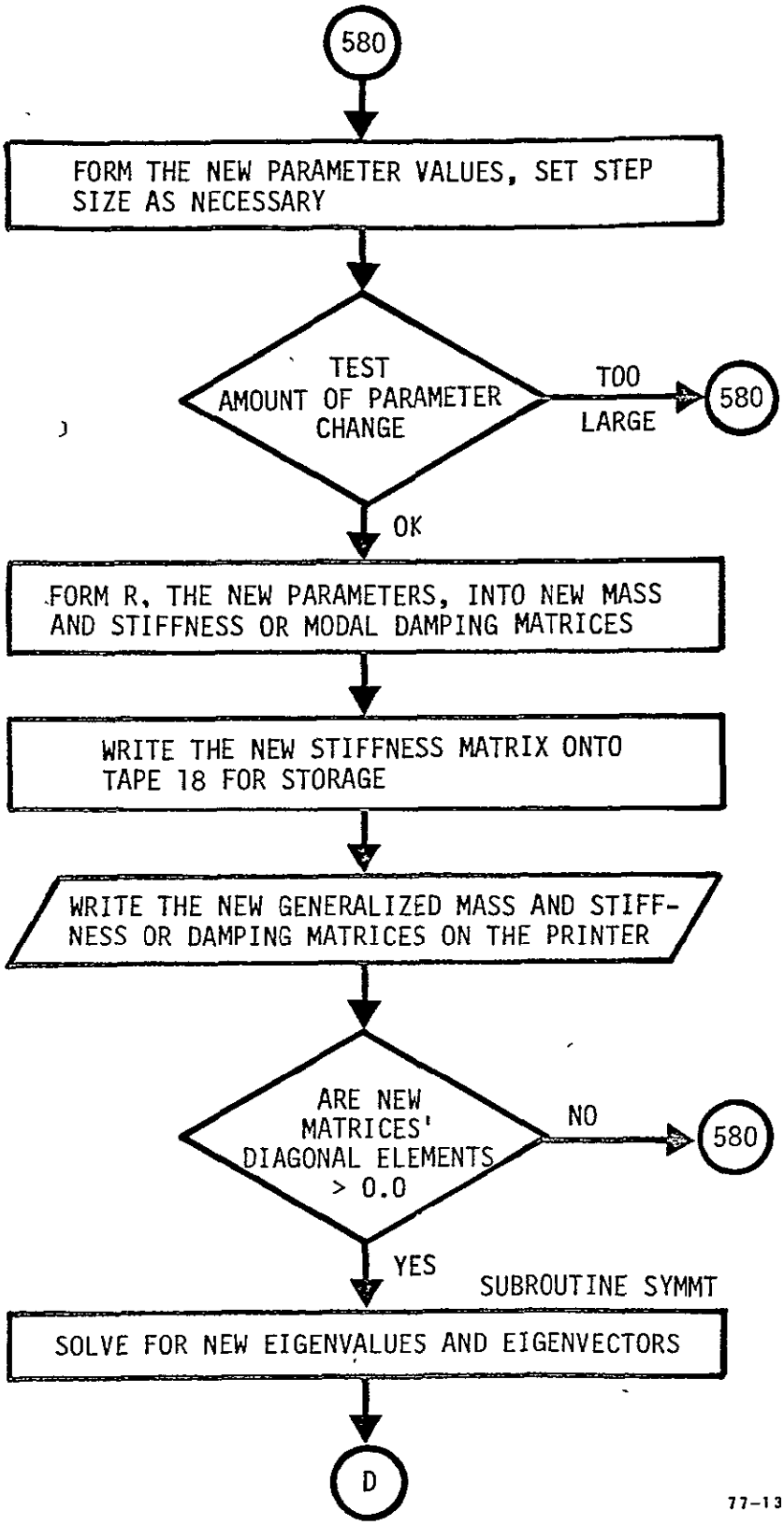
580
FORM THE NEW PARAMETER VALUES, SET STEP SIZE AS NECESSARY
TEST AMOUNT OF PARAMETER CHANGE
TOO LARGE
580
OK
FORM R, THE NEW PARAMETERS, INTO NEW MASS AND STIFFNESS OR MODAL DAMPING MATRICES
WRITE THE NEW STIFFNESS MATRIX ONTO TAPE 18 FOR STORAGE
WRITE THE NEW GENERALIZED MASS AND STIFFNESS OR DAMPING MATRICES ON THE PRINTER
ARE NEW MATRICES' DIAGONAL ELEMENTS > 0.0
NO
580
YES
SUBROUTINE SYMMT
SOLVE FOR NEW EIGENVALUES AND EIGENVECTORS
D
77-1300

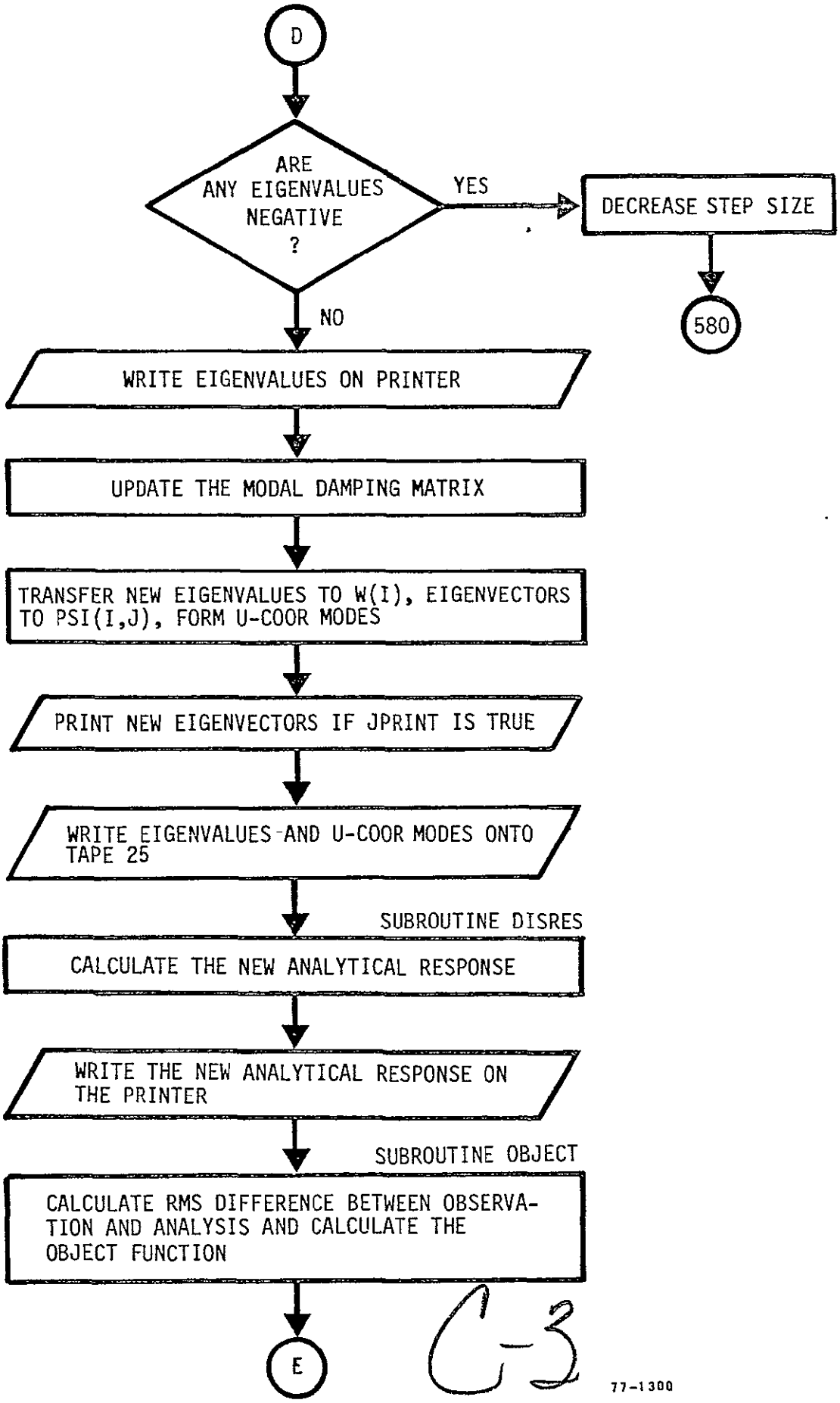
D
ARE ANY EIGENVALUES NEGATIVE ?
YES
DECREASE STEP SIZE
580
NO
WRITE EIGENVALUES ON PRINTER
UPDATE THE MODAL DAMPING MATRIX
TRANSFER NEW EIGENVALUES TO W(I), EIGENVECTORS TO PSI(I,J), FORM U-COOR MODES
PRINT NEW EIGENVECTORS IF JPRINT IS TRUE
WRITE EIGENVALUES AND U-COOR MODES ONTO TAPE 25
SUBROUTINE DISRES
CALCULATE THE NEW ANALYTICAL RESPONSE
WRITE THE NEW ANALYTICAL RESPONSE ON THE PRINTER
SUBROUTINE OBJECT
CALCULATE RMS DIFFERENCE BETWEEN OBSERVATION AND ANALYSIS AND CALCULATE THE OBJECT FUNCTION
E
C-3
77-1300

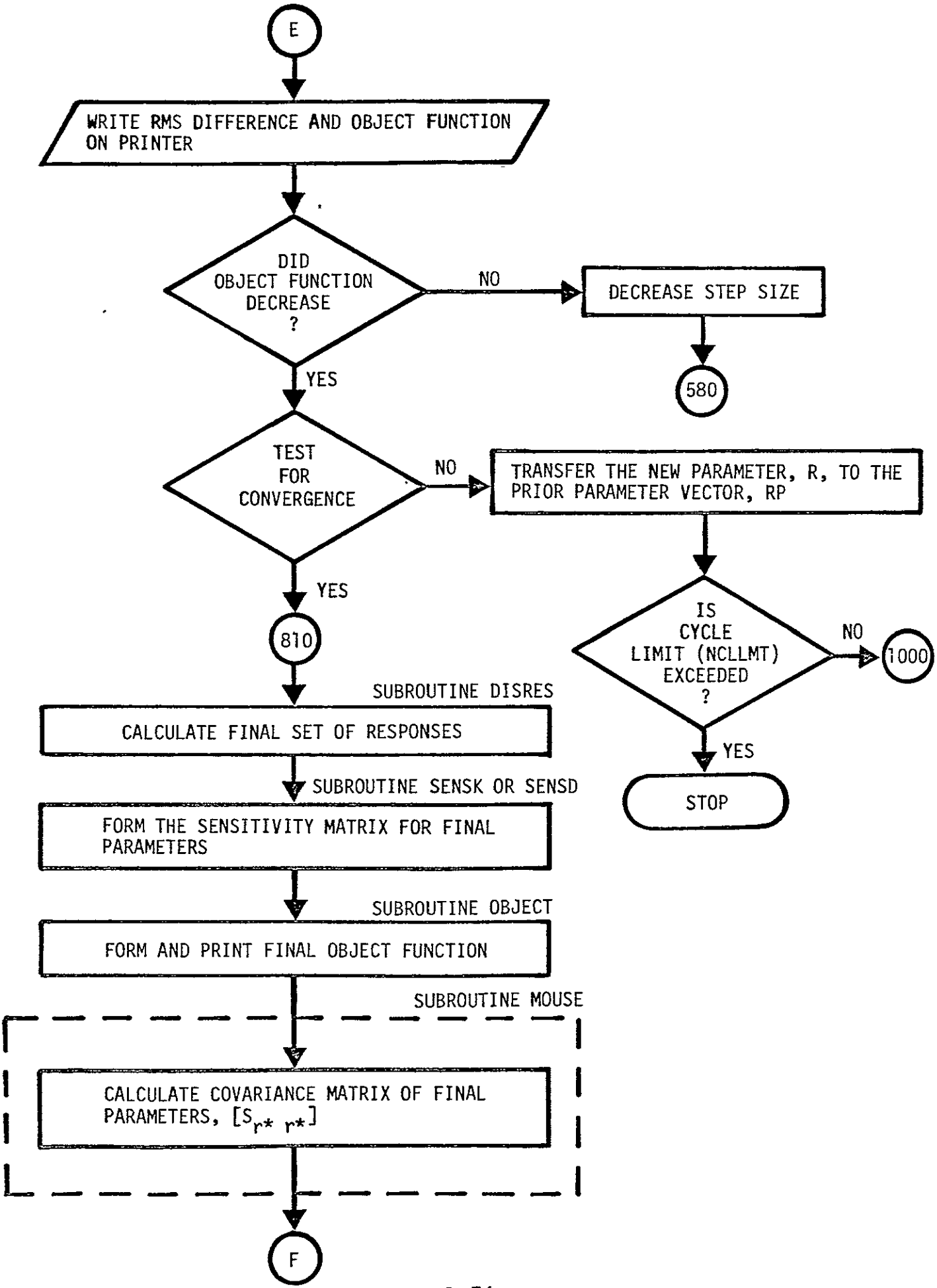
E
WRITE RMS DIFFERENCE AND OBJECT FUNCTION ON PRINTER
DID OBJECT FUNCTION DECREASE ?
NO
DECREASE STEP SIZE
580
YES
TEST FOR CONVERGENCE
NO
TRANSFER THE NEW PARAMETER, R, TO THE PRIOR PARAMETER VECTOR, RP
YES
810
IS CYCLE LIMIT (NCLLMT) EXCEEDED ?
NO
1000
YES
STOP
SUBROUTINE DISRES
CALCULATE FINAL SET OF RESPONSES
SUBROUTINE SENSK OR SENSD
FORM THE SENSITIVITY MATRIX FOR FINAL PARAMETERS
SUBROUTINE OBJECT
FORM AND PRINT FINAL OBJECT FUNCTION
SUBROUTINE MOUSE
CALCULATE COVARIANCE MATRIX OF FINAL PARAMETERS, [S r* r*]
F

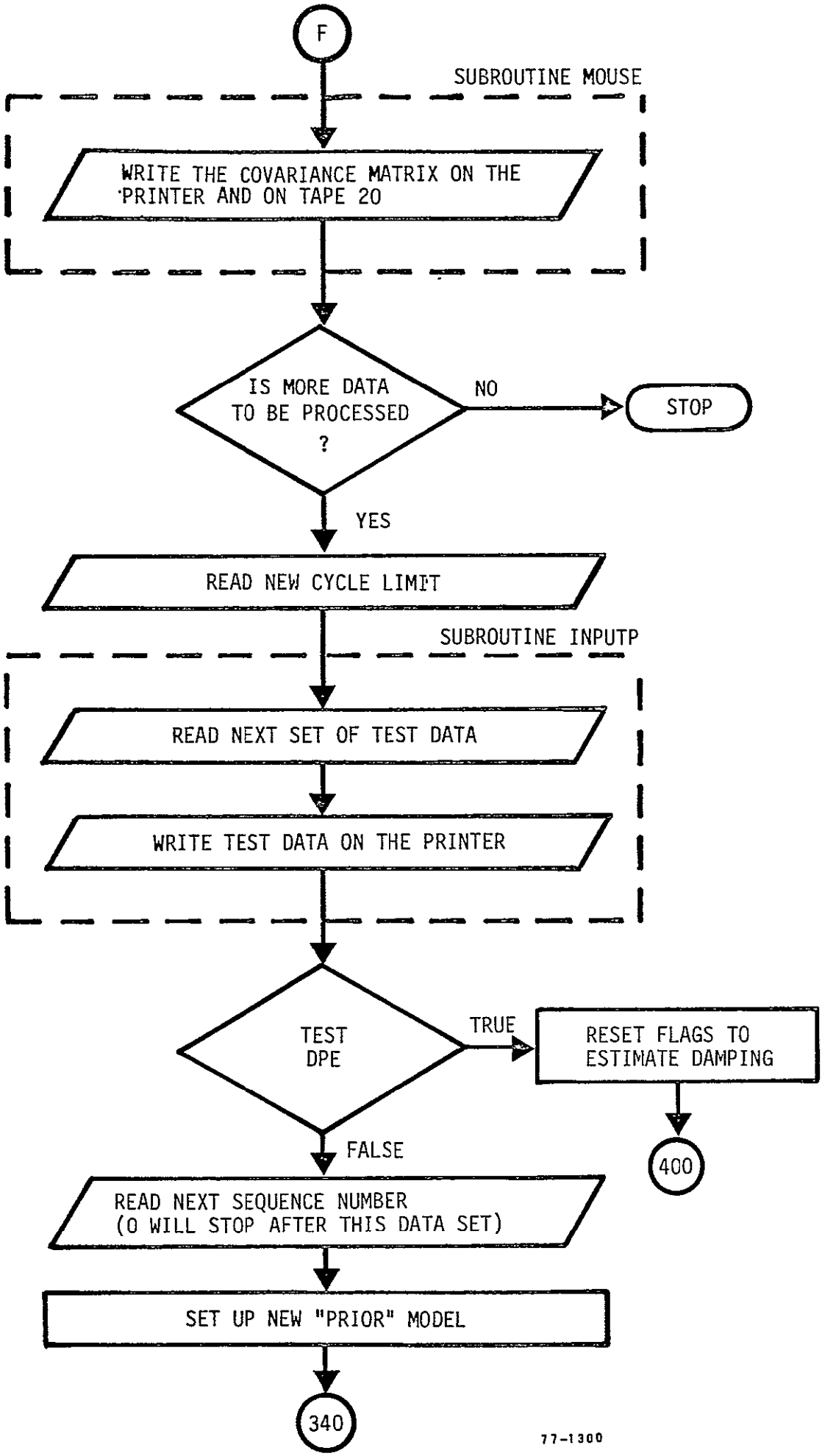
F
SUBROUTINE MOUSE
WRITE THE COVARIANCE MATRIX ON THE PRINTER AND ON TAPE 20
IS MORE DATA TO BE PROCESSED ?
NO
STOP
YES
READ NEW CYCLE LIMIT
SUBROUTINE INPUTP
READ NEXT SET OF TEST DATA
WRITE TEST DATA ON THE PRINTER
TEST DPE
TRUE
RESET FLAGS TO ESTIMATE DAMPING
400
FALSE
READ NEXT SEQUENCE NUMBER (0 WILL STOP AFTER THIS DATA SET)
SET UP NEW "PRIOR" MODEL
340
77-1300

D

ESTIMA INPUT

Cards 1 to 3 provide information on input-output requirements, on the convergence criteria, and the elements to be estimated.

Card One

IPRINT, JPRINT, DPE			
L10,	L10,	L10	FORMAT

where

IPRINT — is a flag which controls printing of the modal orthogonality check.
- =T print the entire orthogonality check.
- =F print only bad elements of orthogonality check

JPRINT — is a flag which controls printing of the various intermediate matrices.
- =T print intermediate matrices
- =F do not print intermediate matrices

DPE — is flag for estimating damping.
- =T estimate modal damping
- =F do not estimate modal damping

Card Two

NCLLMT, NB, IFIRST, PDATA, TDATA					
I5,	I5,	I5,	I5,	I5,	FORMAT

where

NCLLMT	is the maximum number of iterations allowed on the first set of test data.
NB	is the bandwidth within which new elements are to be estimated. >0 number of elements in each row of matrix to be estimated (starting with the diagonal element and going to the right). <0 total number of elements to be estimated (indices of elements given on next card, always include all diagonal elements, use only off-diagonal terms from right side of diagonal).
IFIRST	is a flag which controls reading and implementation of first order corrections to original model. =0 do not use first order correction =1 use first order correction
PDATA	is the location of the prior-model data (Data Set Three). =0,5, or blank read data from cards =23 read data from tape 23 =anything else not permitted
TDATA	is the location of the test data (Data Set Four). =0,5, or blank read data from cards =24 read data from tape 24 =anything else not permitted

Card Two-A (use only if NB <0)

(NI(J), NJ(J)), J= 1, NP
16I5 FORMAT

where

NI(J), NJ(J) =I, J indice of each element of the generalized stiffness and mass matrix to be estimated (include all diagonal terms, plus as many terms from right of diagonal as desired up to a maximum of 50). NP = absolute value of NB.

Card Three

CONLMT, CONLM2, CONST, CHANGE
F10.0, F10.0, F10.0, F10.0 FORMAT

CONLMT is a convergence criterion (change in successive values of the object function as a fraction of the initial value of the object function). Default = .005.

CONLM2 is a second convergence criterion (maximum change in successive values of the parameters being estimated as a fraction of the initial value of the parameter). Default = .01.

CONST parameter used by MOUSE algorithm to control step size. Default = 1.0.

CHANGE parameter used to control step size. Maximum allowable change in any parameter as a fraction of its standard deviation. Default = 0.1.

Cards 4 to 9 provide data on the prior model. This data is provided on cards unless PDATA = 23 when it is read from a tape or disk file.

Card Four

LAB(I), I = 1, 8	
8A4	CARD FORMAT
8A4	TAPE FORMAT

where

LAB(I) is a title with up to 32 characters.

Card Five

NM, NC	
I5, I5,	CARD FORMAT
I5, I5,	TAPE FORMAT

where

NM is the number of modes being used.

NC is the number of degrees of freedom in the u-coordinate system.

Card Six

W(I), I = 1, NM	
8F10.0	CARD FORMAT
4E20.14	TAPE FORMAT

where

W(I) are the natural frequencies (in Hertz) of the original analytic model being used for this estimation.

Card Seven

NDMPFL	
I5	CARD FORMAT
I5	TAPE FORMAT

where

NDMPFL is the control flag which specifies the type of damping information to be read.

=0 read the critical damping ratios for the NM modes of the prior model

=1 read the full NM by NM damping matrix for the prior model

Card Eight (when NDMPFL = 0)

ZET(I), I = 1, NM	
8F10.0	CARD FORMAT
4E20.14	TAPE FORMAT

where

ZET(I) are the critical damping ratios for the NM modes of the prior model being used for this estimation.

Card Eight (when NDMPFL = 1)

(ETA(I,J), I = 1, NM), J = 1, NM	
8F10.0	CARD FORMAT
8F10.0	TAPE FORMAT

where

ETA(I,J) are the NM times NM elements of the modal damping matrix for the prior model being used for this estimation. All elements of the matrix must be input.

Card Nine

(PHI(I,J), I = 1, NC), J = 1, NM	
8F10.0	CARD FORMAT
4E20.14	TAPE FORMAT

where

PHI(I,J)	are the NC elements of the original modal matrix for the NM modes being used for this estimation.

Cards 10 to 12 provide the variances of the prior model. This data is always read from cards.

Card Ten

SRPRP(I), I = 1, NP	
8F10.0	FORMAT

where

SRPRP(I)	are the initial variances of the elements of the generalized stiffness matrix that are to be estimated. The program determines NP based on the band width specified and the number of modes or from the number of elements to be estimated. Only the diagonal and upper right elements are estimated.

Card Eleven

SRPRP(I), I = NP+1, 2*NP	
8F10.0	FORMAT

where

SRPRP(I)	are the initial variances of the elements of the generalized mass matrix that are to be estimated. These elements correspond to the elements of the stiffness matrix being estimated.

Card Twelve

SRPRPD(I), I = 1, NP	
8F10.0	FORMAT

where

SRPRPD(I)	are the initial variances of the generalized damping matrix. These elements correspond to the elements of the stiffness matrix being estimated.

Cards 13 to 17 provide the observation data (i.e., test data). Successive sets of observation data may be processed (see card 17). Subroutine INPUTP reads the data. It may be on cards or tape 24 (TDATA).

Card Thirteen

LAB(I), I = 1, 8	
8A4	CARD FORMAT
8A4	TAPE FORMAT

where

LAB(I) is a title with up to 32 characters.

Card Fourteen

NF	
I5	CARD FORMAT
I5	TAPE FORMAT

where

NF is the number of excitation frequencies for which observation data is being read.

Card Fifteen

FQ(I), I = 1, NF	
8F10.0	CARD FORMAT
4E20.14	TAPE FORMAT

where

FQ(I) are the observation frequencies (Hertz).

Card Sixteen (a block of cards)

This block of cards must be provided for each of the NF observation frequencies. L is the index of the observation frequencies. A maximum of 10 observation frequencies are allowed.

Card Sixteen A

NCT(L), NCF(L)	
I5, I5,	CARD FORMAT
I5, I5,	TAPE FORMAT

where

NCT — is the number of coordinates with observation data (maximum value = 20).

NCF — is the number of coordinates being forced (i.e., with shakers, maximum value = 17).

Card Sixteen B

ICT(I,L), I = 1, NCT(L)	
16I5	CARD FORMAT
16I5	TAPE FORMAT

where

ICT(I,L) — are the locations (i.e., the degrees of freedom) of the observation data (i.e., the measured response). Up to 20 response points are allowed at each excitation frequency.

Card Sixteen C

ICF(I,L), I = 1, NCF(L)	
16I5	CARD FORMAT
16I5	TAPE FORMAT

where

ICF(I,L)	are the locations (i.e., the degrees of freedom) of the coordinates being forced. Up to 17 forced points are allowed at each excitation frequency.

Card Sixteen D

PR(I,L), I = 1, NCF(L)	
8F10.0	CARD FORMAT
4E20.14	TAPE FORMAT

where

PR(I,L)	are the real components of the excitation forces(in-phase).

Card Sixteen E

PI(I,L), I = 1, NCF(L)	
8F10.0	CARD FORMAT
4E20.14	TAPE FORMAT

where

PI(I,L)	are the imaginary components of the excitation forces(out-of-phase).

Card Sixteen F

UTEST(I), I = 1, NO	
8F10.0	CARD FORMAT
4E20.14	TAPE FORMAT

where

UTEST(I) are the observed responses arranged as followed:

UTEST(1) = freq. 1, location 1
UTEST(2) = freq. 1, location 2
≡
freq. 1, location NCT(1)
freq. 2, location 1
≡
freq. 2, location NCT(2)
≡
UTEST(NO)= freq. NF, location NCT(NF)

through all observation frequencies. Repeat for all locations.

A total of 150 observations are allowed. This is less than the maximum number of observation frequencies (10) times the maximum number of observations per frequency (20).

NO is calculated by the program and is the total number of responses = $\sum_{i=1}^{NF} NCTC(i)$.

Card Sixteen G

SEE(I), I = 1, NO	
8F10.0	CARD FORMAT
4E20.14	TAPE FORMAT

where

SEE(I)	are the variances of the observed response arranged as described above.

Card Seventeen

NSEQ	
I5	FORMAT

where

NSEQ	is the number of the next set of sequential data to be processed. Set NSEQ to 0 if no further data is to be processed. If more data is to be read, program reads data starting with Card Two (NCLLMT only).

Card Eighteen (a block of data)

This data block provides the first order correction (FOC) data required when IFIRST = 1. It must be provided on a binary tape

or disk file prepared prior to the ESTIMA run. Subroutine FOC reads the data.

Record Eighteen A

```
NVEC, NM2
- - - - - - - - - - - - - - - - - - - - - - - - - - - - - -
binary record
```

where

NVEC	is the number of elements to be read for stiffness or mass matrices. NVEC = (NM + 1) NM/2.
NM2	is the number of modes being used. Should equal NM.

Record Eighteen B

```
ZZ(I), I = 1, NVEC
- - - - - - - - - - - - - - - - - - - - - - - - - - - - - -
binary record
```

where

ZZ(I)	are the changes to the generalized stiffness matrix caused by application of the First Order Correction. All elements of the right-diagonal-half of the matrix must be input, by row.

Record Eighteen C

ZZ(I), I = 1, NVEC
binary record

where

ZZ(I)	are the changes to the generalized mass matrix caused by application of the First Order Correction. All elements of the right diagonal half of the matrix must be input, by row.

E

ESTIMA Job Control Cards

Compile and store relocatable on CDC computer

```
job card
account card
REQUEST, LGO, *PF.
FTN, R = 3.
CATALOG, LGO, ESTIMA, ID = xxxxx.
AUDIT, AI = P, ID = xxxxx.
¶ - end of record
source deck
¶ - end of record
¶ - end of information
```

Execute using cards for input data and disk file for program

```
job card
account card
REQUEST, TAPE20, *PF.
ATTACH, OLD, ESTIMA, ID = xxxxx.
MAP, OFF.
OLD.
CATALOG, TAPE20, covar. matrix, ID = xxxxx.
¶ - end of record
card data
¶ - end of record
¶ - end of information
```

Execute using existing disk files for program and data

```
job card
account card
```

```
REQUEST, TAPE20, *PF.
ATTACH, TAPE22, first order correction data, ID = xxxxx.
ATTACH, TAPE23, prior model data, ID = xxxxx.
ATTACH, TAPE24, test data, ID = xxxxx.
ATTACH, OLD, ESTIMA, ID = xxxxx.
MAP, OFF.
OLD.
CATALOG, TAPE20, covar. matrix, ID = xxxxx.
¶ - end of record
card data
¶ - end of record
¶ - end of information
```

APPENDIX 6

Program ESTIMB

USER's Instructions

A - General Description

B - Subroutines

C - Flow Chart

D - Input

E - Job Control Cards

A

General Description of ESTIMB

This program, the third and final member of the family, performs the Phase II estimation: the estimate of mass and stiffness scaling parameters. The program is presently sized for five mass sub-matrices and five stiffness sub-matrices, one each of which is a non-scaled component. The theoretical basis for all of the operations performed here is described in the interim and final project reports.

The program consists of a main routine plus six subroutines (Section B). Four of the subroutines perform matrix manipulation (printing, multiplying, and inverting) and the other two perform the parameter estimation. The parameter estimation routines (MOUSE, OBJECT) are only slightly different from the subroutines used by ESTIMA. A flow chart of the main routine is provided in Section C.

The program input consists of data sets described in detail in Section D. Data Set One consists of the program print control, file numbers for the other data sets, the variances of the scaling parameters, the elements of [m] and [k] being used as observation data, and certain other program parameters. Data Set Two is the set of stiffness sub-matrices and Data Set Three is the set of mass sub-matrices. Both sets may be provided on cards, or from a binary disk, or one set may be on cards and the other on a disk file. Up to five sub-matrices may be provided for each set. Although the number of stiffness sub-matrices need not be the same as the number of mass sub-matrices, at least one of each (the non-scaled portion) must be provided.

The stiffness sub-matrices must be such that when added together and pre- and post-multiplied by the original modes, the eigenvalue matrix is obtained:

$$[\phi_o]^t \left(\sum_i [K]_i \right) [\phi_o] = [\Omega^2]$$

Similarly, the mass matrices must yield the identity matrix

$$[\phi_o]^t \left(\sum_i [M]_i \right) [\phi_o] = [I]$$

Data Set Four is the modal deflections, $[\phi_o]$, for the original analytic model. It may be provided on cards or from a binary disk file as described in Section D.

Data Set Five is the covariance matrix of the observations. Each element of [m] and [k] being input constitutes an observation. Only elements from the right-diagonal-half of the matrices can be input and they must be in pairs of one generalized mass element and one generalized stiffness element. This data may be provided on cards or on a binary disk file as described in Section D. This matrix must be taken from the same ESTIMA run that provided [m] and [k].

To minimize data handling, it is recommended that disk files be used whenever more than 10 dynamic degrees-of-freedom are involved. Printing of the input data is controlled by one of the program control flags. Printing the input will result in an extensive amount of output for the larger problems. The program is sized for 125 dynamic degrees-of-freedom.

A set of sample job control cards is presented in Section E for use on a CDC computer. The program source code has been designed for easy comprehension. It is extensively annotated and is keyed to both the input description and the flow chart. Most of the mnemonics are defined at the beginning of the code.

B

ESTIMB Subroutines

INVERT — Inverts a real symmetric matrix. Identical to the INVERT subroutine used for Phase I. Uses the Choleski SDS decomposition method.

MATOUT — Prints all non-zero terms of a matrix with titles and paging. It is identical to the MATOUT subroutine used for Phase I.

MATOU2 — Prints all non-zero terms of a matrix without pages, page headings, or a matrix identification.

MMULRR — Performs matrix multiplication of two real matrices without destroying either one. Can perform [A][B], $[A]^T[B]$, or $[A][B]^T$.

MOUSE — Estimates new scaling parameters (α_j). Provides the covariance matrix of the new parameters. Almost identical to the MOUSE subroutine used for Phase I.

OBJECT — Calculates the value of the object function (i.e., the function which the MOUSE subroutine minimizes).

C

ESTIMB FLOW CHART

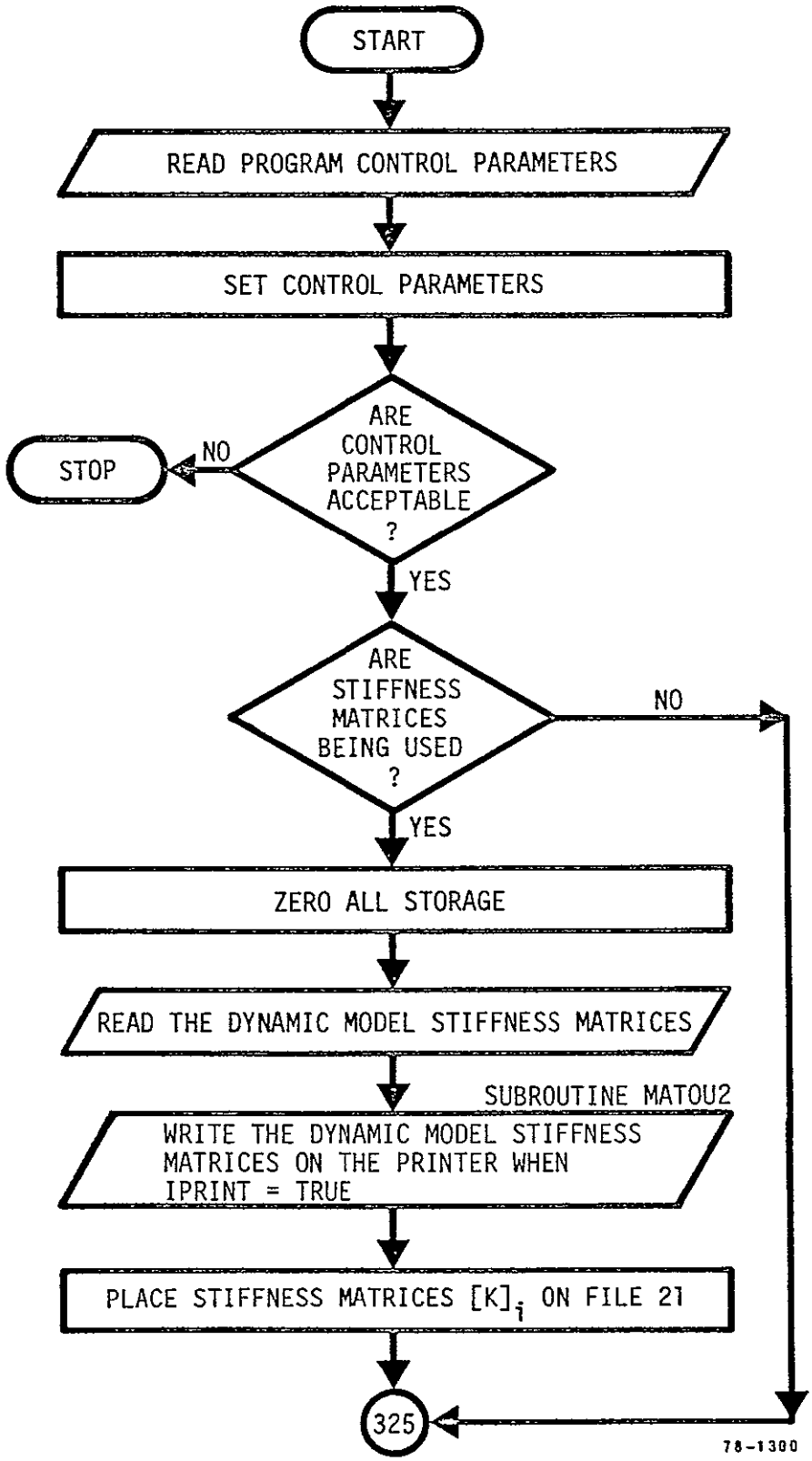

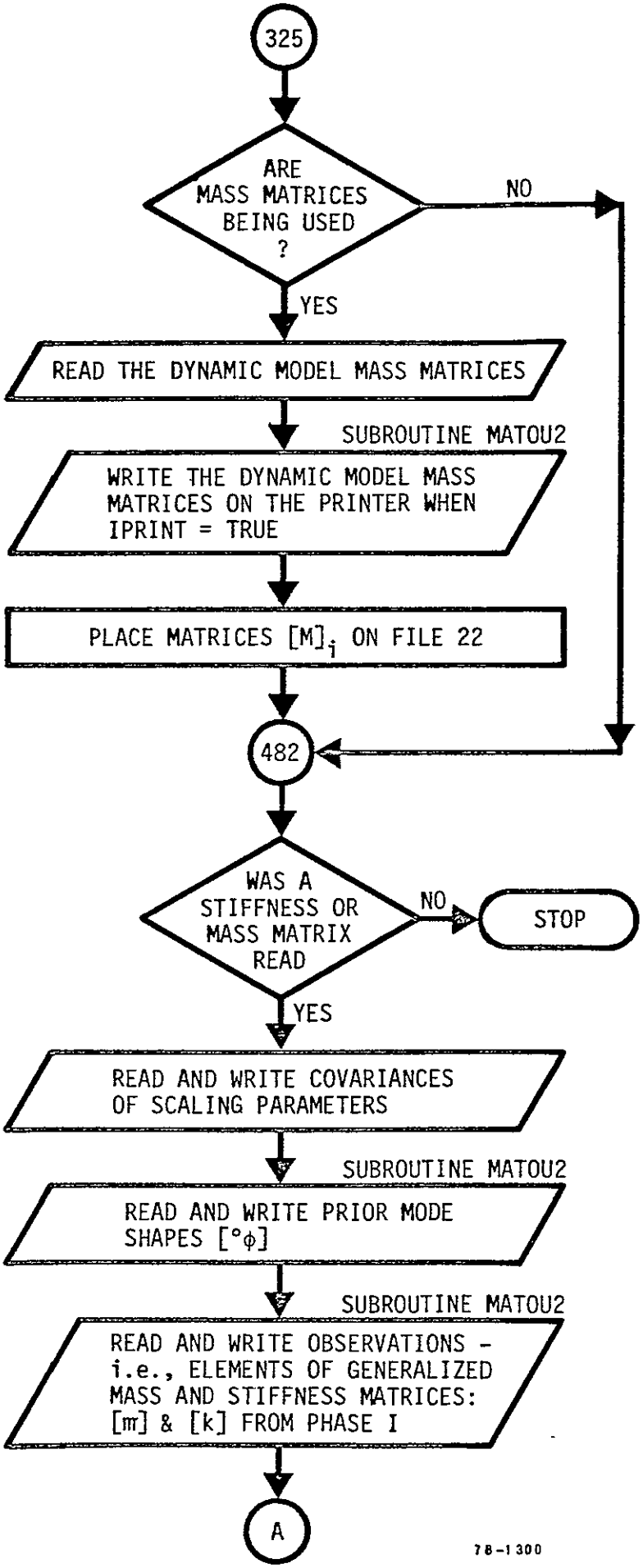
325
ARE MASS MATRICES BEING USED ?
NO
YES
READ THE DYNAMIC MODEL MASS MATRICES
SUBROUTINE MATOU2
WRITE THE DYNAMIC MODEL MASS MATRICES ON THE PRINTER WHEN IPRINT = TRUE
PLACE MATRICES [M]i ON FILE 22
482
WAS A STIFFNESS OR MASS MATRIX READ
NO
STOP
YES
READ AND WRITE COVARIANCES OF SCALING PARAMETERS
SUBROUTINE MATOU2
READ AND WRITE PRIOR MODE SHAPES [°φ]
SUBROUTINE MATOU2
READ AND WRITE OBSERVATIONS - i.e., ELEMENTS OF GENERALIZED MASS AND STIFFNESS MATRICES: [m] & [k] FROM PHASE I
A
78-1300

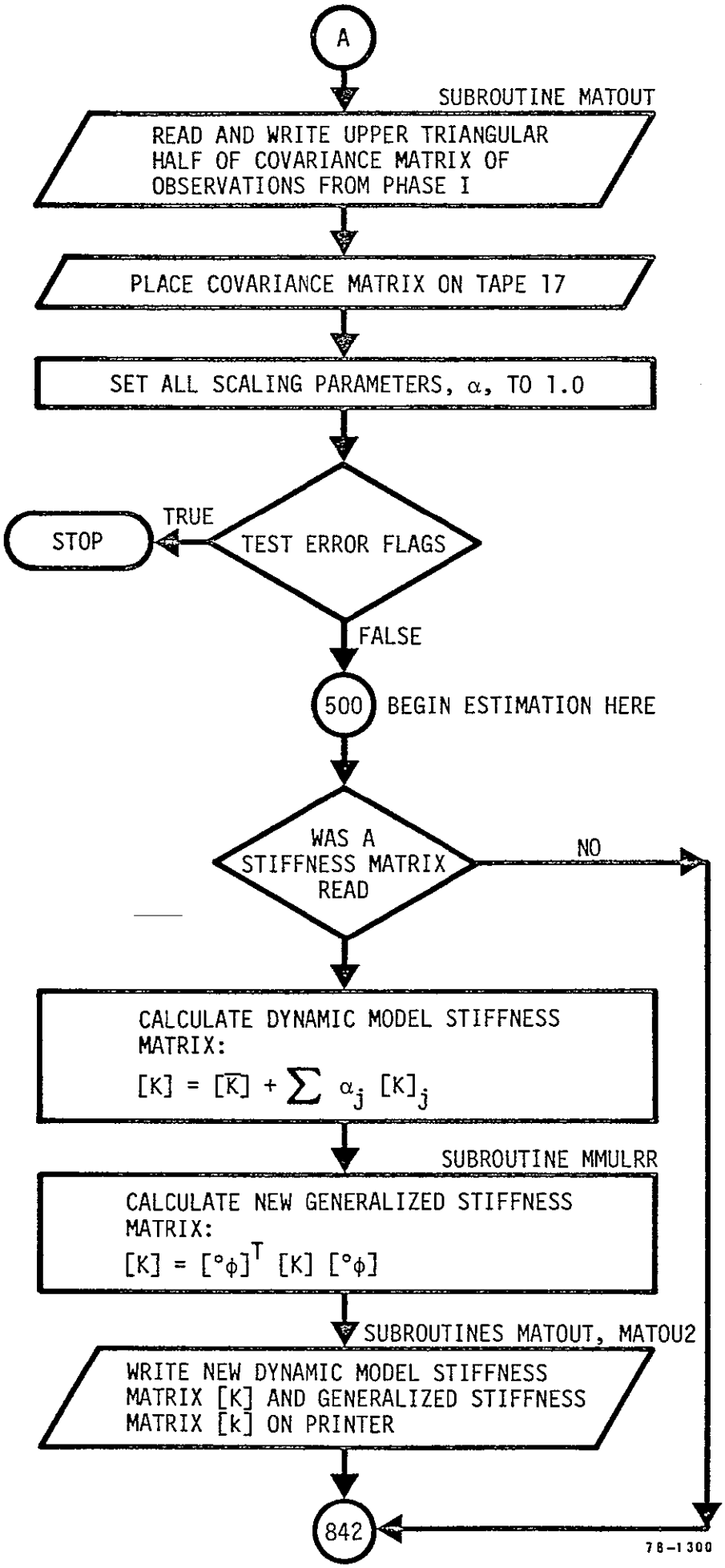
A
SUBROUTINE MATOUT
READ AND WRITE UPPER TRIANGULAR HALF OF COVARIANCE MATRIX OF OBSERVATIONS FROM PHASE I
PLACE COVARIANCE MATRIX ON TAPE 17
SET ALL SCALING PARAMETERS, α, TO 1.0
TEST ERROR FLAGS
TRUE
STOP
FALSE
500
BEGIN ESTIMATION HERE
WAS A STIFFNESS MATRIX READ
NO
CALCULATE DYNAMIC MODEL STIFFNESS MATRIX:
$[K] = [\overline{K}] + \sum \alpha_j [K]_j$
SUBROUTINE MMULRR
CALCULATE NEW GENERALIZED STIFFNESS MATRIX:
$[K] = [^{\circ}\phi]^T [K] [^{\circ}\phi]$
SUBROUTINES MATOUT, MATOU2
WRITE NEW DYNAMIC MODEL STIFFNESS MATRIX [K] AND GENERALIZED STIFFNESS MATRIX [k] ON PRINTER
842
78-1300

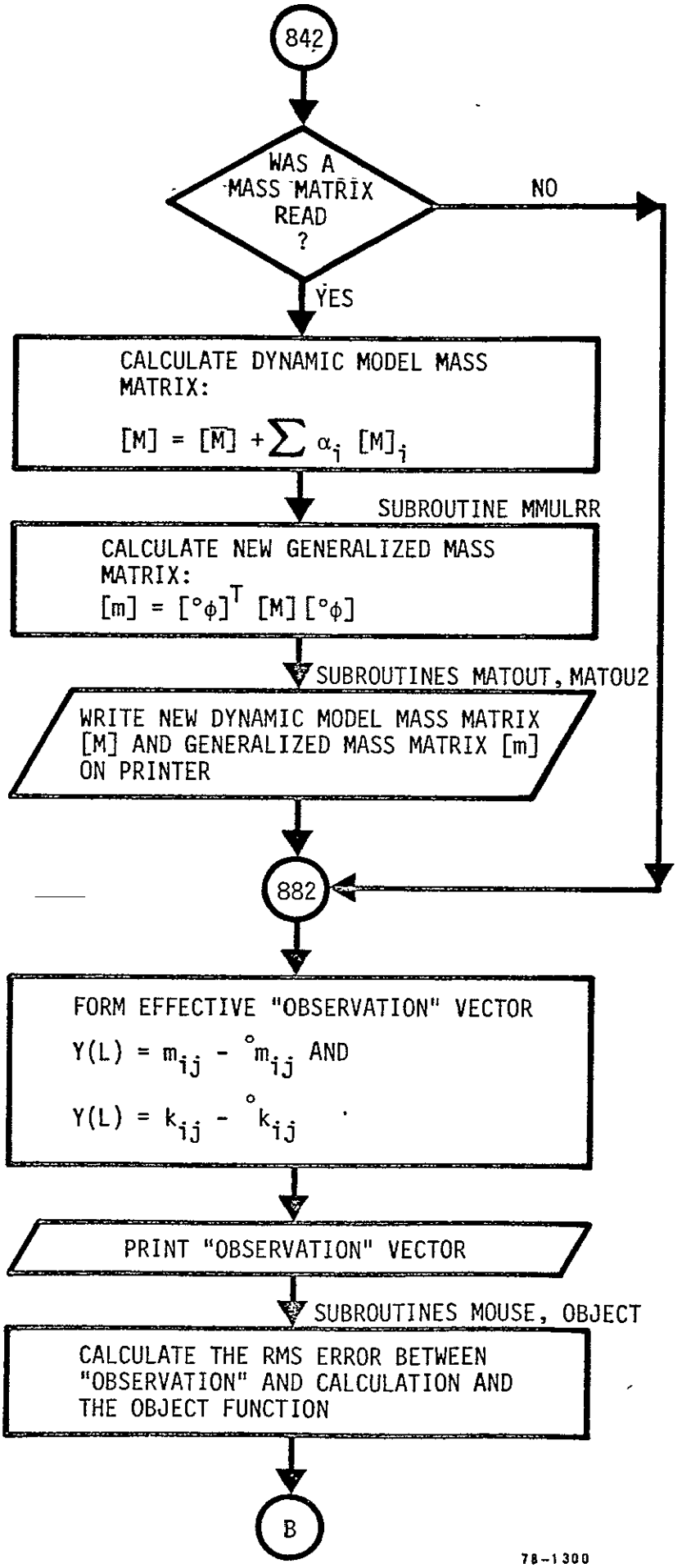
842
WAS A MASS MATRIX READ ?
NO
YES
CALCULATE DYNAMIC MODEL MASS MATRIX:
$[M] = [\bar{M}] + \sum \alpha_i [M]_i$
SUBROUTINE MMULRR
CALCULATE NEW GENERALIZED MASS MATRIX:
$[m] = [{}^{\circ}\phi]^T [M] [{}^{\circ}\phi]$
SUBROUTINES MATOUT, MATOU2
WRITE NEW DYNAMIC MODEL MASS MATRIX [M] AND GENERALIZED MASS MATRIX [m] ON PRINTER
882
FORM EFFECTIVE "OBSERVATION" VECTOR
$Y(L) = m_{ij} - {}^{\circ}m_{ij}$ AND
$Y(L) = k_{ij} - {}^{\circ}k_{ij}$
PRINT "OBSERVATION" VECTOR
SUBROUTINES MOUSE, OBJECT
CALCULATE THE RMS ERROR BETWEEN "OBSERVATION" AND CALCULATION AND THE OBJECT FUNCTION
B

78-1300

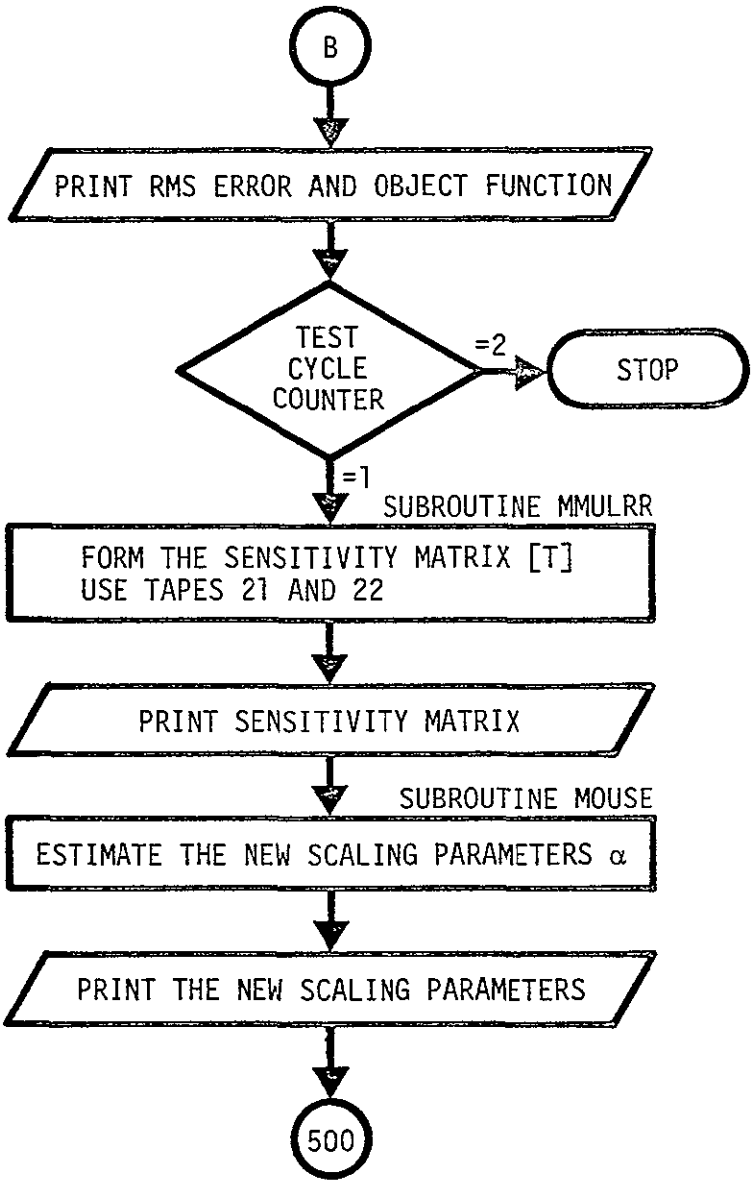
B
PRINT RMS ERROR AND OBJECT FUNCTION
TEST CYCLE COUNTER
=2
STOP
=1
SUBROUTINE MMULRR
FORM THE SENSITIVITY MATRIX [T]
USE TAPES 21 AND 22
PRINT SENSITIVITY MATRIX
SUBROUTINE MOUSE
ESTIMATE THE NEW SCALING PARAMETERS α
PRINT THE NEW SCALING PARAMETERS
500
76-1300

ESTIMB INPUT

Data Set One

Data Set One provides the card data always required by the program. The data included here consists of the program control parameters, the variances of the scaling parameters, and the observation data.

Card One

JPRINT, IPRINT	
L10,	L10 FORMAT

where

JPRINT is a flag which controls printing of intermediate operations.

=T print intermediate matrices.

=F do not print intermediate matrices.

IPRINT is a flag which controls printing of input data.

=T print input data.

=F do not print input data.

Card Two

KTAPE, MTAPE, OTAPE, STAPE				
I5,	I5,	I5,	I5	FORMAT

where

KTAPE is the location of the NK stiffness matrices (Data Set Two).

=30 data provided on a binary file, File 30.

≠30 defaults to 5, data provided on cards.

MTAPE is the location of the NM mass matrices (Data Set Three).

=30 data provided on a binary file, File 30.

≠30 defaults to 5, data provided on cards.

OTAPE is the location of the mode shapes (Data Set Four).

=25 data provided on a binary file, File 25.

≠25 defaults to 5, data provided on cards.

STAPE is the location of the covariance matrix of the observation data (Data Set Five).

=20 data provided on a binary file, File 20.

≠25 defaults to 5, data provided on cards.

Card Three

NK, NM, NS	
I5, I5, I5	FORMAT

where

NK is the number of K-matrix sub-matrices including $[\bar{K}]$ (maximum value = 5).

NM is the number of M-matrix sub-matrices including $[\bar{M}]$ (maximum value = 5).

NS is the size (degrees-of-freedom) of the dynamic model (maximum value = 125).

When stiffness matrices are being input on cards, the cards must be inserted here.

See Data Set Two

When mass matrices are being input

on cards, the cards must be inserted here.

See Data Set Three

Card Four

SRPRP(I), I = 1, NP	
8F10.0	FORMAT

where

SRPRP(I) are the variances of the original scaling parameters. NP = NM + NK - 2.

Use as many cards as necessary to read all of the variances. A maximum of 8 values is presently allowed: 4 for K-matrix parameters, 4 for M-matrix parameters.

Card Five

ND	
I5	FORMAT

where

ND	is the number of modes of the dynamic model that are being used.

When the modes are being input on cards, the cards must be inserted here.

See Data Set Four

Card Six

NO2
I5 FORMAT

where

NO2	is the total number of observation points being read. NO2 = number of mass matrix elements plus the number of stiffness matrix elements. Only the non-zero elements need be read, but if a value is supplied to one matrix it must also be supplied for the other. The elements may be read in any sequence but care must be exercised to insure that the covariance matrix is properly keyed to these data.

Card Seven

(IO(I), JO(I), KO(I), MO(I)) I = 1, NO
2(I5, I5, E15.9, E15.9) FORMAT

where

IO(I)	are the i indices (row index) of the i^{th} observation.
JO(I)	are the j indices (column index) of the i^{th} observation.
KO(I)	are the i^{th} elements of the generalized stiffness matrix, [k].
MO(I)	are the i^{th} elements of the generalized mass matrix, [m].
——	NO = NO2/2. The KO(I) elements become the first NO observations; the MO(I) become the second NO observations.

Use as many cards as necessary with each card, except the last one, full. A maximum of 100 observations may be read (50 for generalized stiffness matrix, 50 for mass).

When the covariance matrix of the observation data

is being input on cards, the cards must be inserted here.

See Data Set Five

ESTIMB INPUT

Data Set Two

Data Set Two is the stiffness matrix data including all of the submatrices which, when added together, form the dynamic model stiffness matrix. Up to five submatrices may presently be used, including the non-varying component. These data may be provided either on cards inserted into the run stream or on a binary file prepared beforehand. If a binary file is used it must be assigned to TAPE 30.

Each submatrix is retrieved from the file as follows:

```
      Do 410 L = 1, NK
         READ (30) N
         DO 405 I = 1, NS
            READ (30) (K(I,J),J = 1, NS)
405      CONTINUE
410   CONTINUE
```

The first record is the index of the submatrix (1,2,3,4, or 5). The submatrix assigned the index number of 1 is taken to be the non-varying component. Following the index number are NS records, one for each row of the matrix, with only the right-diagonal-half of the matrix being read.

When cards are used, they must be inserted into the run stream as shown in Data Set One. The card formats are shown below. The parameters NK, the number of matrices to read, and NS, the number of degrees-of-freedom in the matrices, are provided in Data Set One.

Card One

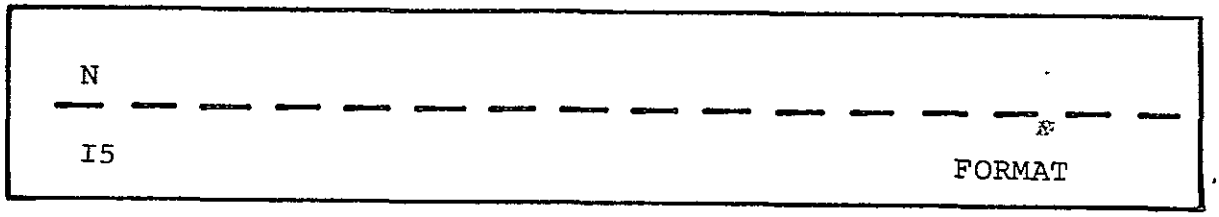

where

N	is the index number of the stiffness-matrix portion to be read next.

Card Two

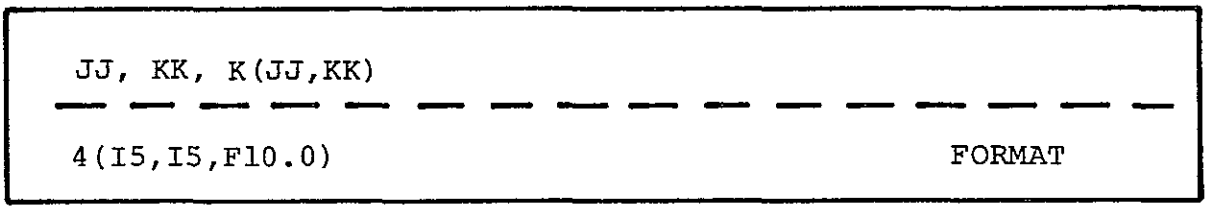

where

JJ	is the first index of the element.
KK	is the second index of the element. KK must $\geq$ JJ.
K(JJ,KK)	is the JJ,KK element of the portion of K-matrix being read.

Values of JJ, KK, and K(JJ,KK) are read until a value of 0 is read for JJ. Use as many cards as necessary with 4 elements per card.

Repeat cards one and two until all portions of the prior stiffness matrix are read. The program will continue to read stiffness matrix blocks until a value of 0 is read for N. Only the upper right-hand elements of the stiffness matrices must be read.

ESTIMB INPUT

Data Set Three

Data Set Three is the mass matrix data including all of the submatrices which, when added together, form the dynamic model mass matrix. Up to five submatrices may presently be used, including the non-varying component. This data may be provided either on cards inserted into the run stream or on a binary file prepared beforehand. If a binary file is used it must be assigned to TAPE 30. If both mass and stiffness matrices are provided from a binary file, both types of matrices must be on TAPE 30 with the NM mass matrices following the NK stiffness matrices.

Each mass submatrix is retrieved from the file as follows:

```
      DO 460 L = 1, NM
         READ (30) N
         DO 455 I = 1, NS
            READ (30) (M(I,J),J = I, NS)
455      CONTINUE
460   CONTINUE
```

The first record is the index of the submatrix (1,2,3,4, or 5). The submatrix assigned the index number of 1 is taken to be the non-varying component. Each submatrix must be provided on NS records, one for each row of the matrix. Only the right diagonal-half of the matrix is used.

When cards are used, they must be inserted into the run stream as shown in Data Set One. The card formats are shown below. The parameters NM, the number of matrices being read, and NS,

the number of degrees-of-freedom in the matrices, are provided in Data Set One.

Card One

N
I5 FORMAT

where

N	is the index number of the mass-matrix portion to be read next.

Card Two

JJ, KK, M(JJ,KK)
4(I5, I5, F10.0) FORMAT

where

JJ	is the first index of the element.
KK	is the second index of the element. KK must $\geq$ JJ.
M(JJ,KK)	is the JJ,KK element of the portion of the mass matrix being read.

Values of JJ, KK, and M(JJ,KK) are read until a value of 0 is read for JJ. Use as many cards as necessary with 4 elements per card.

Repeat cards one and two until all portions of the prior mass-matrix are read. The program will continue to read mass matrix blocks until a value of 0 is read for N. Only the upper right-hand elements of the mass matrices must be read.

ESTIMB INPUT

Data Set Four

Data Set Four provides the modal data. One analytic mode must be provided for each row in the generalized mass or stiffness matrix. This data may also be provided on cards inserted into the run stream, or on a binary file prepared beforehand. If a binary file is used it must be assigned to TAPE 25. The file must consist of ND+1 records with one record for each mode. The file format is:

```
      READ (25) ND
      DO 494 I = 1, ND
         READ (25) (PHIP(J,I), J = I, NS)
494   CONTINUE
```

ND is the number of modes to read and NS the number of degrees-of-freedom. The ND read here supercedes the one read in Data Set One. When cards are used they must be inserted into the run stream as shown in Data Set One. The card format is:

PHIP(J,I), J = 1, NS
8F10.0 FORMAT

where

PHIP(J,I) is the j^{th} element of the i^{th} mode shape.

Use as many cards as necessary to complete each mode shape. Repeat for each mode shape. A maximum of 12 modes with 125 elements per mode may be read.

ESTIMB INPUT

Data Set Five

Data Set Five provides the covariance matrix of the observation data. It may be provided on cards in the run stream, or on a binary data file prepared beforehand by the user.

The binary file, FILE 20, must consist of NO2 records with one record for each column of the matrix. All elements of the row, including zeros, must be provided. The read code is as follows:

```
     DO 550 J = 1,NO2
        READ (20) (SEE(I,J), J = 1, NO2)
550  CONTINUE
```

When input as card data, the cards must be inserted into the run stream as shown in Data Set One. The following cards are required:

Card One

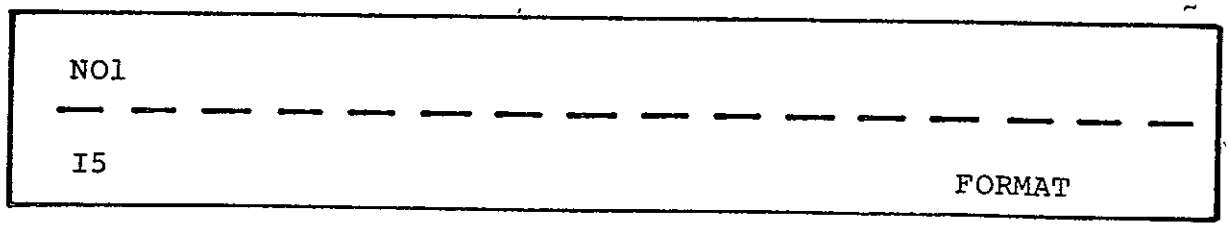

where

NO1 is the number of cards with covariance data.

Card Two

JJ, KK, SEE(JJ,KK)
4(I4,I4, E12.4) FORMAT

where

JJ is the first index of the element.

KK is the second index of the element. KK must $\geq$ JJ.

SEE(JJ,KK) is the JJ,KK element of the covariance matrix of the "observation" data.

Only read the upper right-hand elements of the covariance matrix. Although the elements may be read in any order, care must be taken to insure that the i^{th} row of this matrix corresponds to the i^{th} observation. From 1 to 4 elements sets (J, K, value) may be input per card. Use as many cards as desired, with the exact number of cards specified on card one.

E

ESTIMB Job Control Cards

Compile and store relocatable on CDC computer

```
job card
account card
REQUEST, LGO, *PF.
FTN, R = 3
CATALOG, LGO, ESTIMB, ID = xxxxx.
AUDIT, AI = P, ID = xxxxx.
¶ - end of record
source deck
¶ - end of record
¶ - end of information
```

Execute using cards for input data and disk file for program

```
job card
account card
ATTACH, OLD, ESTIMB, ID = xxxxx.
MAP, OFF.
OLD.
¶ - end of record
card data
¶ - end of record
¶ - end of information
```

Execute using existing disk files for program and data

```
job card
account card
ATTACH, OLD, ESTIMB, ID = xxxxx.
```

```
ATTACH, TAPE20, covar. matrix, ID = xxxxx.
ATTACH, TAPE25, prior modes, ID = xxxxx.
ATTACH, TAPE30, mass and stiffness matrices, ID = xxxxx.
MAP, OFF.
¶ - end of record
card data
¶ - end of record
¶ - end of information
```